

# NAVAL POSTGRADUATE SCHOOL Monterey, California



## THESIS

**A DESIGN PROCEDURE FOR SEAKEEPING ANALYSIS  
OF CLOSE PROXIMITY SHIP TOWING**

by

Orhan Barbaros Okan

March 2002

Thesis Advisor:

Fotis A. Papoulias

Approved for Public Release; Distribution is Unlimited.

THIS PAGE INTENTIONALLY LEFT BLANK

REPORT DOCUMENTATION PAGE			Form Approved OMB No. 0704-0188	
Public reporting burden for this collection of information is estimated to average 1 hour per response, including the time for reviewing instruction, searching existing data sources, gathering and maintaining the data needed, and completing and reviewing the collection of information. Send comments regarding this burden estimate or any other aspect of this collection of information, including suggestions for reducing this burden, to Washington headquarters Services, Directorate for Information Operations and Reports, 1215 Jefferson Davis Highway, Suite 1204, Arlington, VA 22202-4302, and to the Office of Management and Budget, Paperwork Reduction Project (0704-0188) Washington DC 20503.				
<b>1. AGENCY USE ONLY (Leave blank)</b>		<b>2. REPORT DATE</b> March 2002	<b>3. REPORT TYPE AND DATES COVERED</b> Master's Thesis	
<b>4. TITLE AND SUBTITLE</b> A Design Procedure for Seakeeping Analysis of Close Proximity Ship Towing			<b>5. FUNDING NUMBERS</b>	
<b>6. AUTHOR</b> Orhan Barbaros Okan				
<b>7. PERFORMING ORGANIZATION NAME(S) AND ADDRESS(ES)</b> Naval Postgraduate School Monterey, CA 93943-5000			<b>8. PERFORMING ORGANIZATION REPORT NUMBER</b>	
<b>9. SPONSORING / MONITORING AGENCY NAME(S) AND ADDRESS(ES)</b> N/A			<b>10. SPONSORING / MONITORING AGENCY REPORT NUMBER</b>	
<b>11. SUPPLEMENTARY NOTES</b> The views expressed in this thesis are those of the author and do not reflect the official policy or position of the Department of Defense or the U.S. Government.				
<b>12a. DISTRIBUTION / AVAILABILITY STATEMENT</b> Approved for Public Release; Distribution is Unlimited.			<b>12b. DISTRIBUTION CODE</b>	
<b>13. ABSTRACT (maximum 200 words)</b>  The purpose of this thesis is to develop an efficient analysis and design procedure for assessing the seakeeping behavior of surface ships in close proximity towing. The problem is formulated by using the heave and pitch equations of motion in regular waves. The vertical plane relative motions between the trailing and the leading ships are matched through the speed-resistance characteristics of the trailing ship. A sea state degradation factor is introduced. This factor characterizes the expected seakeeping performance penalty resulting from the connection. A series of parametric studies is conducted for various geometric properties and environmental characteristics. The results can be used to evaluate the response of the system and provide insight into parameter selection for motion minimization.				
<b>14. SUBJECT TERMS</b> SLICE, KAIMALINO, SEAKEEPING, SWATH, RAO, SPEED POLAR PLOT			<b>15. NUMBER OF PAGES</b> 115	
			<b>16. PRICE CODE</b>	
<b>17. SECURITY CLASSIFICATION OF REPORT</b> Unclassified	<b>18. SECURITY CLASSIFICATION OF THIS PAGE</b> Unclassified	<b>19. SECURITY CLASSIFICATION OF ABSTRACT</b> Unclassified	<b>20. LIMITATION OF ABSTRACT</b> UL	

THIS PAGE INTENTIONALLY LEFT BLANK

**Approved for Public Release; Distribution is Unlimited**

**A DESIGN PROCEDURE FOR SEAKEEPING ANALYSIS OF CLOSE  
PROXIMITY SHIP TOWING**

Orhan Barbaros Okan  
Lieutenant Junior Grade, Turkish Navy  
B.S., Turkish Naval Academy, 1996

Submitted in partial fulfillment of the  
requirements for the degree of

**MASTER OF SCIENCE IN MECHANICAL ENGINEERING**

from the

**NAVAL POSTGRADUATE SCHOOL  
March 2002**

Author: Orhan Barbaros Okan

Approved by: Fotis A. Papoulias, Thesis Advisor

Terry R. McNelley, Chairman  
Mechanical Engineering Department

THIS PAGE INTENTIONALLY LEFT BLANK

## **ABSTRACT**

The purpose of this thesis is to develop an efficient analysis and design procedure for assessing the seakeeping behavior of surface ships in close proximity towing. The problem is formulated by using the heave and pitch equations of motion in regular waves. The vertical plane relative motions between the trailing and the leading ships are matched through the speed-resistance characteristics of the trailing ship. A sea state degradation factor is introduced. This factor characterizes the expected seakeeping performance penalty resulting from the connection. A series of parametric studies is conducted for various geometric properties and environmental characteristics. The results can be used to evaluate the response of the system and provide insight into parameter selection for motion minimization.

THIS PAGE INTENTIONALLY LEFT BLANK

## TABLE OF CONTENTS

<b>I.</b>	<b>INTRODUCTION.....</b>	<b>1</b>
<b>A.</b>	<b>MOTIVATION.....</b>	<b>1</b>
<b>B.</b>	<b>PREVIOUS WORK.....</b>	<b>1</b>
<b>II.</b>	<b>REGULAR WAVES RESPONSE.....</b>	<b>3</b>
<b>III.</b>	<b>RANDOM WAVES RESPONSE.....</b>	<b>11</b>
<b>IV.</b>	<b>SEAKEEPING EVALUATIONS.....</b>	<b>15</b>
<b>V.</b>	<b>CONCLUSIONS AND RECOMMENDATIONS.....</b>	<b>17</b>
<b>A.</b>	<b>CONCLUSIONS.....</b>	<b>17</b>
<b>B.</b>	<b>RECOMMENDATIONS.....</b>	<b>17</b>
<b>APPENDIX A.</b>	<b>REGULAR WAVES RESULTS.....</b>	<b>19</b>
<b>APPENDIX B.</b>	<b>RANDOM WAVES RESULTS.....</b>	<b>29</b>
<b>APPENDIX C.</b>	<b>SEAKEEPING RESULTS.....</b>	<b>51</b>
<b>APPENDIX D.</b>	<b>HYDRODYNAMICS DATA.....</b>	<b>81</b>
<b>APPENDIX E.</b>	<b>MATLAB CODES FOR REGULAR WAVES.....</b>	<b>83</b>
<b>APPENDIX F.</b>	<b>MATLAB CODES FOR RANDOM WAVES.....</b>	<b>91</b>
<b>APPENDIX G.</b>	<b>MATLAB CODES FOR SEAKEEPING EVALUATION.....</b>	<b>95</b>
	<b>LIST OF REFERENCES.....</b>	<b>97</b>
	<b>INITIAL DISTRIBUTION LIST.....</b>	<b>99</b>

THIS PAGE INTENTIONALLY LEFT BLANK

## LIST OF FIGURES

Figure 1.	Sign Convention for Ship Motions (From: Beck).....	4
Figure 2.	Connection Force and Motions of the Ships.....	6
Figure 3.	Tension.....	9
Figure 4.	Wave Spectrum and Addition of Waves (From: Cummins).....	11
Figure 5.	A notional ship operability envelope mapping.....	16
Figure A-1.	Exciting Forces for $V=10\text{kts}$ , $l/L=0.1$ and $\beta=0^\circ$ .....	20
Figure A-2.	Motions of the Ships for $V=10\text{kts}$ , $l/L=0.1$ and $\beta=0^\circ$ .....	20
Figure A-3.	Exciting Forces for $V=10\text{kts}$ , $l/L=0.1$ and $\beta=90^\circ$ .....	21
Figure A-4.	Motions of the Ships for $V=10\text{kts}$ , $l/L=0.1$ and $\beta=90^\circ$ .....	21
Figure A-5.	Exciting Forces for $V=10\text{kts}$ , $l/L=0.1$ and $\beta=180^\circ$ .....	22
Figure A-6.	Motions of the Ships for $V=10\text{kts}$ , $l/L=0.1$ and $\beta=180^\circ$ .....	22
Figure A-7.	Force Variation for Different Headings when $V=10\text{kts}$ and $l/L=0.1$ .....	23
Figure A-8.	SLICE Motion for Different Headings when $V=10\text{kts}$ and $l/L=0.1$ .....	23
Figure A-9.	KAIMALINO Motion for Different Headings when $V=10\text{kts}$ and $l/L=0.1$ .....	24
Figure A-10.	Connection Force for Different Towing Lengths when $V=10\text{kts}$ and $\beta=45^\circ$ .....	24
Figure A-11.	SLICE Motion for Different Towing Lengths when $V=10\text{kts}$ and $\beta=45^\circ$ .....	25
Figure A-12.	KAIMALINO Motion for Different Towing Lengths when $V=10\text{kts}$ and $\beta=45^\circ$ .....	25
Figure A-13.	Connection Forces for Different Ship Speeds when $l/L=0.1$ and $\beta=45^\circ$ .....	26
Figure A-14.	SLICE Motion for Different Ship Speeds when $l/L=0.1$ and $\beta=45^\circ$ .....	26
Figure A-15.	KAIMALINO Motion for Different Ship Speeds when $l/L=0.1$ and $\beta=45^\circ$ .....	27
Figure B-1.	RMS of Connection Force vs. Heading when $V=10\text{kts}$ and $l/L=0.01$ .....	30
Figure B-2.	RMS of Heave Force vs. Heading when $V=10\text{kts}$ and $l/L=0.01$ .....	30
Figure B-3.	RMS of Vertical Motion vs. Heading when $V=10\text{kts}$ and $l/L=0.01$ .....	31
Figure B-4.	Normalized Force ( $f/F_3$ ) vs. Heading when $V=10\text{kts}$ and $l/L=0.01$ .....	31
Figure B-5.	Vertical Motion vs. Heading when $V=10\text{kts}$ and $l/L=0.01$ .....	32
Figure B-6.	RMS of Connection Force vs. Heading when $V=10\text{kts}$ and $l/L=0.1$ .....	32
Figure B-7.	RMS of Heave Force vs. Heading when $V=10\text{kts}$ and $l/L=0.1$ .....	33
Figure B-8.	RMS Value of Vertical Motion vs. Heading when $V=10\text{kts}$ and $l/L=0.1$ .....	33
Figure B-9.	Normalized Force ( $f/F_3$ ) vs. Heading as a Function of Sea State when $V=10\text{kts}$ and $l/L=0.1$ .....	34
Figure B-10.	Vertical Motion vs. Heading when $V=10\text{kts}$ and $l/L=0.1$ .....	34
Figure B-11.	RMS of Connection Force vs. Heading as a Function of Sea State when $V=10\text{kts}$ and $l/L=1$ .....	35
Figure B-12.	RMS of Heave Force vs. Heading when $V=10\text{kts}$ and $l/L=1$ .....	35
Figure B-13.	RMS Value of Vertical Motion vs. Heading when $V=10\text{kts}$ and $l/L=1$ .....	36
Figure B-14.	Normalized Force ( $f/F_3$ ) vs. Heading when $V=10\text{kts}$ and $l/L=1$ .....	36
Figure B-15.	Normalized Vertical Motion vs. Heading when $V=10\text{kts}$ and $l/L=1$ .....	37
Figure B-16.	RMS of Connection Force vs. Heading as a Function of $l/L$ when $V=10\text{kts}$ .....	37
Figure B-17.	RMS of Heave Force vs. Heading as a Function of $l/L$ when $V=10\text{kts}$ .....	38

Figure B-18.	RMS Value of Vertical Motion vs. Heading as a Function of $l/L$ when $V=10\text{kts}$ .....	38
Figure B-19.	Normalized Force ( $f/F_3$ ) vs. Heading as a Function of $l/L$ when $V=10\text{kts}$ .....	39
Figure B-20.	Vertical Motion vs. Heading as a Function of $l/L$ when $V=10\text{kts}$ .....	39
Figure B-21.	RMS of Connection Force vs. Heading when $V=5\text{kts}$ and $l/L=0.1$ .....	40
Figure B-22.	RMS of Heave Force vs. Heading when $V=5\text{kts}$ and $l/L=0.1$ .....	40
Figure B-23.	RMS Value of Vertical Motion vs. Heading when $V=5\text{kts}$ and $l/L=0.1$ .....	41
Figure B-24.	Normalized Force ( $f/F_3$ ) vs. Heading when $V=5\text{kts}$ and $l/L=0.1$ .....	41
Figure B-25.	Vertical Motion vs. Heading when $V=5\text{kts}$ and $l/L=0.1$ .....	42
Figure B-26.	RMS of Connection Force vs. Heading when $V=15\text{kts}$ and $l/L=0.1$ .....	42
Figure B-27.	RMS of Heave Force vs. Heading when $V=15\text{kts}$ and $l/L=0.1$ .....	43
Figure B-28.	RMS Value of Vertical Motion vs. Heading when $V=15\text{kts}$ and $l/L=0.1$ .....	43
Figure B-29.	Normalized Force ( $f/F_3$ ) vs. Heading when $V=15\text{kts}$ and $l/L=0.1$ .....	44
Figure B-30.	Normalized Vertical Motion vs. Heading when $V=15\text{kts}$ and $l/L=0.1$ .....	44
Figure B-31.	RMS of Connection Force vs. Heading when $V=20\text{kts}$ and $l/L=0.1$ .....	45
Figure B-32.	RMS of Heave Force vs. Heading when $V=20\text{kts}$ when $l/L=0.1$ .....	45
Figure B-33.	RMS Value of Vertical motion vs. Heading when $V=20\text{kts}$ and $l/L=0.1$ .....	46
Figure B-34.	Normalized Force ( $f/F_3$ ) vs. Heading when $V=20\text{kts}$ and $l/L=0.1$ .....	46
Figure B-35.	Vertical Motion vs. Heading when $V=20\text{kts}$ and $l/L=0.1$ .....	47
Figure B-36.	RMS of Connection Force vs. Heading when $l/L=0.1$ and Sea State 4 .....	47
Figure B-37.	RMS of Heave Force vs. Heading when $l/L=0.1$ and Sea State 4 .....	48
Figure B-38.	RMS Value of Vertical Motion vs. Heading when $l/L=0.1$ and Sea State 4... 48	
Figure B-39.	Normalized Force ( $f/F_3$ ) vs. Heading when $l/L=0.1$ and Sea State 4 .....	49
Figure B-40.	Vertical Motion vs. Heading when $l/L=0.1$ and Sea State 4.....	49
Figure C-1.	Sea state variation when $V=10\text{kts}$ , $l/L=0.01$ and Sea State 1.....	52
Figure C-2.	Sea state degradation when $V=10\text{kts}$ , $l/L=0.01$ and Sea State 1 .....	52
Figure C-3.	Sea state variation when $V=10\text{kts}$ , $l/L=0.01$ and Sea State 2.....	53
Figure C-4.	Sea state degradation when $V=10\text{kts}$ , $l/L=0.01$ and Sea State 2.....	53
Figure C-5.	Sea state variation when $V=10\text{kts}$ , $l/L=0.01$ and Sea State 3.....	54
Figure C-6.	Sea state degradation when $V=10\text{kts}$ , $l/L=0.01$ and Sea State 3 .....	54
Figure C-7.	Sea state variation when $V=10\text{kts}$ , $l/L=0.01$ and Sea State 4.....	55
Figure C-8.	Sea state degradation when $V=10\text{kts}$ , $l/L=0.01$ and Sea State 4 .....	55
Figure C-9.	Sea state variation when $V=10\text{kts}$ , $l/L=0.01$ and Sea State 5.....	56
Figure C-10.	Sea state degradation when $V=10\text{kts}$ , $l/L=0.01$ and Sea State 5 .....	56
Figure C-11.	Sea state variation when $V=10\text{kts}$ , $l/L=0.01$ and Sea State 6.....	57
Figure C-12.	Sea state degradation when $V=10\text{kts}$ , $l/L=0.01$ and Sea State 6 .....	57
Figure C-13.	Sea state variation when $V=10\text{kts}$ , $l/L=0.01$ and Sea State 7.....	58
Figure C-14.	Sea state degradation when $V=10\text{kts}$ , $l/L=0.01$ and Sea State 7 .....	58
Figure C-15.	Sea state variation when $V=10\text{kts}$ , $l/L=0.1$ and Sea State 1.....	59
Figure C-16.	Sea state degradation when $V=10\text{kts}$ , $l/L=0.1$ and Sea State 1 .....	59
Figure C-17.	Sea state variation when $V=10\text{kts}$ , $l/L=0.1$ and Sea State 2.....	60
Figure C-18.	Sea state degradation when $V=10\text{kts}$ , $l/L=0.1$ and Sea State 2 .....	60
Figure C-19.	Sea state variation when $V=10\text{kts}$ , $l/L=0.1$ and Sea State 3.....	61
Figure C-20.	Sea state degradation when $V=10\text{kts}$ , $l/L=0.1$ and Sea State 3 .....	61
Figure C-21.	Sea state variation when $V=10\text{kts}$ , $l/L=0.1$ and Sea State 4.....	62

Figure C-22.	Sea state degradation when $V=10\text{kts}$ , $l/L=0.1$ and Sea State 4.....	62
Figure C-23.	Sea state variation when $V=10\text{kts}$ , $l/L=0.1$ and Sea State 5.....	63
Figure C-24.	Sea state degradation when $V=10\text{kts}$ , $l/L=0.1$ and Sea State 5.....	63
Figure C-25.	Sea state variation when $V=10\text{kts}$ , $l/L=0.1$ and Sea State 6.....	64
Figure C-26.	Sea state degradation when $V=10\text{kts}$ , $l/L=0.1$ and Sea State 6.....	64
Figure C-27.	Sea state variation when $V=10\text{kts}$ , $l/L=0.1$ and Sea State 7.....	65
Figure C-28.	Sea state degradation when $V=10\text{kts}$ , $l/L=0.1$ and Sea State 7.....	65
Figure C-29.	Sea state variation when $V=10\text{kts}$ , $l/L=0.5$ and Sea State 1.....	66
Figure C-30.	Sea state degradation when $V=10\text{kts}$ , $l/L=0.5$ and Sea State 1.....	66
Figure C-31.	Sea state variation when $V=10\text{kts}$ , $l/L=0.5$ and Sea State 2.....	67
Figure C-32.	Sea state degradation when $V=10\text{kts}$ , $l/L=0.5$ and Sea State 2.....	67
Figure C-33.	Sea state variation when $V=10\text{kts}$ , $l/L=0.5$ and Sea State 3.....	68
Figure C-34.	Sea state degradation when $V=10\text{kts}$ , $l/L=0.5$ and Sea State 3.....	68
Figure C-35.	Sea state variation when $V=10\text{kts}$ , $l/L=0.5$ and Sea State 4.....	69
Figure C-36.	Sea state degradation when $V=10\text{kts}$ , $l/L=0.5$ and Sea State 4.....	69
Figure C-37.	Sea state variation when $V=10\text{kts}$ , $l/L=0.5$ and Sea State 5.....	70
Figure C-38.	Sea state degradation when $V=10\text{kts}$ , $l/L=0.5$ and Sea State 5.....	70
Figure C-39.	Sea state variation when $V=10\text{kts}$ , $l/L=0.5$ and Sea State 6.....	71
Figure C-40.	Sea state degradation when $V=10\text{kts}$ , $l/L=0.5$ and Sea State 6.....	71
Figure C-41.	Sea state variation when $V=10\text{kts}$ , $l/L=0.5$ and Sea State 7.....	72
Figure C-42.	Sea state degradation when $V=10\text{kts}$ , $l/L=0.5$ and Sea State 7.....	72
Figure C-43.	Sea state variation when $V=10\text{kts}$ , $l/L=1$ and Sea State 1.....	73
Figure C-44.	Sea state degradation when $V=10\text{kts}$ , $l/L=1$ and Sea State 1.....	73
Figure C-45.	Sea state variation when $V=10\text{kts}$ , $l/L=1$ and Sea State 2.....	74
Figure C-46.	Sea state degradation when $V=10\text{kts}$ , $l/L=1$ and Sea State 2.....	74
Figure C-47.	Sea state variation when $V=10\text{kts}$ , $l/L=1$ and Sea State 3.....	75
Figure C-48.	Sea state degradation when $V=10\text{kts}$ , $l/L=1$ and Sea State 3.....	75
Figure C-49.	Sea state variation when $V=10\text{kts}$ , $l/L=1$ and Sea State 4.....	76
Figure C-50.	Sea state degradation when $V=10\text{kts}$ , $l/L=1$ and Sea State 4.....	76
Figure C-51.	Sea state variation when $V=10\text{kts}$ , $l/L=1$ and Sea State 5.....	77
Figure C-52.	Sea state degradation when $V=10\text{kts}$ , $l/L=1$ and Sea State 5.....	77
Figure C-53.	Sea state variation when $V=10\text{kts}$ , $l/L=1$ and Sea State 6.....	78
Figure C-54.	Sea state degradation when $V=10\text{kts}$ , $l/L=1$ and Sea State 6.....	78
Figure C-55.	Sea state variation when $V=10\text{kts}$ , $l/L=1$ and Sea State 7.....	79
Figure C-56.	Sea state degradation when $V=10\text{kts}$ , $l/L=1$ and Sea State 7.....	79

THIS PAGE INTENTIONALLY LEFT BLANK

## LIST OF TABLES

Table 1.	Significant Wave Height.....	15
----------	------------------------------	----

THIS PAGE INTENTIONALLY LEFT BLANK

# **I. INTRODUCTION**

## **A. MOTIVATION**

Close proximity towing of surface ships is a matter of interest to the U.S. Navy and the Office of Naval Research. Several possible applications have been suggested including the SLICE/KAIMALINO connection (Nash) and the SEA LANCE configuration (TSSE). Advantages of ship towing are cost effectiveness when towing large expensive loads with a denser vehicle and being able to tow various kinds of platforms to carry various kinds of loads (Nash). One of the problems that need to be overcome is the evaluation of motions of the two ships when in close proximity towing operations. This thesis addresses this problem, and suggests a possible design methodology.

## **B. PREVIOUS WORK**

Nash utilized strip theory calculations (Beck and Troesch) in order to develop the coupled heave/pitch equations of motion of the two ships. A brief discussion on strip theory is available in “Principles of Naval Architecture, Volume III, Chapter VIII, Section 3.4.” The matching condition that was used was that of a generic spring/damper connector. In this thesis, we want to utilize a more realistic matching condition based on the speed/resistance profile of the ships. In order to avoid the excessive computational burden of fully coupled hydrodynamic and structural analyses (Korsmeyer and Kring), we wish to develop a simpler design procedure that can be effectively utilized in design. This procedure could be applied in cases where only the operational envelopes of the ships are known, and not necessarily their individual hydrodynamic properties.

THIS PAGE INTENTIONALLY LEFT BLANK

## II. REGULAR WAVES RESPONSE

Beck and Reed describe ship seakeeping as one of the most challenging problems in the marine hydrodynamics field. The complexities of wave resistance, maneuvering problems and unsteadiness due to incident waves as well as some of the nonlinearities associated with free surface problems, coupled with the need for easy implementation in a design environment, contribute to the challenges we face in seakeeping assessment.

In our study, we assumed that the water is incompressible, the density is constant and the flow is irrotational. These are standard assumptions in seakeeping studies. We also assumed that the ships operate in infinitely deep water.

In this chapter, the waves that the ships are encountering are assumed to be regular waves. This motion of waves is two dimensional, sinusoidal in time with radian frequency  $\omega$ . The wave propagates with velocity  $V$  such that, to an observer moving with this velocity, the waves appears as steady-state (Newman). Wave surface elevation can then be defined as

$$\eta(x,t) = \cos(kx - \omega t) \quad (1)$$

where the parameter  $k = \omega/V$ , which is called the wave number, the number of waves per unit distance along the  $x$ -axis. Clearly,  $k = 2\pi/\lambda$ , where the wavelength  $\lambda$  is the distance between two points on the wave with the same phase. For infinitely deep water, the dispersion relation states that  $k = \omega^2/g$  (Newman).

The frequency of the wave encounter by the ship is defined as

$$\omega_e = \omega + Vk \cos \beta \quad (2)$$

where  $\beta$  is the relative wave heading and  $V$  becomes the ship speed relative to water (McCreight).

We can derive the equations of motion for free oscillations of a rigid body moving in sea. Motion of that body can be described in six degrees of freedom system. Three translational (surge, sway, and yaw), and three rotational (roll, pitch, and yaw) motions

are required for this system. Figure 1 illustrates these motions and the standard sign convention used in seakeeping calculations.

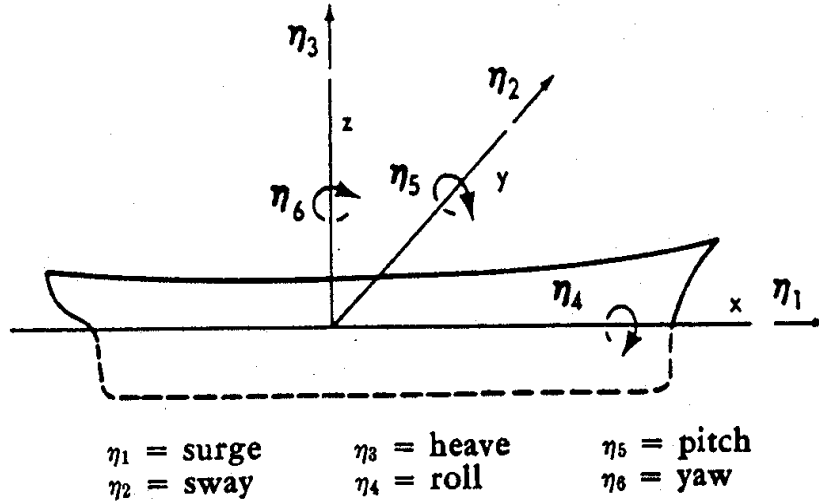


Figure 1. Sign Convention for Ship Motions (From: Beck)

From Newton's second law of motion, a translational displacement is defined as

$$\Delta \ddot{\eta} = F \quad (3)$$

where  $\Delta$  is the apparent displacement of the body and  $F$  is the total force acting on the body. For rotational motion we have

$$I \ddot{\eta} = F \quad (4)$$

where  $I$  is the mass moment of inertia about that axis and  $F$  is the total moment acting on the body.

For the simplified case, the total force and moment consist mainly of hydrostatic and hydrodynamic forces

$$F(t) = F_{\text{ex}}(t) + F_H(t) \quad (5)$$

where  $F_{\text{ex}}$  is the exciting force due to waves and  $F_H$  is the radiation force due to motion of the ship.

The exciting force can be defined in frequency domain as  $F_{ex}(t) = F_{ex} e^{i\omega_e t}$ .

For sinusoidal motions, the hydrodynamic radiation force and moment can be defined as

$$F_H = -[A(\omega)\ddot{\eta} + B(\omega)\dot{\eta} + C(\omega)\eta] \quad (6)$$

where A is the added mass, B is the hydrodynamic damping, and C is the restoring force or moment.

Since our equation is linear, it is usually carried out in the frequency domain for easier calculations. Now we can define the motion and its derivatives in the frequency domain as

$$\begin{aligned} \eta(t) &= \bar{\eta} e^{i\omega_e t} \\ \dot{\eta}(t) &= i\omega_e \bar{\eta} e^{i\omega_e t} \\ \ddot{\eta}(t) &= -\omega_e^2 \bar{\eta} e^{i\omega_e t} \end{aligned}$$

Like a two degrees of freedom system, we can write our equation of motion as

$$[-\omega_e^2(\Delta + A) + i\omega_e B + C]\bar{\eta} = F_{ex} \quad (7)$$

where  $(\Delta + A)$ , B and C are the mass, damping and stiffness matrices respectively.

For six degrees of freedom system, this equation has to be defined for six different motions.

Now, let's define the equations of motions for a point on SLICE and a point on KAIMALINO.

$$\begin{aligned} [\Delta_S + A_S]\{\ddot{\eta}\} + [B_S]\{\dot{\eta}\} + [C_S]\{\eta\} &= \{F_{ex}\} + \{f_S\} \\ [\Delta_K + A_K]\{\ddot{\eta}\} + [B_K]\{\dot{\eta}\} + [C_K]\{\eta\} &= \{F_{ex}\} + \{f_K\} \end{aligned} \quad (8)$$

where  $f_S$  and  $f_K$  are the connection forces acting on SLICE and KAIMALINO respectively, where  $f_K = -f_S$ . The connection force and motions are illustrated in Figure 2.

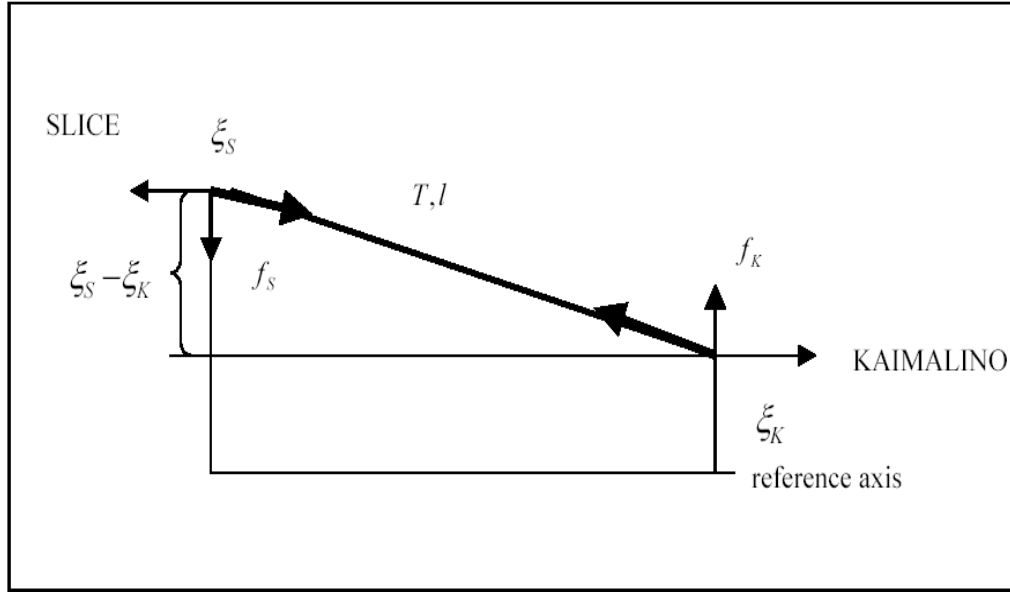


Figure 2. Connection Force and Motions of the Ships

As the derivation procedure is the same for both equations, let's work on a generic one. When we define the equations in the frequency domain,

$$[-\omega_e^2(\Delta + A) + i\omega_e B + C]\{\bar{\eta}\} = \{F_{ex}\} + \{f\}. \quad (9)$$

Since the exponential exists in all terms, it is canceled and the equations of motion in the frequency domain become as follows. Let's define

$$\bar{A} = [-\omega_e^2(\Delta + A) + i\omega_e B + C].$$

We know that  $\bar{A}$  is a 6x6 matrix for six degrees of freedom system.

$$\bar{A}\bar{\eta} = \{F\}$$

$$\bar{\eta} = \text{inv}(\bar{A})\{F\} \quad (10)$$

where  $\{F\} = \{F_{ex}\} + \{f\}$ .

Ship motions due to regular waves of a given wavelength and direction are now determined for a given forward speed ( $V$ ). Motions in vertical and horizontal planes are

usually considered as decoupled and may be solved as two distinct 3x3 systems vice the 6x6 system. We performed our studies on the vertical plane response of the ships. Therefore, only heave and pitch responses and the resultant interactions between SLICE and KAIMALINO in these three degrees of freedom will be analyzed from this point forward. Hence, all motions except  $\eta_3$  and  $\eta_5$  are set to zero. The expanded equations of motion in two degrees of freedom become as

$$\begin{array}{l} \text{heave} - \\ \text{pitch} - \end{array} \left[ \begin{array}{cc} \bar{A}_{33} & \bar{A}_{35} \\ \bar{A}_{53} & \bar{A}_{55} \end{array} \right] \begin{bmatrix} \eta_3 \\ \eta_5 \end{bmatrix} = \begin{bmatrix} F_3 + f \\ F_5 + f x_s \end{bmatrix}. \quad (11)$$

Now we can define the equations of motion in vertical plane (but in two degrees of freedom) for two vehicles as

$$\begin{aligned} \bar{A}_{33,s} \bar{\eta}_{3,S} + \bar{A}_{35,s} \bar{\eta}_{5,S} &= F_{3,S} + f_S \\ \bar{A}_{53,s} \bar{\eta}_{3,S} + \bar{A}_{55,s} \bar{\eta}_{5,S} &= F_{5,S} - f_S x_S \\ \bar{A}_{33,K} \bar{\eta}_{3,K} + \bar{A}_{35,K} \bar{\eta}_{5,K} &= F_{3,K} + f_K \\ \bar{A}_{53,K} \bar{\eta}_{3,K} + \bar{A}_{55,K} \bar{\eta}_{5,K} &= F_{5,K} - f_S x_K \end{aligned} \quad (12)$$

where  $x$  is the distance between the connection point and the center of gravity of that vehicle.

In order to solve these four equations, we make the following substitution.

$$\begin{aligned} \bar{\eta}_{3,S} &= \mu_{3,S} + \nu_{3,S} f_S \\ \bar{\eta}_{5,S} &= \mu_{5,S} + \nu_{5,S} f_S \\ \bar{\eta}_{3,K} &= \mu_{3,K} + \nu_{3,K} f_K \\ \bar{\eta}_{5,K} &= \mu_{5,K} + \nu_{5,K} f_K \end{aligned} \quad (13)$$

where  $f_S = -f_K = -f$ .

Referring to Figure 2, we can form the absolute motion at the connection points as

$$\begin{aligned}\xi_S &= \bar{\eta}_{3,S} - \bar{\eta}_{5,S}x_S \\ \xi_K &= \bar{\eta}_{3,K} - \bar{\eta}_{5,K}x_K\end{aligned}\quad (14)$$

When we combine (13) and (14) as

$$\begin{aligned}\xi_S &= \mu_{3,S} - \nu_{3,S}f - \mu_{5,S}x_S + \nu_{5,S}x_Sf \\ \xi_K &= \mu_{3,K} + \nu_{3,K}f - \mu_{5,K}x_K - \nu_{5,K}x_Kf\end{aligned}\quad (15)$$

Let  $a$  in terms of  $\mu$ 's and  $b$  in terms of  $\nu$ 's be defined as

$$\begin{aligned}a &= \mu_{3,S} - \mu_{3,K} + \mu_{5,K}x_K - \mu_{5,S}x_S \\ b &= -\nu_{3,S} - \nu_{3,K} + \nu_{5,K}x_K + \nu_{5,S}x_S\end{aligned}\quad (16)$$

Therefore, our equation becomes as

$$\xi_S - \xi_K = a - bf. \quad (17)$$

Again referring to Figure 2,

$$f = T \frac{\xi_S - \xi_K}{l}. \quad (18)$$

Combining (17) and (18) gives us our final equation, which gives us the connection force between two ships becomes as

$$f = \frac{a}{\frac{l}{T} + b}. \quad (19)$$

The tension at the connection is assumed to be the tension at steady state. It actually varies with the motions of the ships, but we assume that the influence of its variation on heave/pitch motions is of higher order and can be neglected. Figure 3 shows the tension curve we used in the calculations. This is a curve fit of actual experimental data for the trailing ship, the KAIMALINO. It is of course valid only for the range of speeds shown in the Figure.

The conditions of the regular waves are chosen to be varying speed, heading and towline length. Typical results are presented in Appendix A, Figures A-1 through A-15.

In all figures, motions are dimensionless with respect to a unit wave height, while forces are dimensionless with respect to earth's gravitational constant, ship length, water density, and area, as

$$F_{\text{dimensionless}} = \frac{F}{\rho g A L^2} \quad (20)$$

where  $\rho = 1.9905 \text{ lb/ft}^3$ ,  $g = 32.2 \text{ ft/sec}^2$ ,  $L = 105 \text{ ft}$  and  $A = 1 \text{ ft}^2$ .

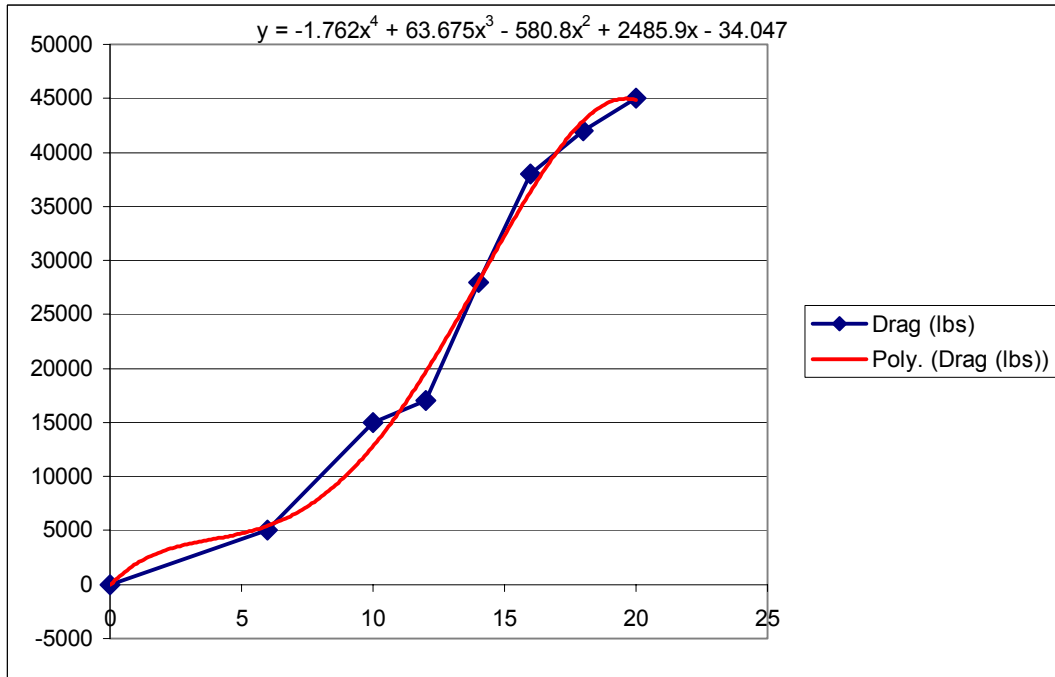


Figure 3. Tension

For consistency, the leading ship (SLICE) length was used as the reference length (105 ft) in the non-dimensionalization of the results. Zero heading corresponds to following seas, while head seas correspond to 180 degrees.

The figures of the motions of the ships show us that when the ships are in tow, they move virtually together at the corresponding connection points. This becomes progressively more accurate as the towline length is reduced. This proves the accuracy of the codes generated.

Based on the results presented in Appendix. A, we can draw the following conclusions.

1. The magnitude of the connection force is of similar order as the magnitude of the wave exciting forces. Therefore, its effect cannot be neglected, and in fact it will influence the resulting motions as much as the exciting waves.
2. The connection force becomes smaller for larger towline lengths as expected.
3. Ship motions at the connection points are closely matched for small towline lengths, while we observe some variation for larger towline lengths. This is consistent with physical intuition.
4. The dependence of the connection force on forward speed is not monotonic. Even though there is a large variation, no significant trend is evident. A similar conclusion holds for ship motions in terms of forward speeds.

### III. RANDOM WAVES RESPONSE

We assumed that the waves were regular waves in Chapter II. If an observer tries to observe the waves encountering his, or her, observation point, it is not difficult to see that waves in real life are random both in space and in time. Hence, it is really difficult to model ocean wave behavior. In addition to this, waves show different characteristics in different regions of the world.

If our observer keeps a record (primarily wave height and period) of the waves for that particular point, and sums those regular waves, a wave system for that point and for that particular time is gained. We call a seaway's "spectrum" as the probabilistic function developed by taking the Fourier transform of the correlation function for free surface elevation (Nash). The correlation factor contains the data our observer recorded. The spectrum  $S(\omega)$  is a measure of the energy contained within a wave system. Figure 5 shows a typical wave spectrum and the algebraic addition of the waves. The area under

the curve represents the mean energy stored in a particular wave system,  $\bar{E} = \int_0^{\infty} S(\omega) d\omega$  (Cummins).

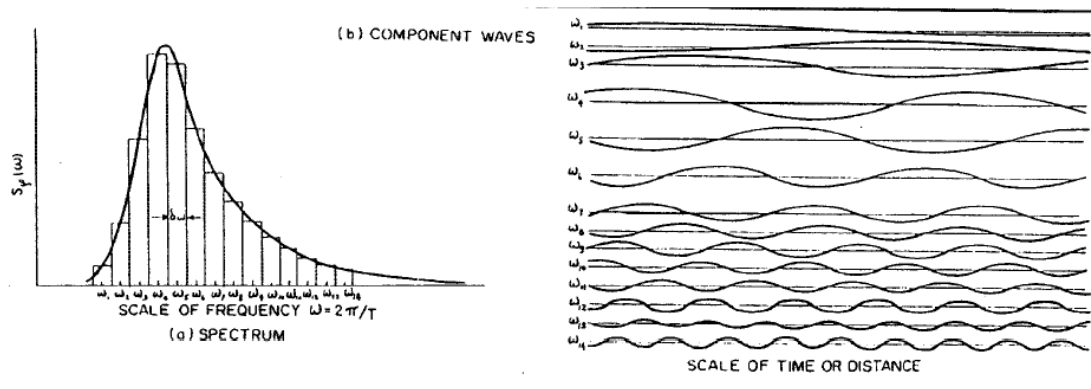


Figure 4. Wave Spectrum and Addition of Waves (From: Cummins)

There are several spectra that are used in random wave computations to compute the ship's response. In our case, the Pierson-Moskowitz spectrum is chosen as a representative spectrum. This two-parameter model predicts the wave spectrum for fully

developed, long crested seas with no swell from other generating areas. Fully developed seas contain waves at equilibrium, independent of fetch and duration of wind. Long crested seas have parallel crests and are assumed to be unidirectional.

The Pierson-Moskowitz spectrum is described by

$$S(\omega) = \frac{\alpha g^2}{\omega^5} \exp[-\beta(g/V_w)^4]. \quad (21)$$

where  $g$  is acceleration of gravity [ $\text{cm}/\text{sec}^2$ ],  $\omega$  is wave frequency [radians/sec],  $\alpha$  is  $8.10 \times 10^{-3}$ ,  $\beta$  is 0.74 and  $V_w$  is wind speed [ $\text{cm}/\text{sec}$ ] at 19.5 m above the surface.

Another parameter considered in random wave calculations is the significant wave height  $H_{1/3}$ , which is the average of the highest one third of all the waves (Newman). Using an empirical relationship between wind speed and significant wave height,  $H_{1/3} = 2 \frac{V_w^2}{g} \left( \frac{\alpha}{\beta} \right)^{0.5}$ , the Pierson-Moskowitz spectrum now becomes a function of significant wave height as

$$S(\omega) = \frac{8.1 \times 10^{-3}}{\omega^5} \exp \left[ \frac{-0.032 \left( \frac{g}{H_{1/3}} \right)^2}{\omega^4} \right]. \quad (22)$$

Also known as the motion transfer function, the response amplitude operator (RAO) maps the complex response of a vessel to a seaway or input spectrum as a function of frequency. The spectrum of the particular response that the RAO has been computed for is calculated from:

$$S_R(\omega) = |RAO(\omega)|^2 S(\omega). \quad (23)$$

In this equation,  $S_R(\omega)$  is the response of the vessel to the input sea spectrum for a given frequency. Ship response then can be calculated for a given wave frequency and significant wave height. For example, the complex absolute motions predicted in regular wave modeling ( $\xi_s, \xi_k$ ) are converted into RAO's for absolute motion as

$$RAO(\xi_{s,k}) = abs(\xi_{s,k}). \quad (24)$$

The response spectrum for absolute motion then becomes as

$$S_{R-\xi_{s,k}}(\omega) = |abs(\xi_{s,k})|^2 S(\omega). \quad (25)$$

For our case, the connection force response can be defined as

$$S_{R-f_{connection}}(\omega) = |abs(f_{connection})|^2 S(\omega). \quad (26)$$

One way to predict a measure of performance over a range of frequencies is by calculating the significant double amplitude of the response. Double amplitudes are obtained by integrating the response with respect to frequency over the frequency range of any input spectrum. For our case, the significant double amplitude of the absolute motion of SLICE at the connection point is  $\sigma_{\xi_s} = \int_{\omega_0}^{\omega_f} S_{R-\xi_s}(\omega) d\omega$ . Now we can make more accurate calculations to make a better design with random wave response.

Different conditions with respect to speed, heading, towing length and significant wave height are chosen for the results. Appendix B., figures B-1 through B-40, shows typical results for these conditions. As in chapter II, all results are non-dimensionalized as shown in equation (20) and the related paragraph. In some cases, designated by f/F3 the connection force is further normalized with respect to the heave wave exciting force.

The results are in root mean square (RMS) form. This is very convenient for further calculations. Multiplying the RMS value by two gives us the significant wave amplitude, which is the average of the highest one third of the amplitudes of the response. Also, multiplying the RMS value by four gives us the eight-hour maximum value, which can be used as design extreme amplitude of the response.

Based on the results presented in Appendix B., we can draw the following conclusions:

1. Connection forces are higher in higher sea states as expected. Head seas produce the highest values of connection forces.

2. Relatively (with regards to wave exciting forces) high values of the connection force exist in headings other than head seas. This may be significant in operations, since even though the actual value of the connection force may be “small” it may be considerably higher than the wave exciting force and may, therefore, significantly limit the operability window of the ships. This item is further addressed in the next chapter.
3. The connection forces are not a monotonic function of the towline length, as Figure B-16 demonstrates. Therefore, it is possible to select a towline length so that the connection force is minimized.
4. In general, higher forward speeds will generate higher RMS values for the connection force, although again the trend is not monotonic. As Figure B-36 shows, it is possible to select a forward speed so that the connection force is minimum.

## IV. SEAKEEPING EVALUATIONS

Pierson and Moscowitz's sea state table is used to obtain the significant wave heights. The mean wave heights, used as the representative significant wave heights in MATLAB computations for different sea states, are shown in Table 1.

SEA STATE	MIN.WAVE HEIGHT	MAX. WAVE HEIGHT	MEAN WAVE HEIGHT
1	0.50	1.20	0.85
2	1.50	3.00	2.25
3	3.50	5.00	4.25
4	6.00	7.50	6.75
5	8.00	12.00	10.00
6	14.00	20.00	17.00
7	25.00	40.00	32.50

Table 1. Significant Wave Heights

Having obtained all the necessary responses in a seaway, we want to introduce a performance degradation factor to be used in design. The question we have to ask ourselves is: If a ship can operate in some condition (speed, heading, sea state) without towing, at what condition can she operate at undertow? The approach we select is to fix the speed and for each heading, calculate the "equivalent" sea state. This equivalent sea state is defined on the basis of heave and connection exciting forces. We call two sea states as "equivalent" for our analysis, if they produce the same total vertical force on the ship. This will be the heave exciting force for the condition without towing, and the sum of the heave exciting force plus the vertical connection force for the condition with towing. Both values are in terms of their RMS. The fact that we use their algebraic sum designates an envisioned worst-case scenario where the phase angles of the two sets of forces are the same.

The results are presented in Appendix C., figures C-1 through C-56. The sea state variation legend in these figures indicates the equivalent sea state (outer envelope) for the ships under towing while the inner curve is the corresponding sea state without towing. The sea state degradation legend in the figures is the one that can be used more directly in design. It maps a given sea state condition (outer envelope) into an equivalent less severity sea state condition under towing (inner envelope). This new sea state, together with the vertical connection force, will match the severity of the initial sea state without towing. Therefore, we can use these results to map an existing operability envelope of a ship without towing to an equivalent operability envelope of the ships under towing. A notional example of such an operability envelope is shown in Figure 5. The triangular area shown in the figure has been mapped to the dark area shown. Using this procedure, we can map any existing operability area of the ships between free running and towing conditions.

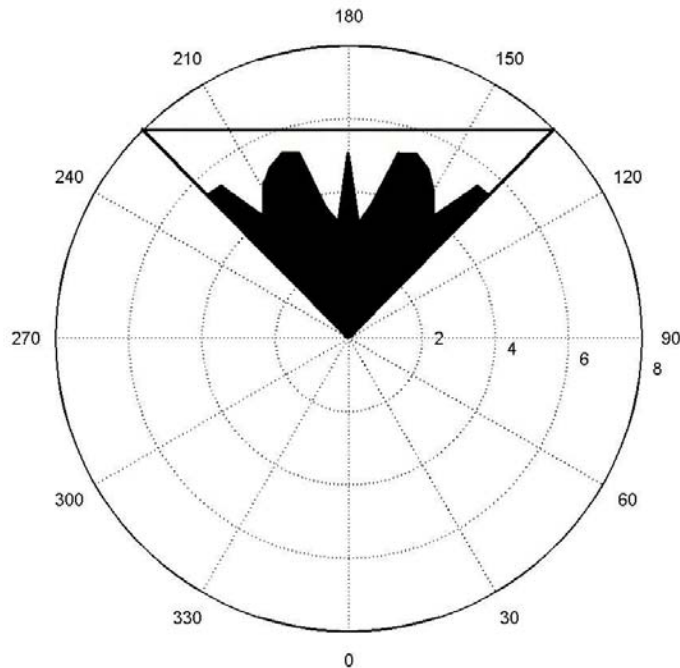


Figure 5. A Notional Ship Operability Envelope Mapping.

## **V. CONCLUSIONS AND RECOMMENDATIONS**

### **A. CONCLUSIONS**

The main conclusions from this work can be summarized as follows:

1. Connection forces under tow are comparable in magnitude to wave (heave) exciting forces.
2. The developed sea state degradation factor may be a viable solution to assessing ship operability envelopes under tow.
3. The developed procedure can be used to maximize the expected operability envelope in a combination of sea states.

### **B. RECOMMENDATIONS**

As recommendations for further research, we suggest the following:

1. What is the effect of tension variations on vertical plane motions? The main assumption that needs to be tested is whether such variations produce higher order effects as we assumed in this thesis.
2. Is there a significant coupling between vertical and horizontal plane motions when the two ships are under towing? In order to answer this we must first produce an estimate of the connection forces in sway.

THIS PAGE INTENTIONALLY LEFT BLANK

## **APPENDIX A. REGULAR WAVES RESULTS**

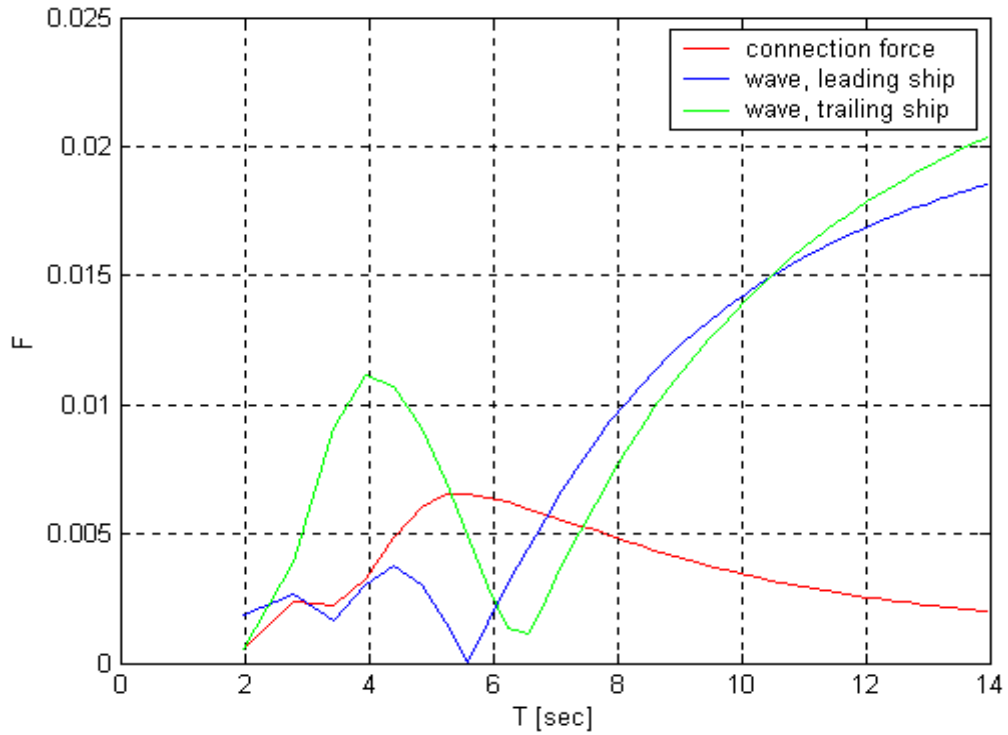


Figure A-1. Exciting Forces for  $V=10\text{kts}$ ,  $l/L=0.1$  and  $\beta=0^\circ$

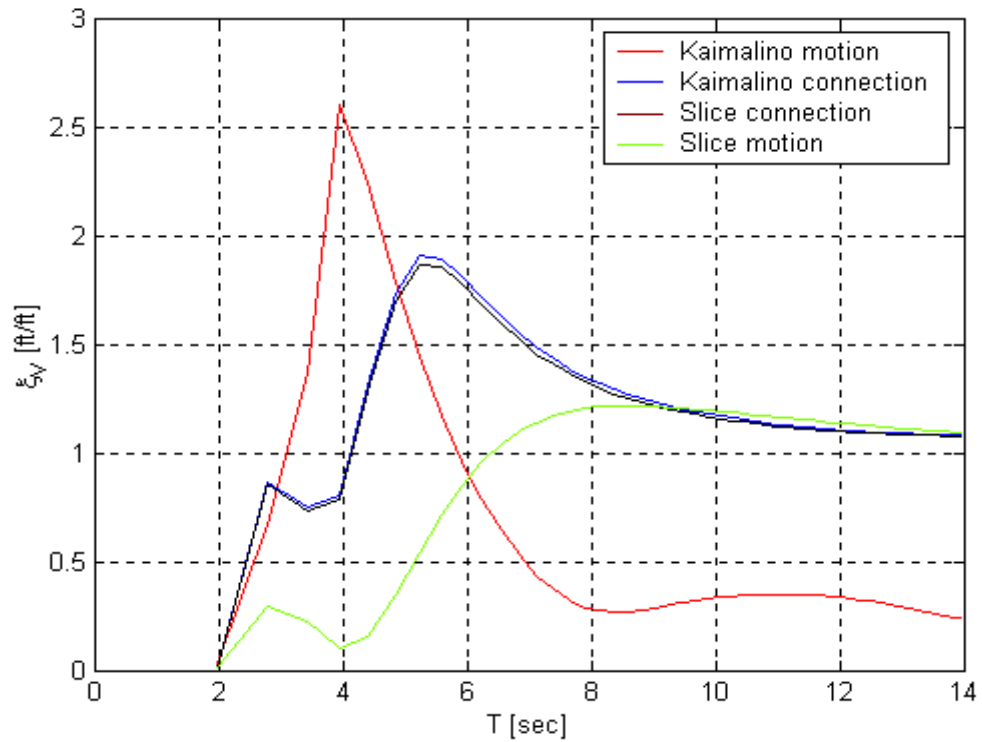


Figure A-2. Motions of the Ships for  $V=10\text{kts}$ ,  $l/L=0.1$  and  $\beta=0^\circ$

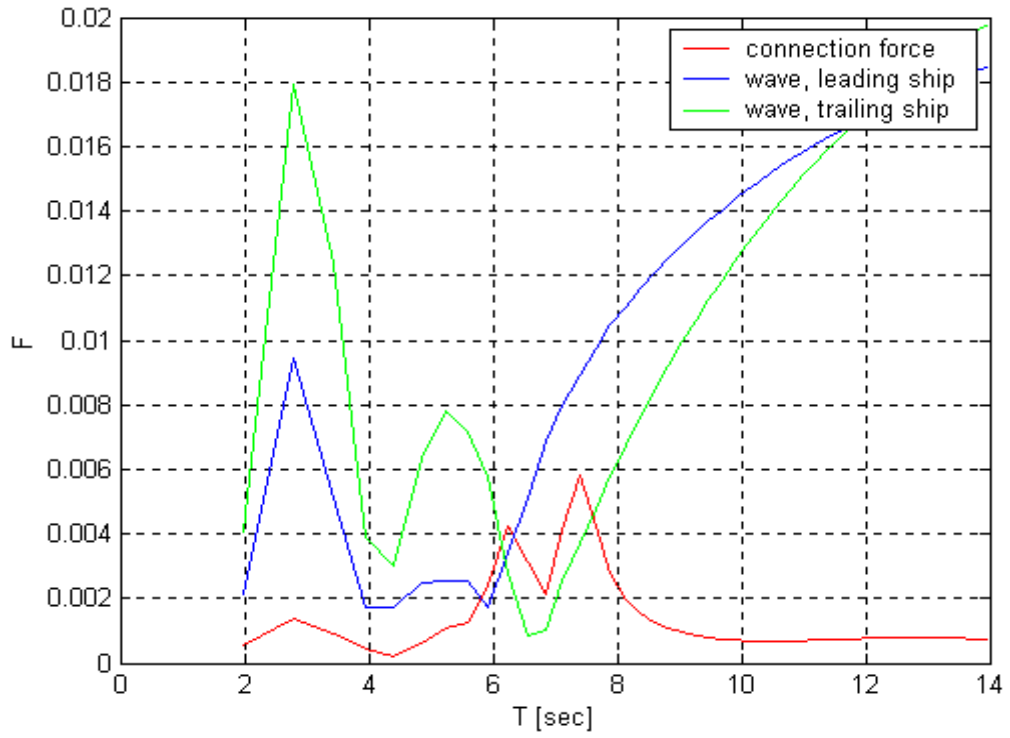


Figure A-3. Exciting Forces for  $V=10\text{kts}$ ,  $l/L=0.1$  and  $\beta=90^\circ$

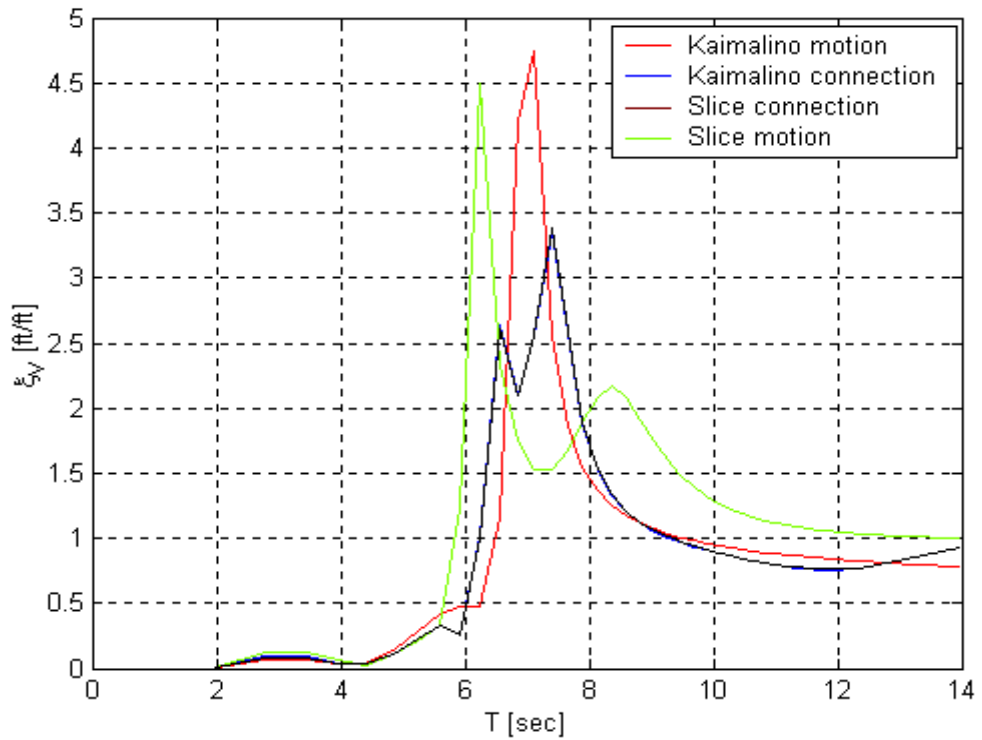


Figure A-4. Motions of the Ships for  $V=10\text{kts}$ ,  $l/L=0.1$  and  $\beta=90^\circ$

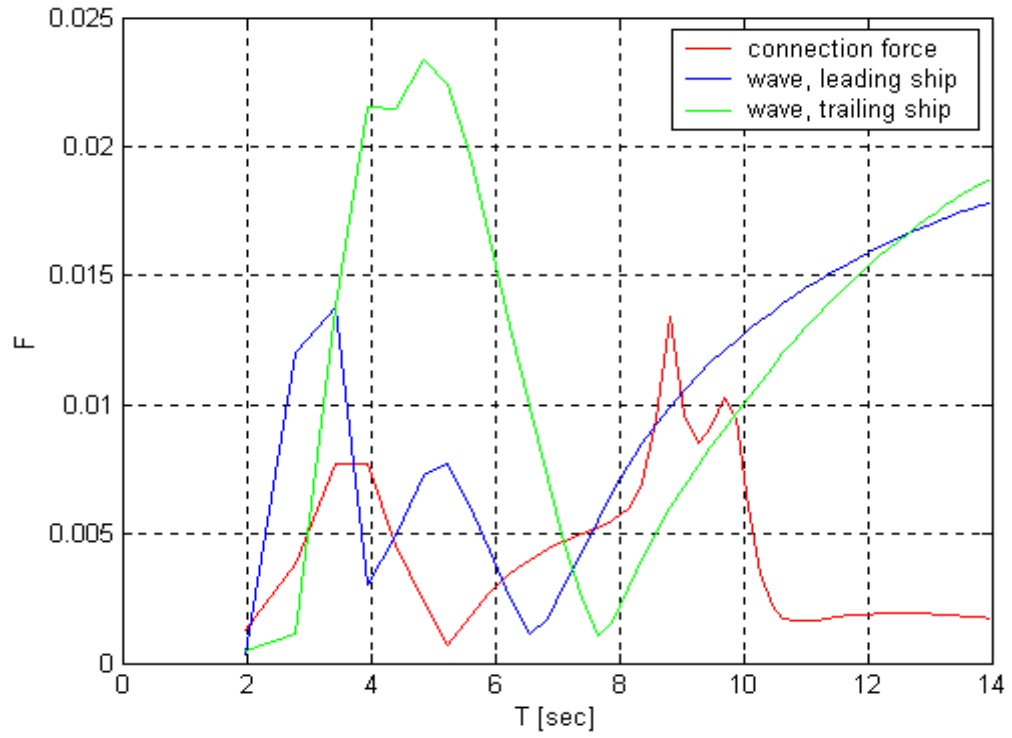


Figure A-5. Exciting Forces for  $V=10\text{kts}$ ,  $l/L=0.1$  and  $\beta=180^\circ$

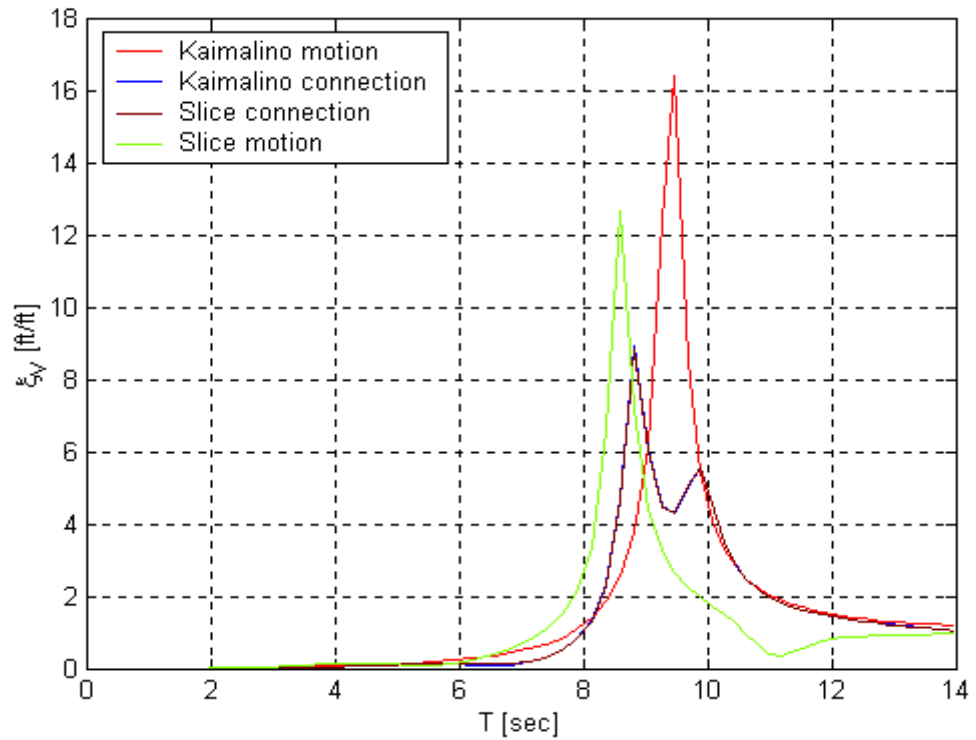


Figure A-6. Motions of the Ships for  $V=10\text{kts}$ ,  $l/L=0.1$  and  $\beta=180^\circ$

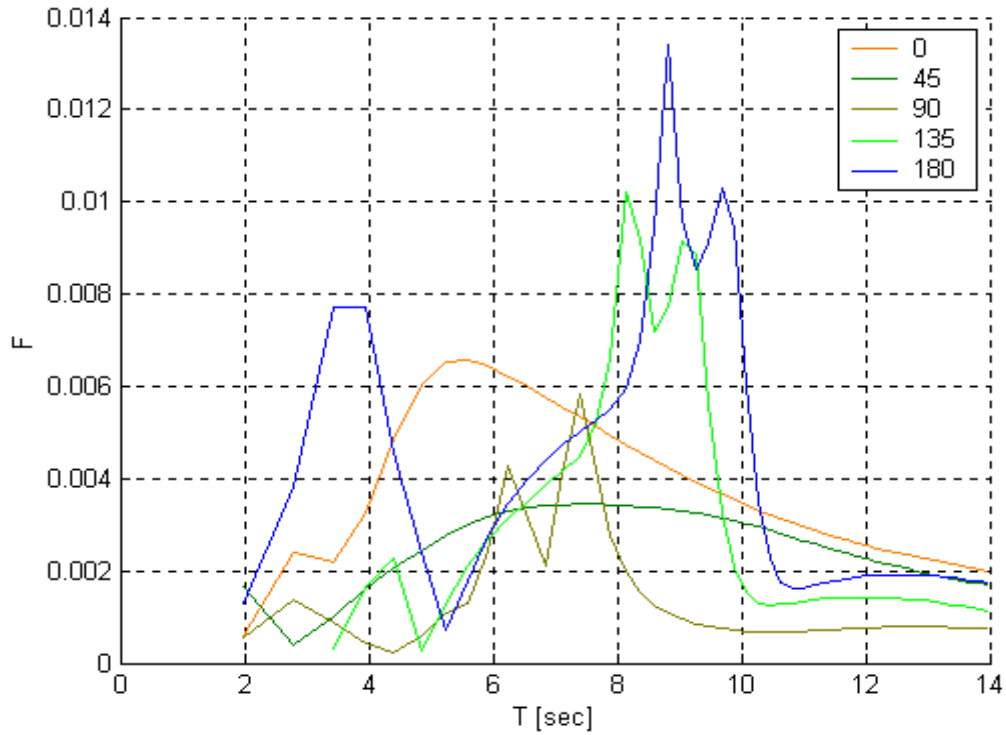


Figure A-7. Force Variation for Different Headings when V=10kts and l/L=0.1

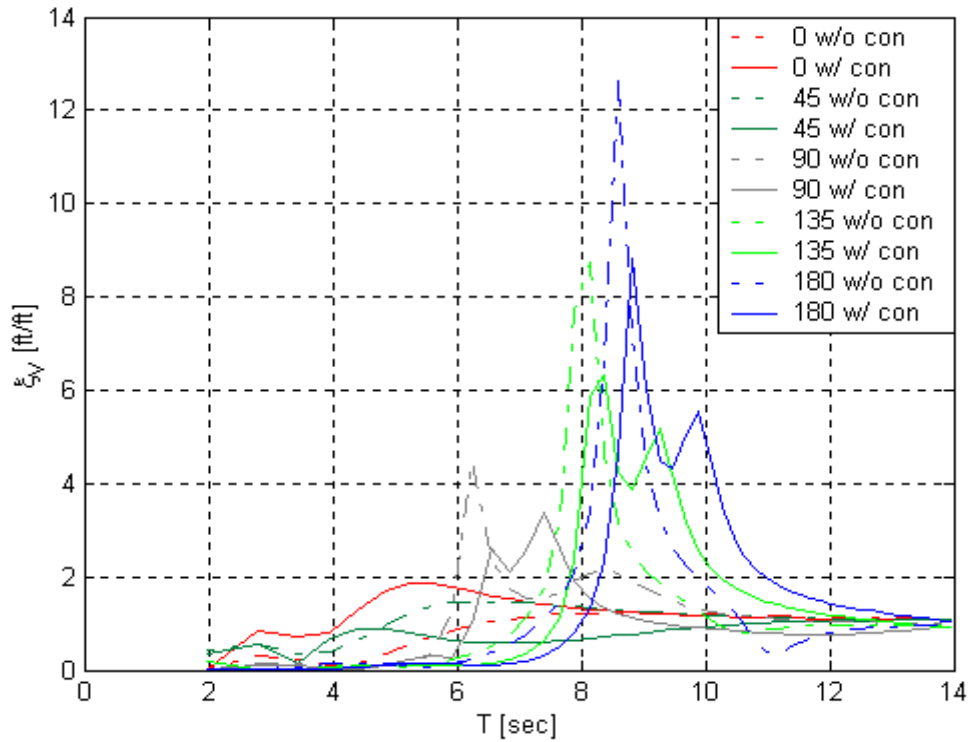


Figure A-8. SLICE Motion for Different Headings when V=10kts and l/L=0.1

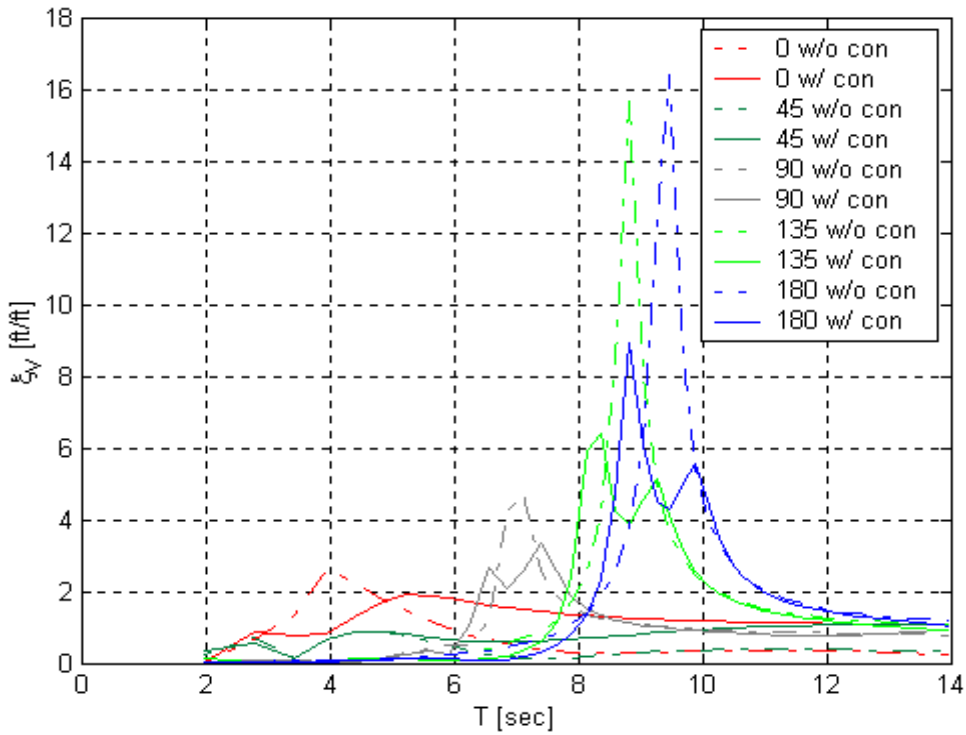


Figure A-9. KAIMALINO Motion for Different Headings when  $V=10$  kts and  $l/L=0.1$

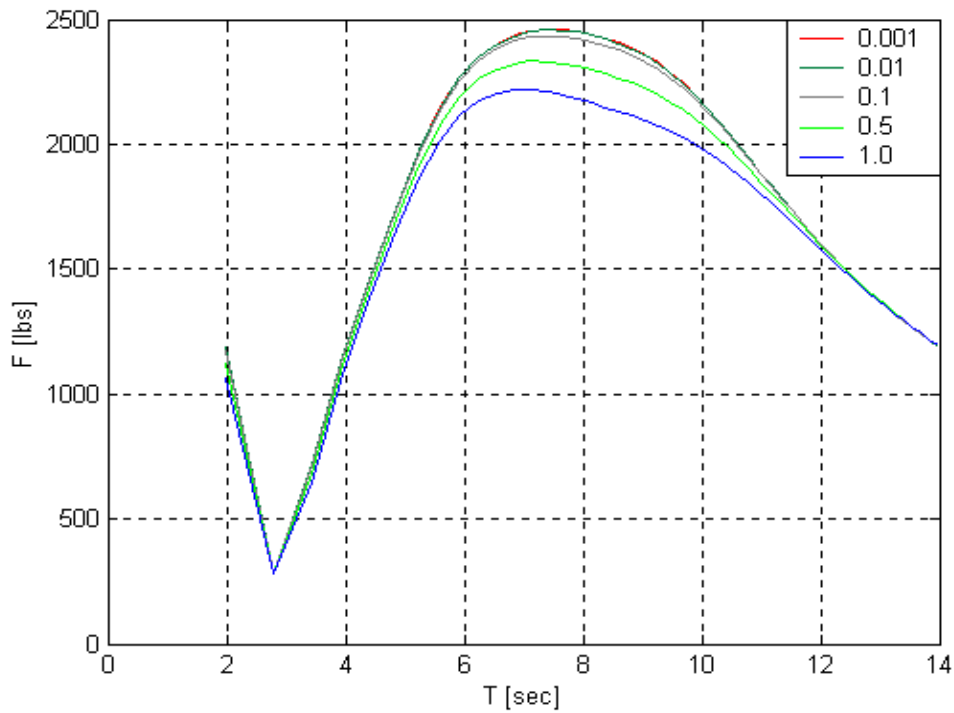


Figure A-10. Connection Force for Different Towing Lengths when  $V=10$  kts and  $\beta=45^\circ$

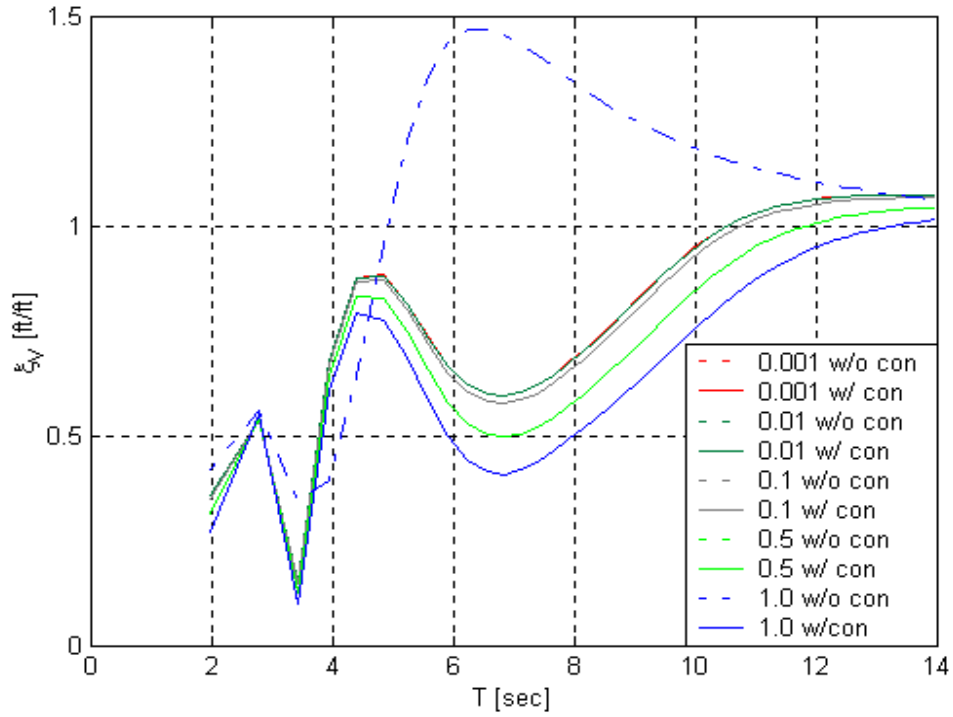


Figure A-11. SLICE Motion for Different Towing Lengths when  $V=10\text{kts}$  and  $\beta=45^\circ$

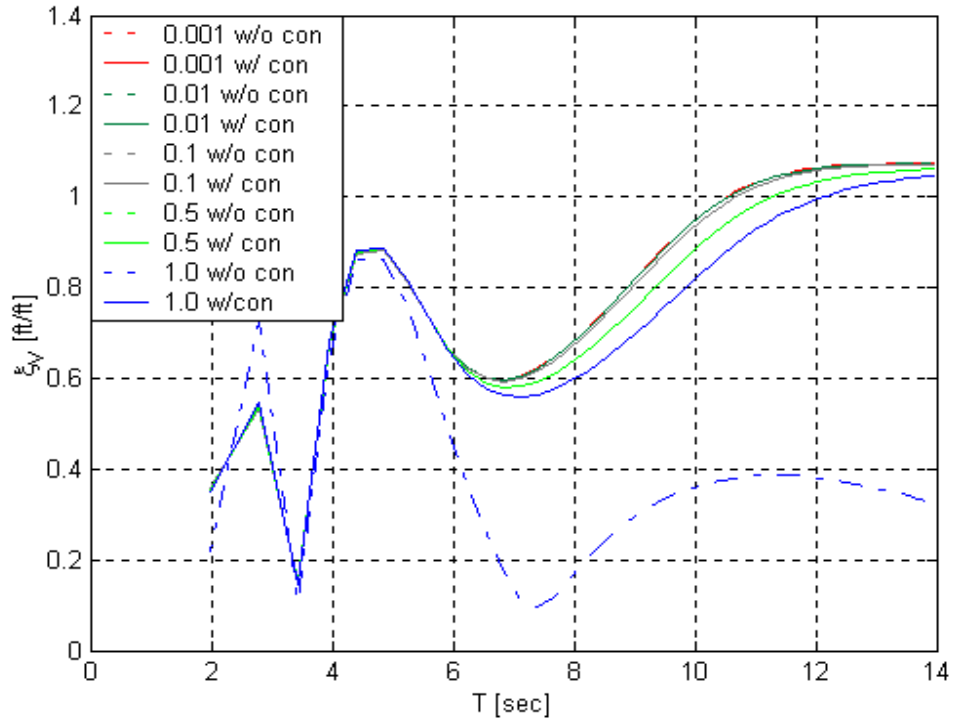


Figure A-12. KAIMALINO Motion for Different Towing Lengths when  $V=10\text{kts}$  and  $\beta=45^\circ$

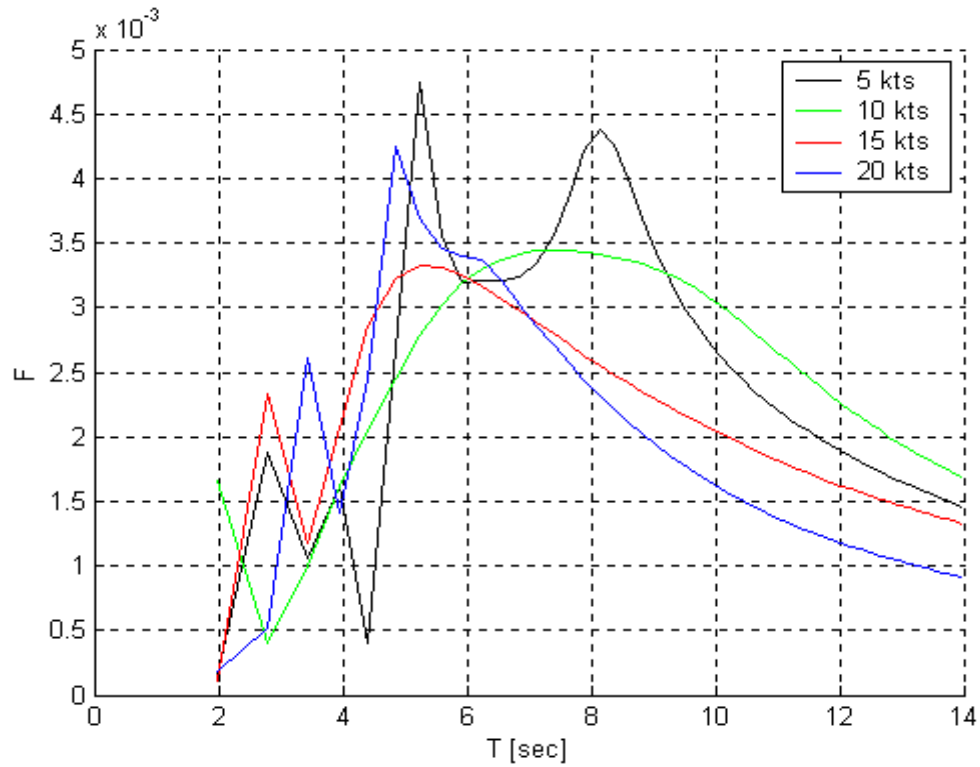


Figure A-13. Connection Forces for Different Ship Speeds when  $l/L=0.1$  and  $\beta=45^\circ$

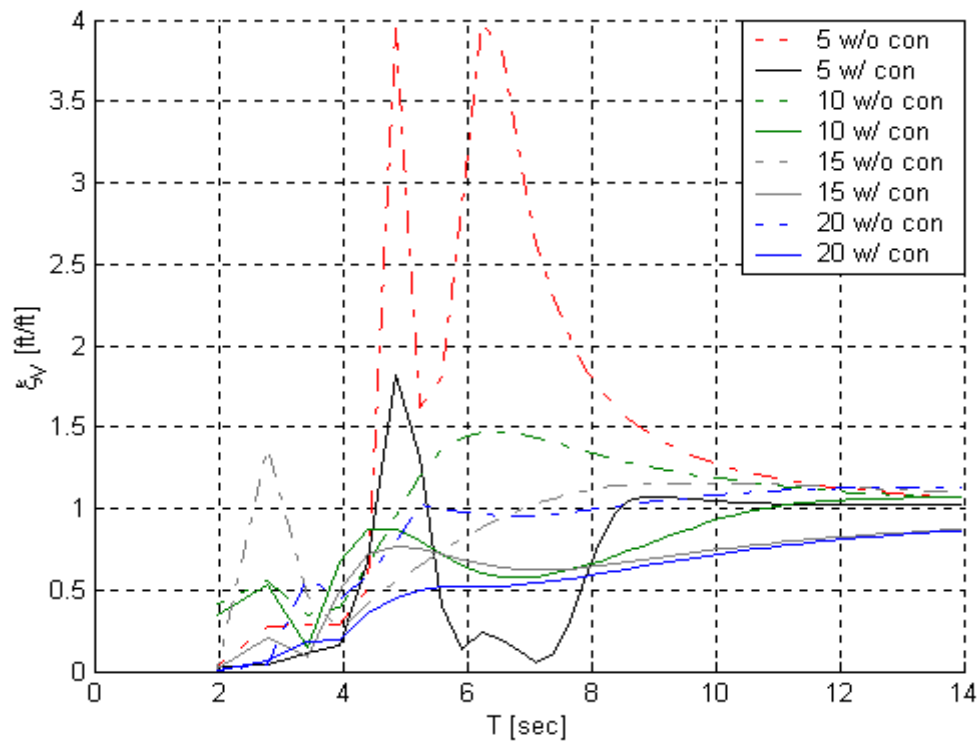


Figure A-14. SLICE Motion for Different Ship Speeds when  $l/L=0.1$  and  $\beta=45^\circ$

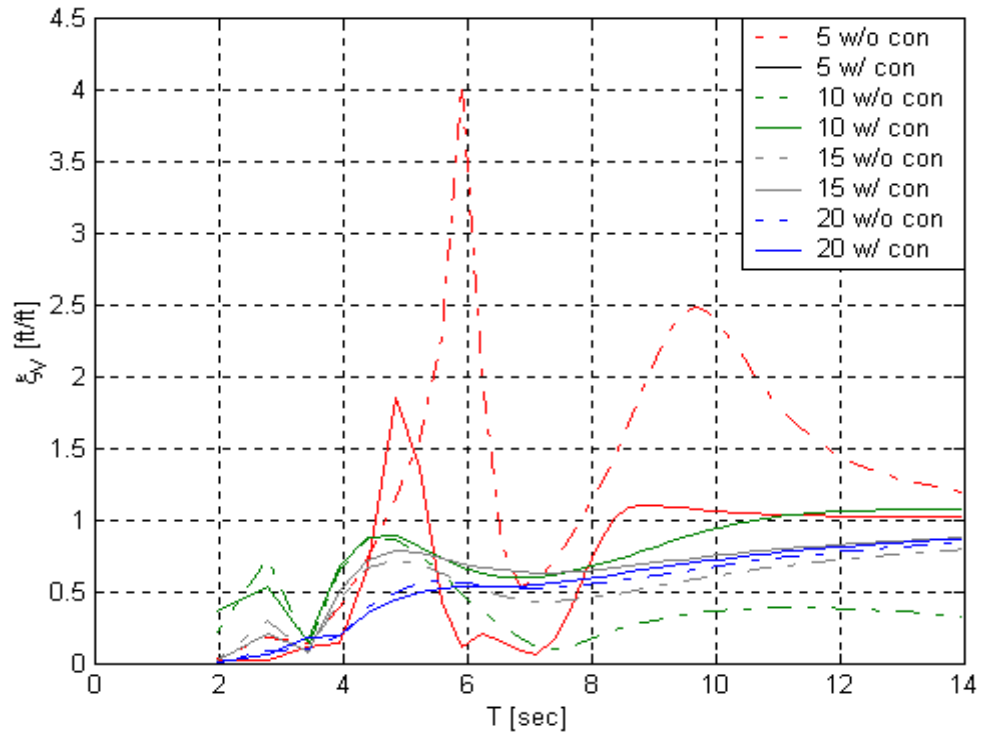


Figure A-15. KAIMALINO Motion for Different Ship Speeds when  $l/L=0.1$  and  $\beta=45^\circ$

THIS PAGE INTENTIONALLY LEFT BLANK

## **APPENDIX B. RANDOM WAVES RESULTS**

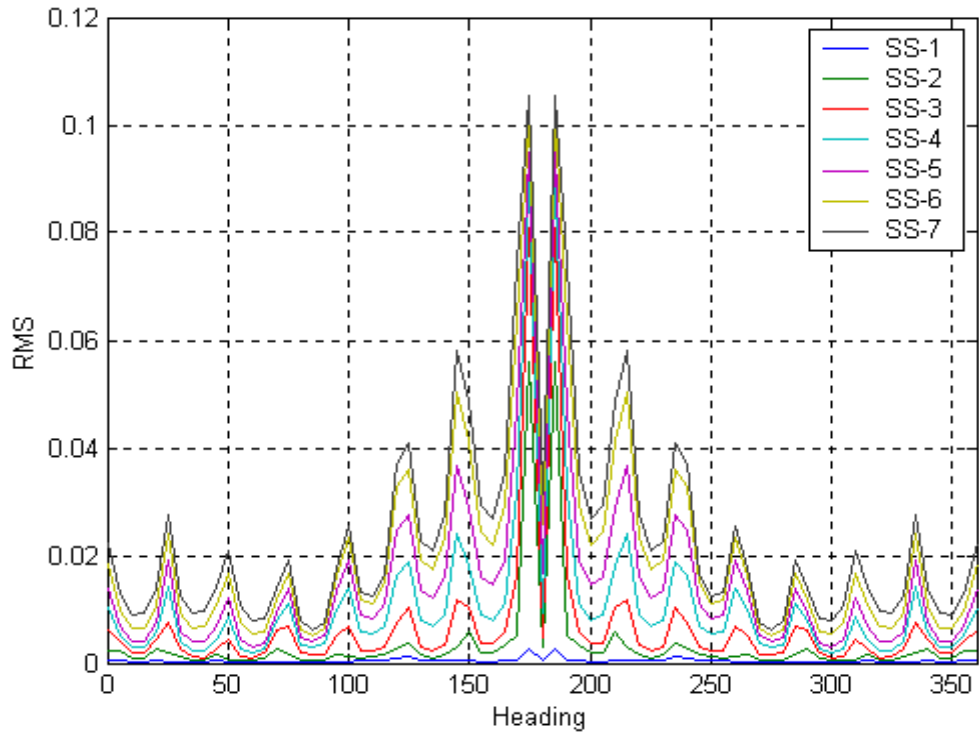


Figure B-1. RMS of Connection Force vs. Heading when  $V=10\text{kts}$  and  $l/L=0.01$

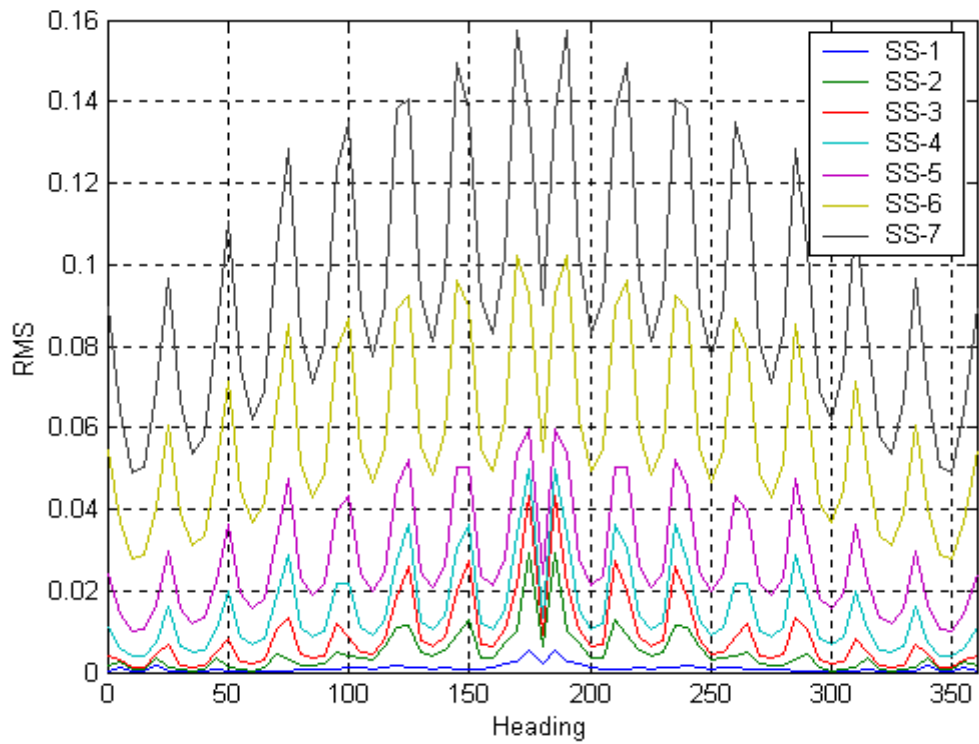


Figure B-2. RMS of Heave Force vs. Heading when  $V=10\text{kts}$  and  $l/L=0.01$

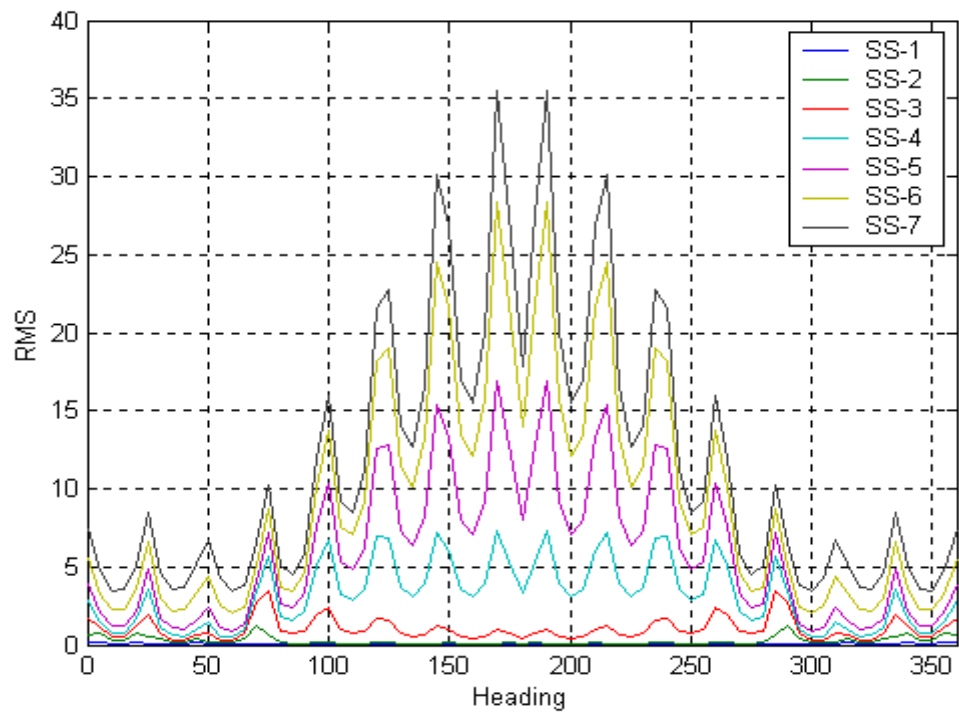


Figure B-3. RMS of Vertical Motion vs. Heading when  $V=10\text{kts}$  and  $l/L=0.01$

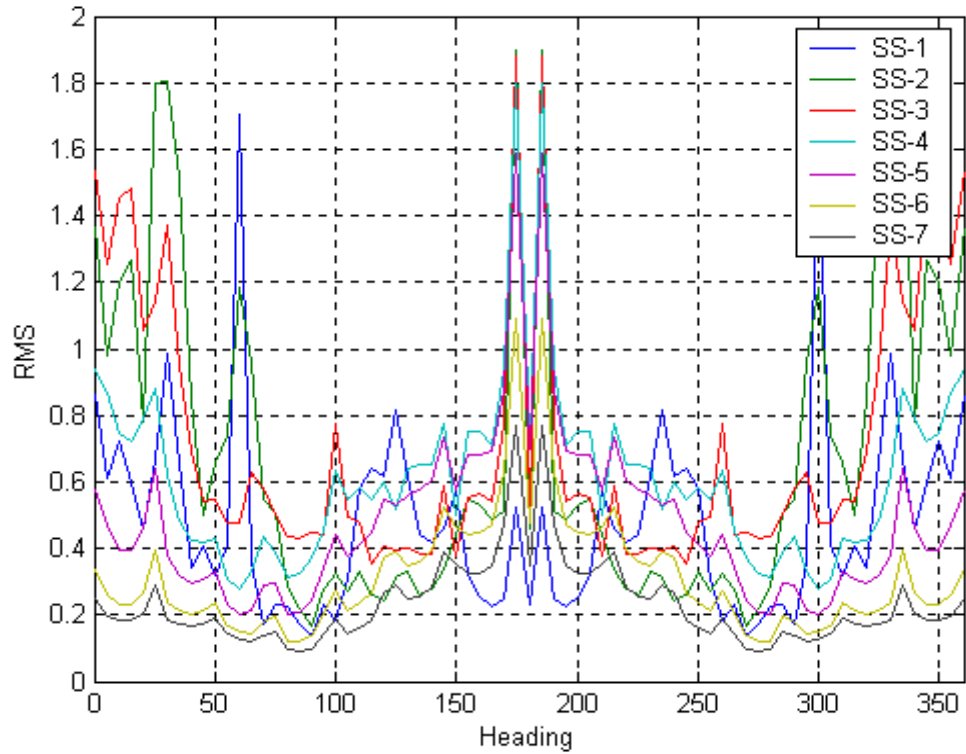


Figure B-4. Normalized Force ( $f/F_3$ ) vs. Heading when  $V=10\text{kts}$  and  $l/L=0.01$

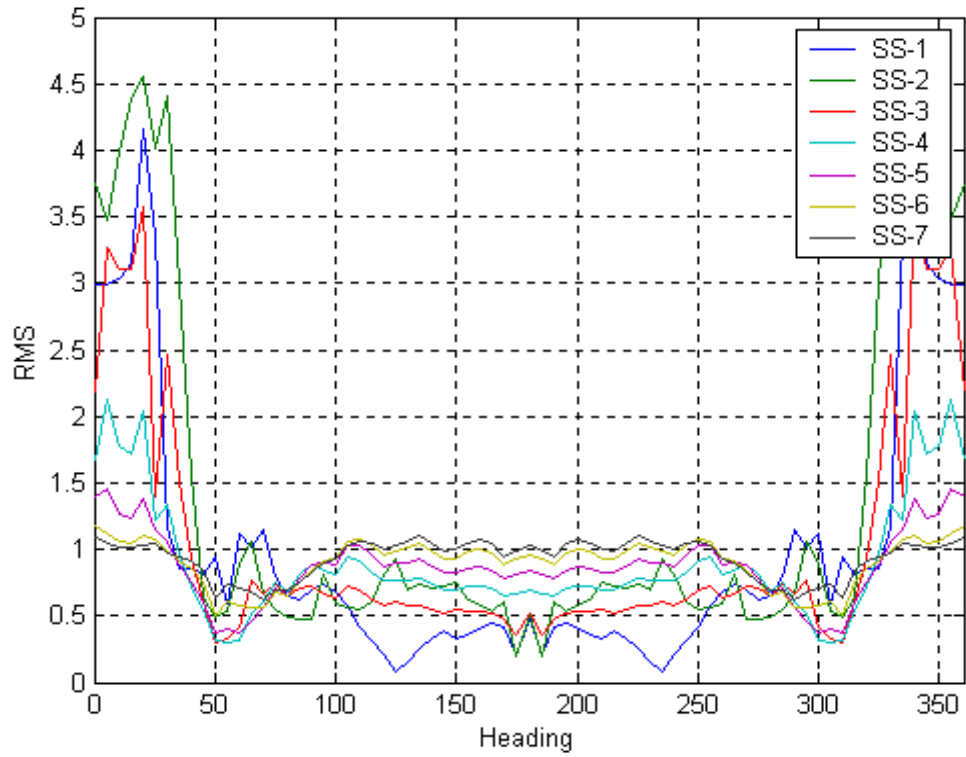


Figure B-5. Vertical Motion vs. Heading when  $V=10\text{kts}$  and  $l/L=0.01$

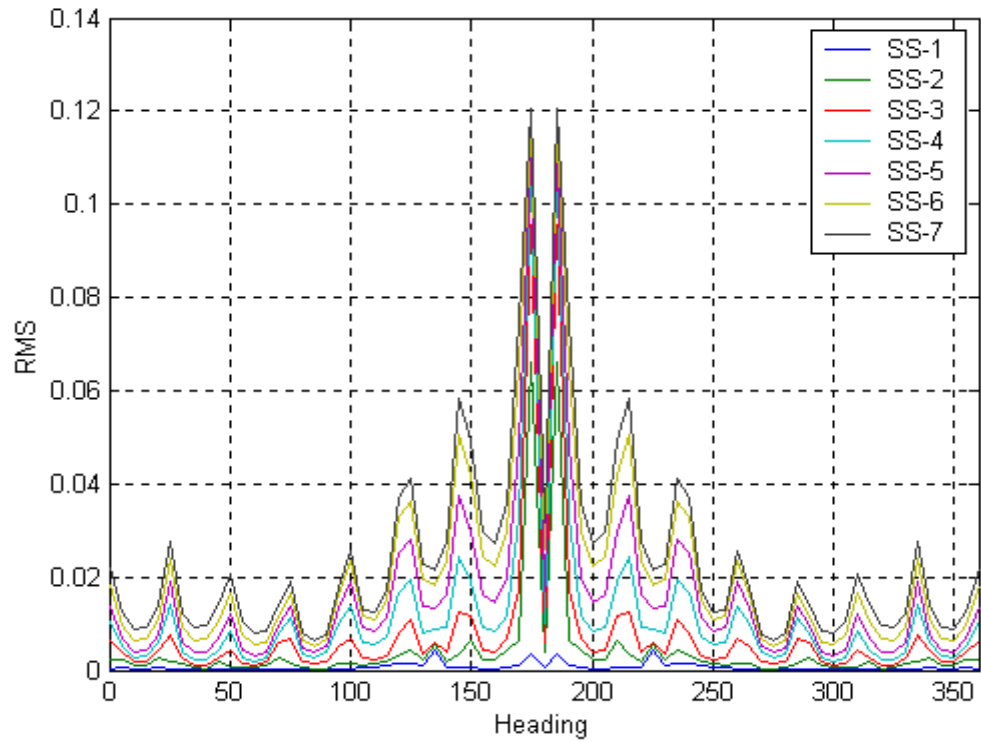


Figure B-6. RMS of Connection Force vs. Heading when  $V=10\text{kts}$  and  $l/L=0.1$

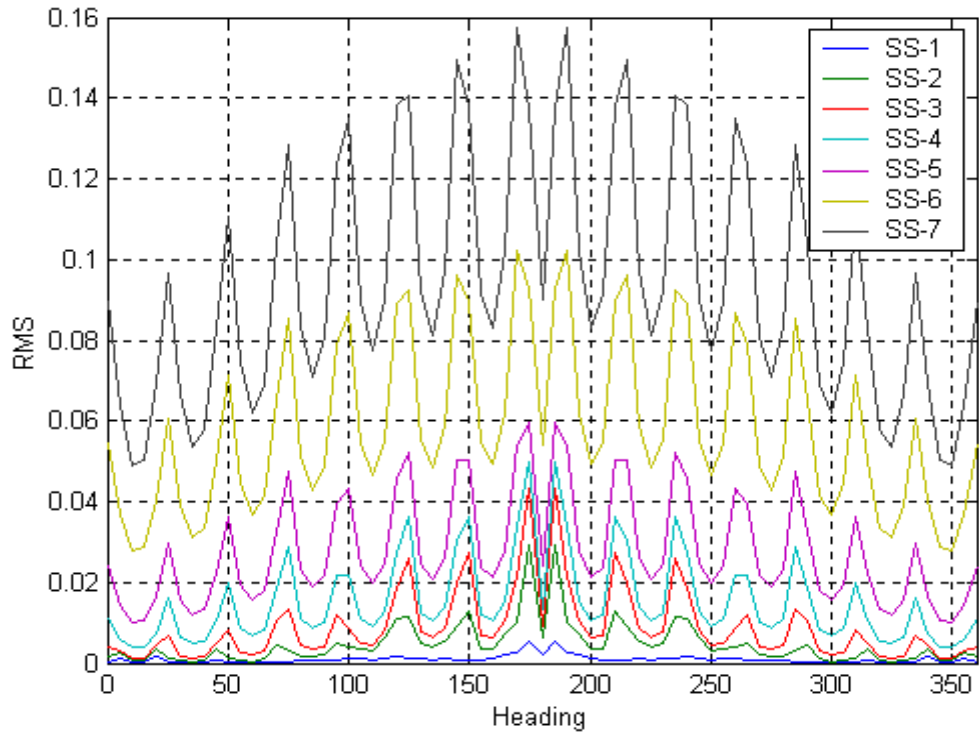


Figure B-7. RMS of Heave Force vs. Heading when  $V=10\text{kts}$  and  $l/L=0.1$

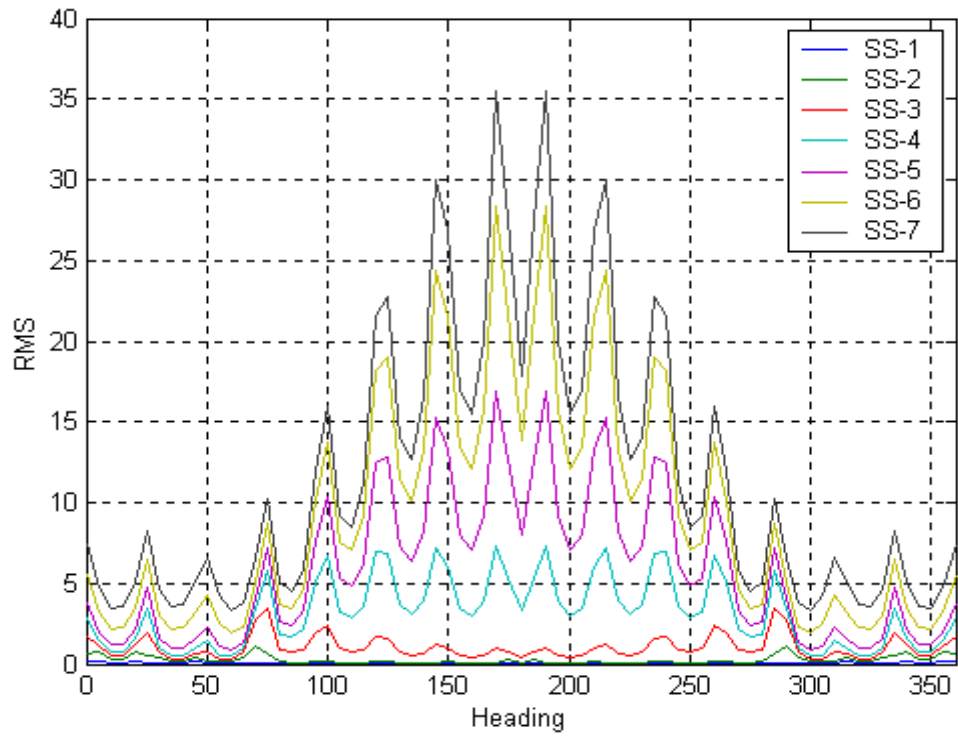


Figure B-8. RMS Value of Vertical Motion vs. Heading when  $V=10\text{kts}$  and  $l/L=0.1$

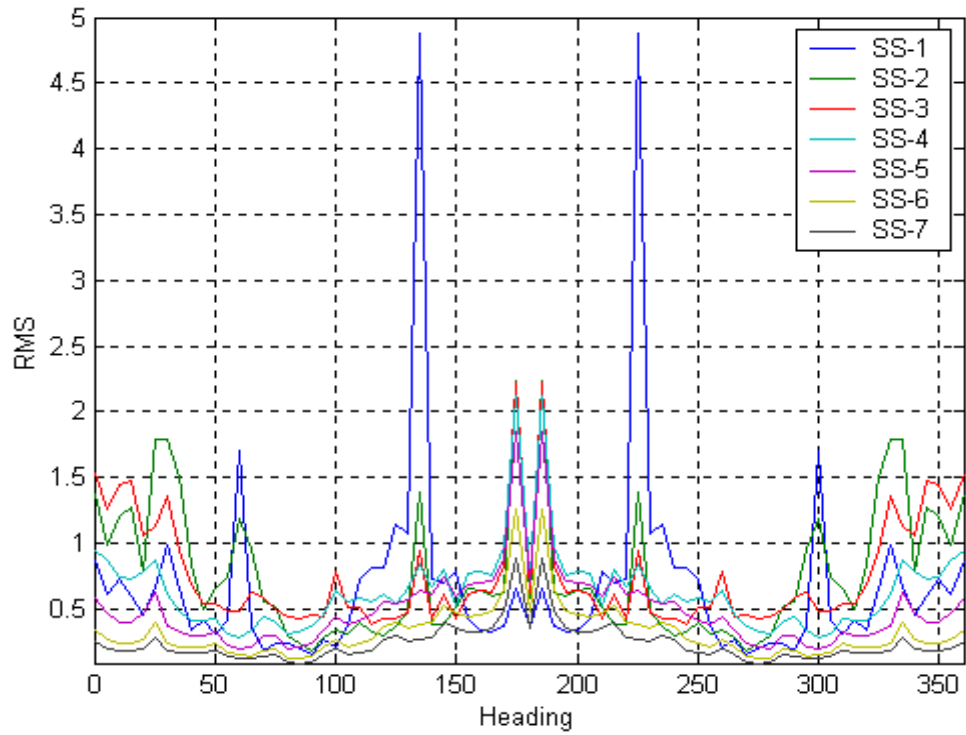


Figure B-9. Normalized Force ( $f/F_3$ ) vs. Heading as a Function of Sea State when  $V=10$  kts and  $l/L=0.1$

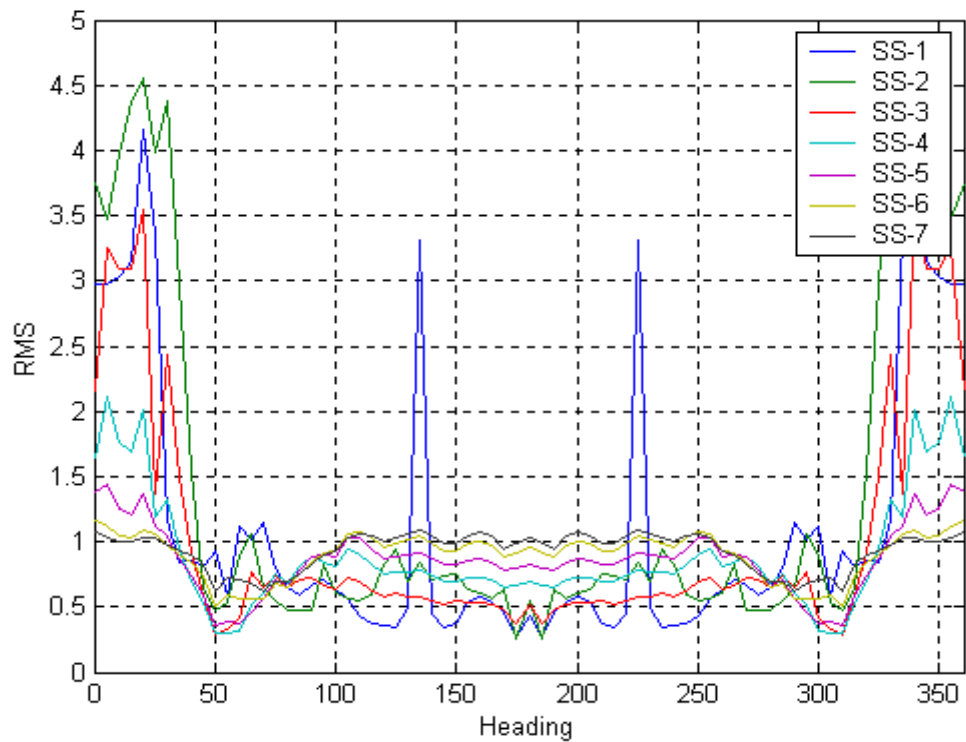


Figure B-10. Vertical Motion vs. Heading when  $V=10$  kts and  $l/L=0.1$

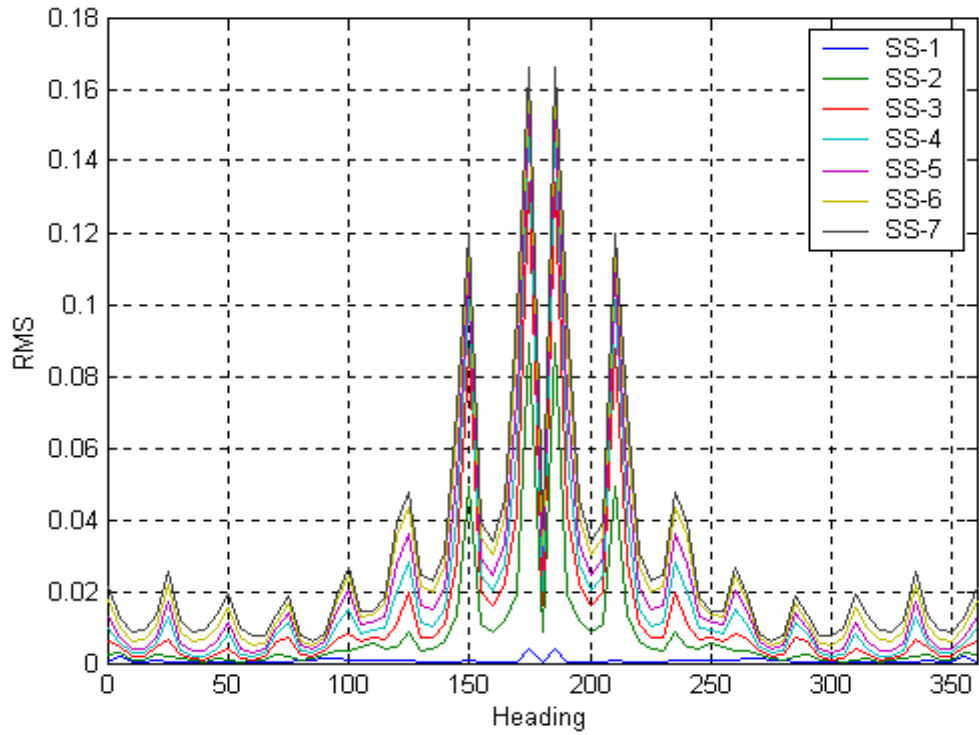


Figure B-11. RMS of Connection Force vs. Heading as a Function of Sea State when  $V=10\text{kts}$  and  $l/L=1$

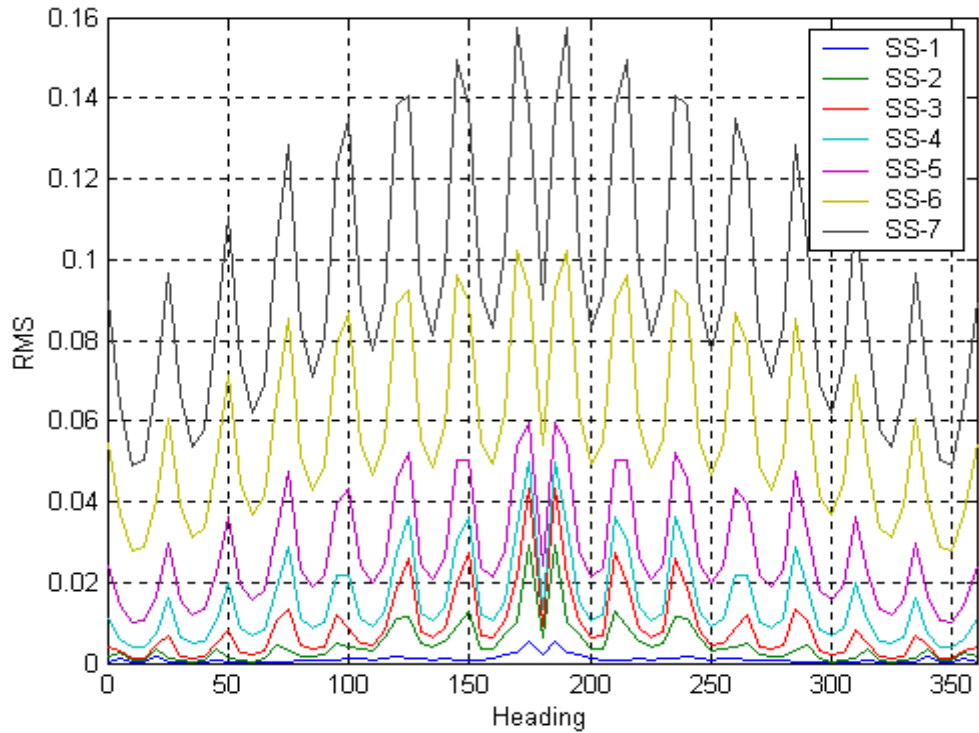


Figure B-12. RMS of Heave Force vs. Heading when  $V=10\text{kts}$  and  $l/L=1$

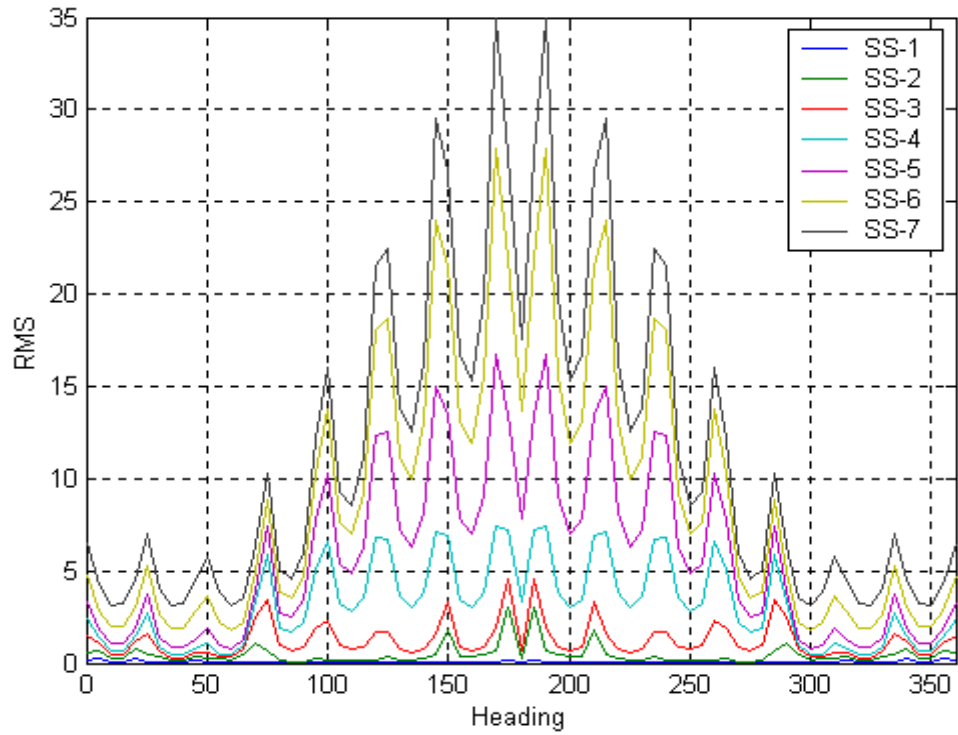


Figure B-13. RMS Value of Vertical Motion vs. Heading when  $V=10\text{kts}$  and  $l/L=1$

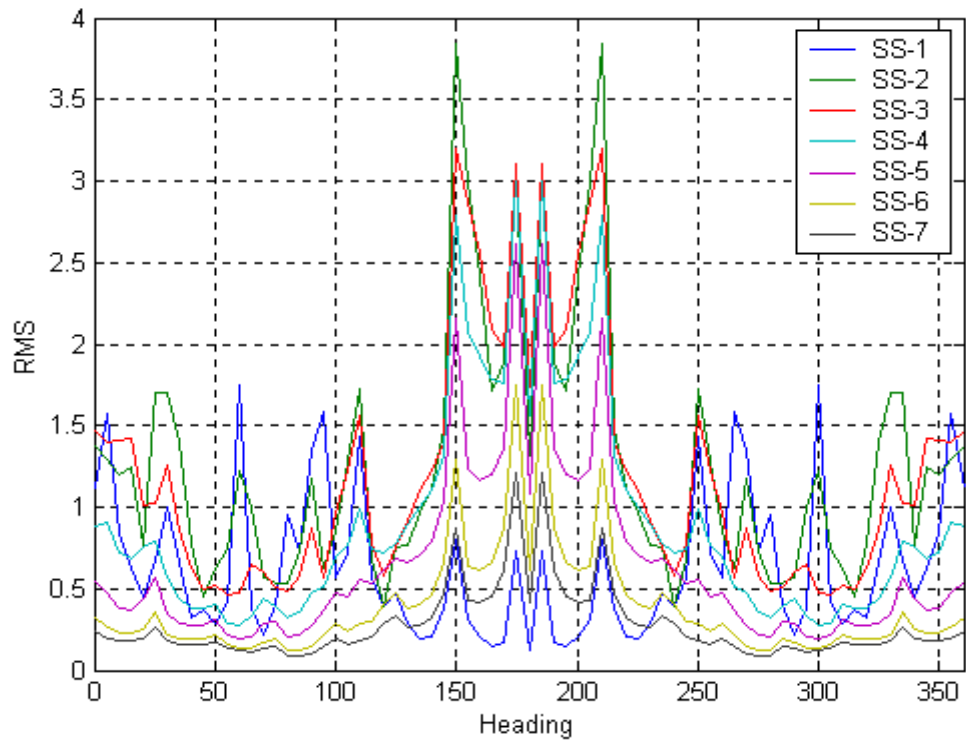


Figure B-14. Normalized Force ( $f/F_3$ ) vs. Heading when  $V=10\text{kts}$  and  $l/L=1$

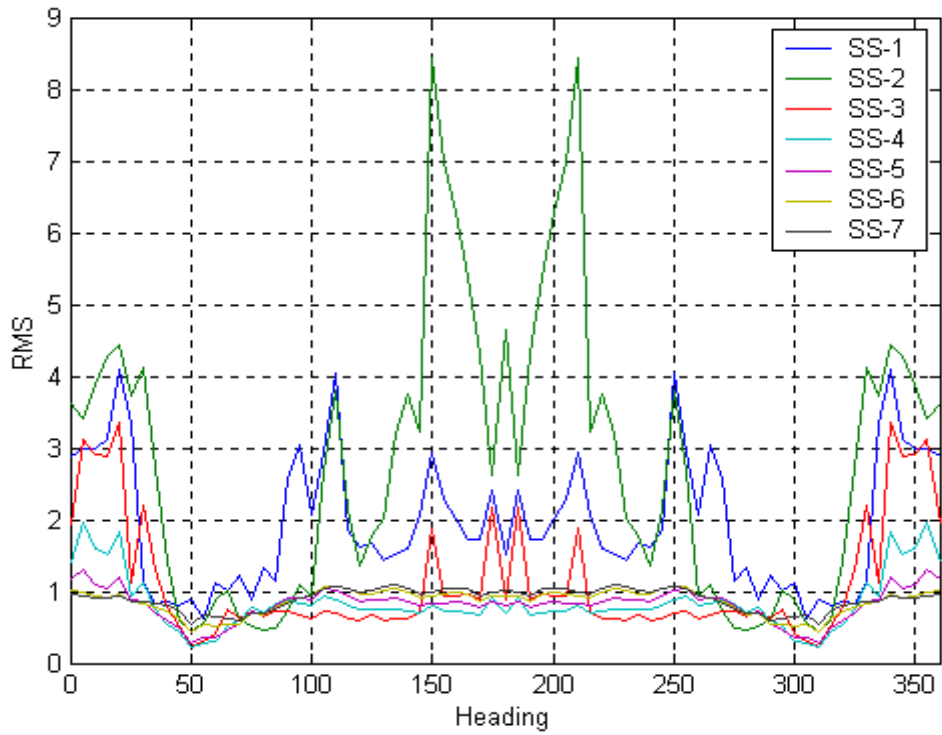


Figure B-15. Normalized Vertical Motion vs. Heading when  $V=10\text{kts}$  and  $l/L=1$

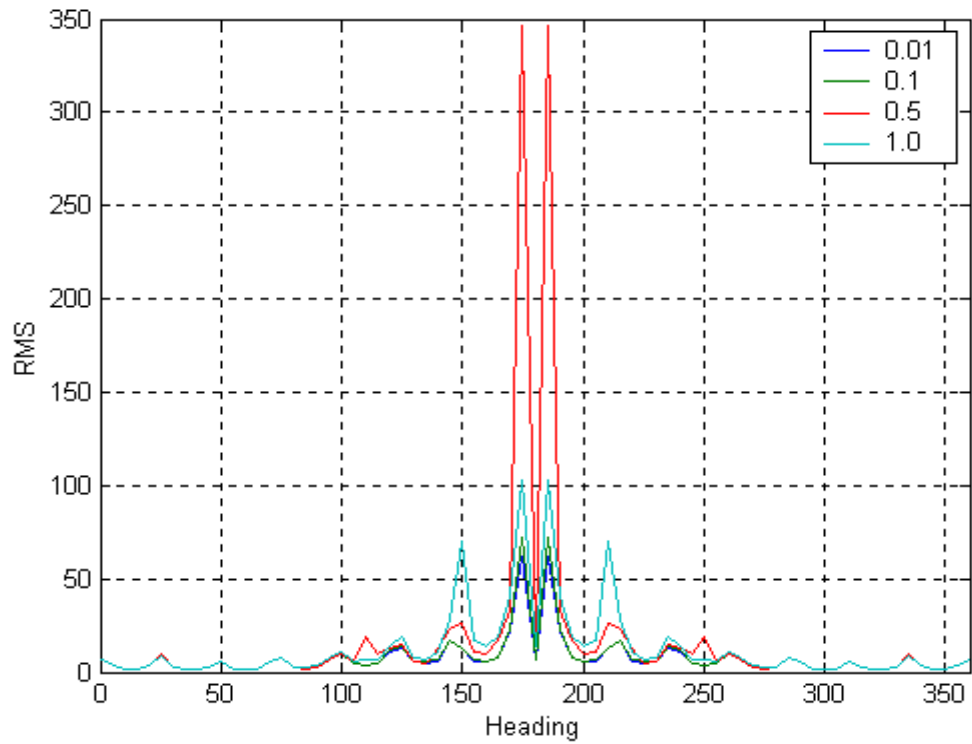


Figure B-16. RMS of Connection Force vs. Heading as a Function of  $l/L$  when  $V=10\text{kts}$

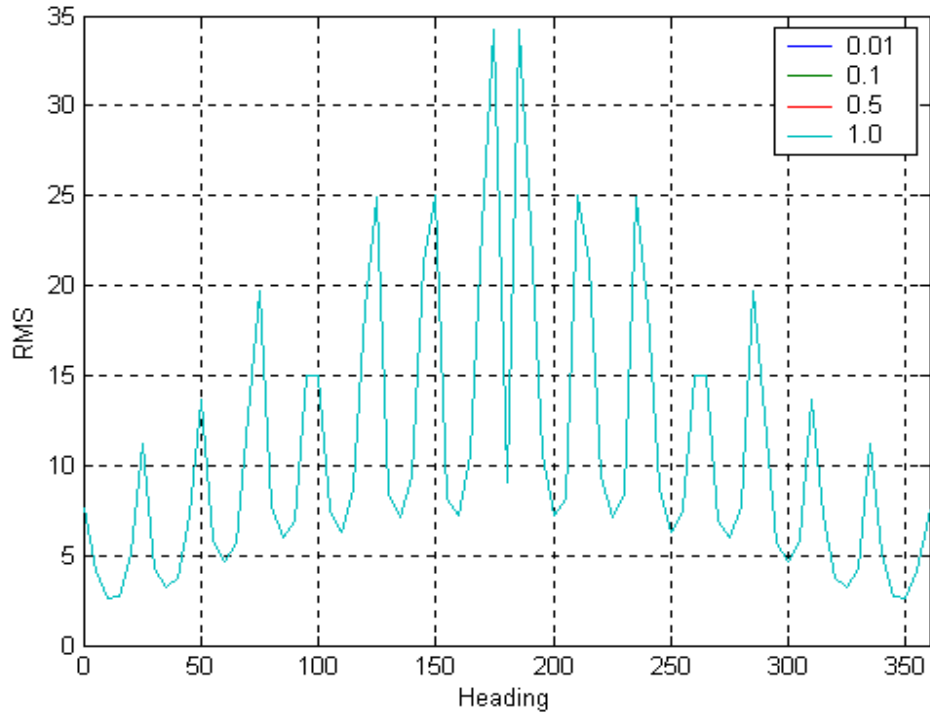


Figure B-17. RMS of Heave Force vs. Heading as a Function of l/L when V=10kts

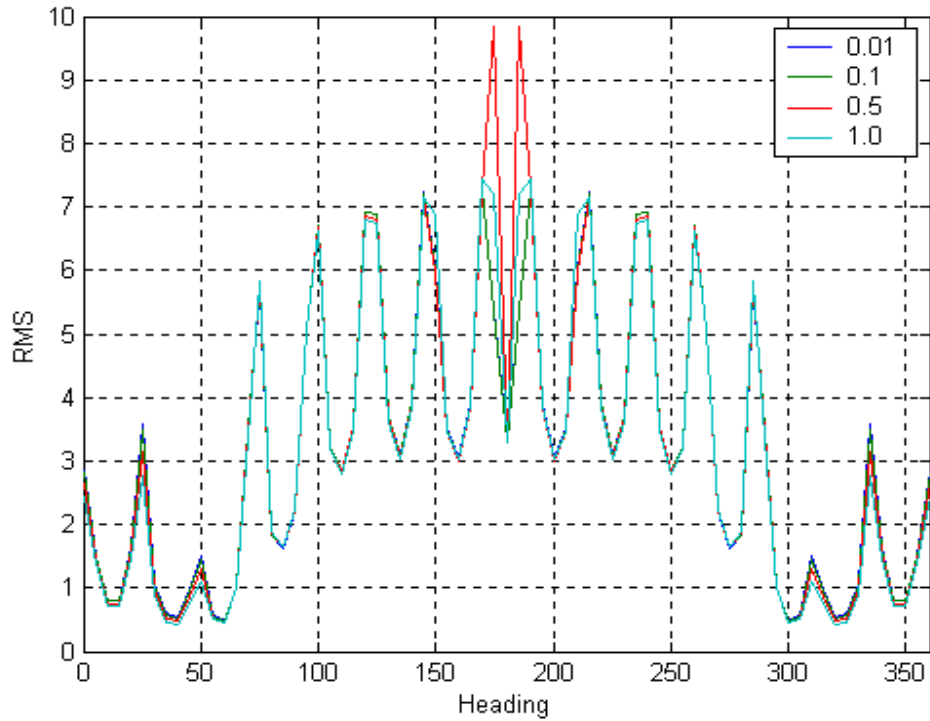


Figure B-18. RMS Value of Vertical Motion vs. Heading as a Function of l/L when V=10kts

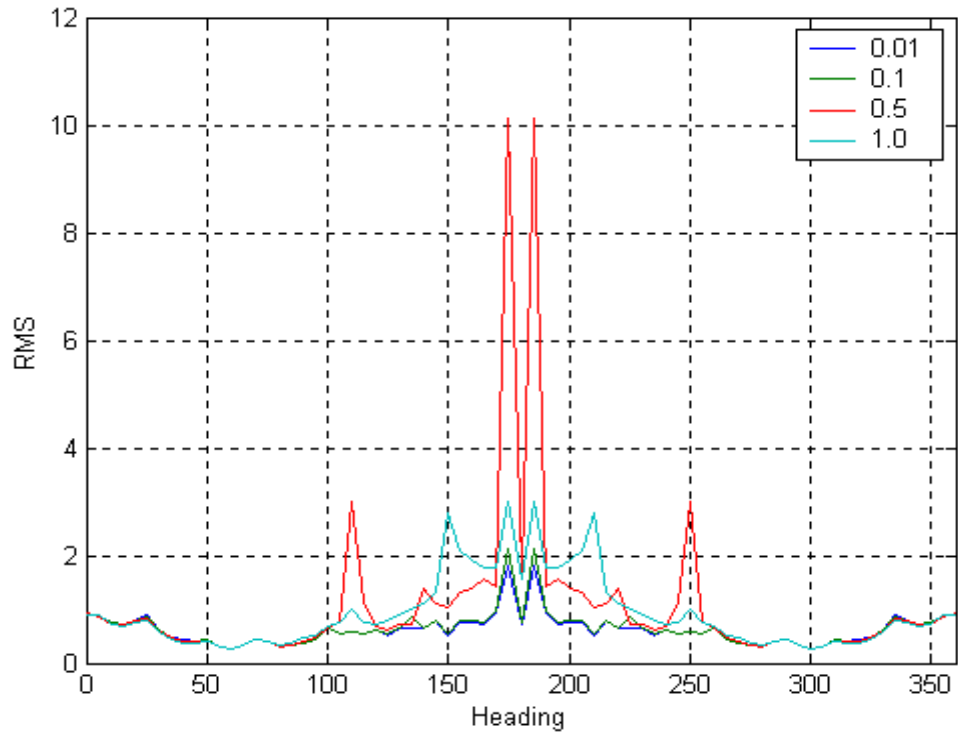


Figure B-19. Normalized Force ( $f/F_3$ ) vs. Heading as a Function of  $l/L$  when  $V=10\text{kts}$

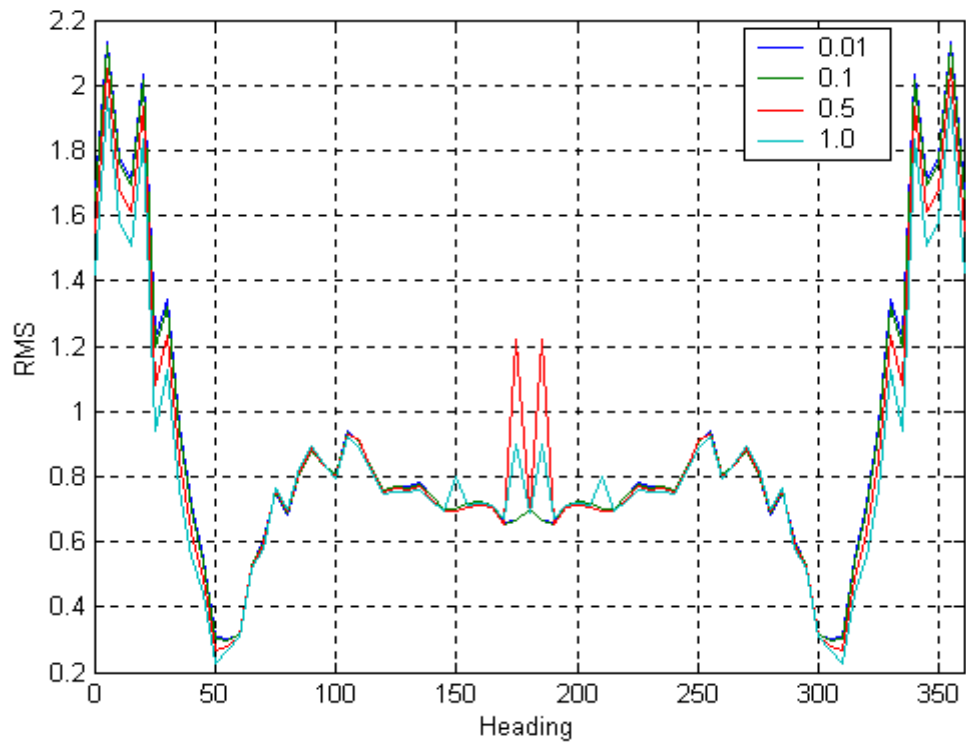


Figure B-20. Vertical Motion vs. Heading as a Function of  $l/L$  when  $V=10\text{kts}$

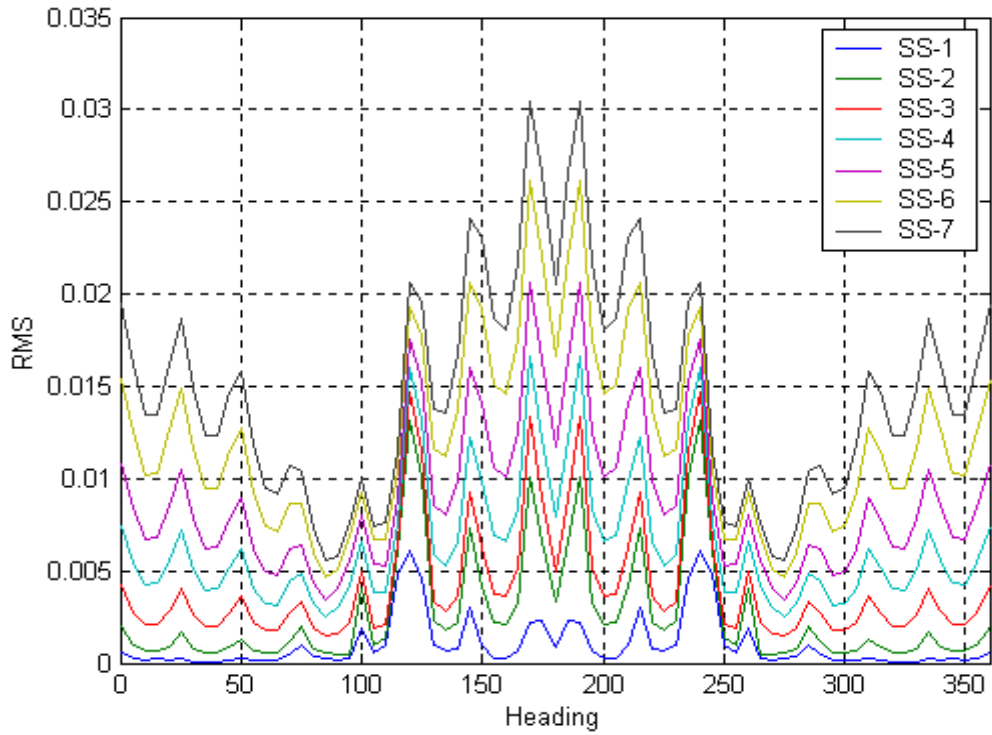


Figure B-21. RMS of Connection Force vs. Heading when  $V=5\text{kts}$  and  $l/L=0.1$

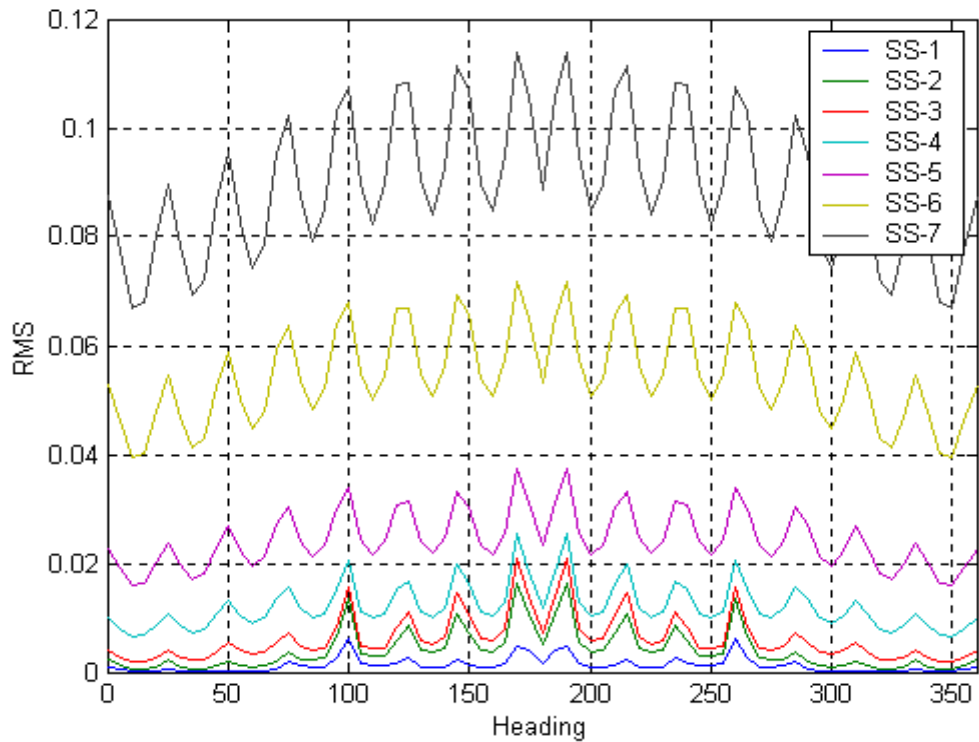


Figure B-22. RMS of Heave Force vs. Heading when  $V=5\text{kts}$  and  $l/L=0.1$

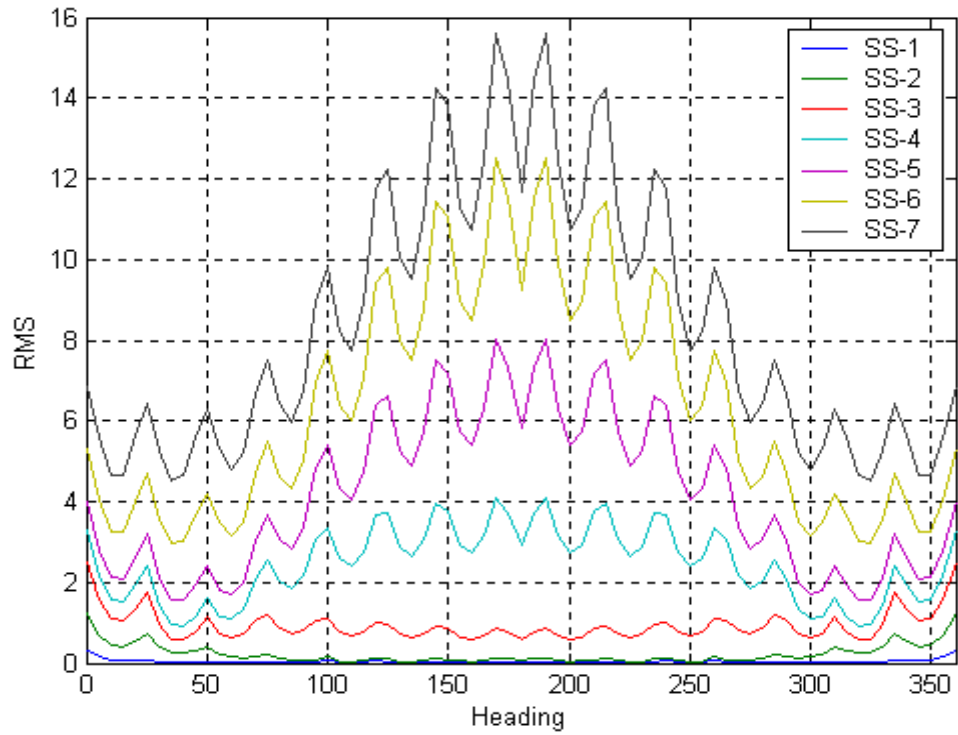


Figure B-23. RMS Value of Vertical Motion vs. Heading when  $V=5\text{kts}$  and  $l/L=0.1$

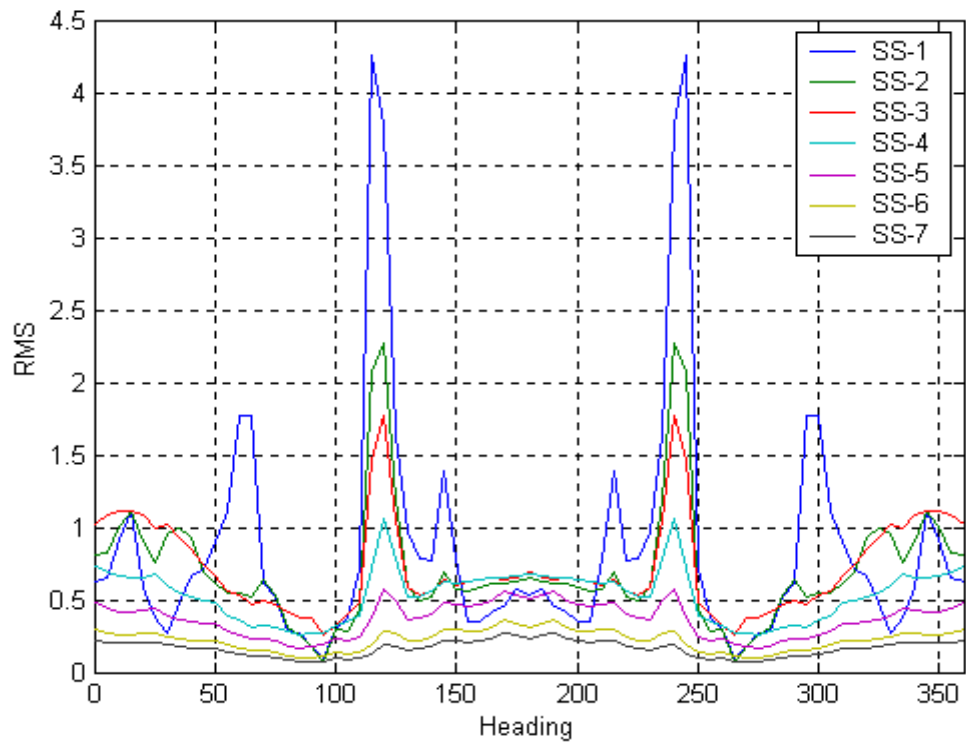


Figure B-24. Normalized Force ( $f/F_3$ ) vs. Heading when  $V=5\text{kts}$  and  $l/L=0.1$

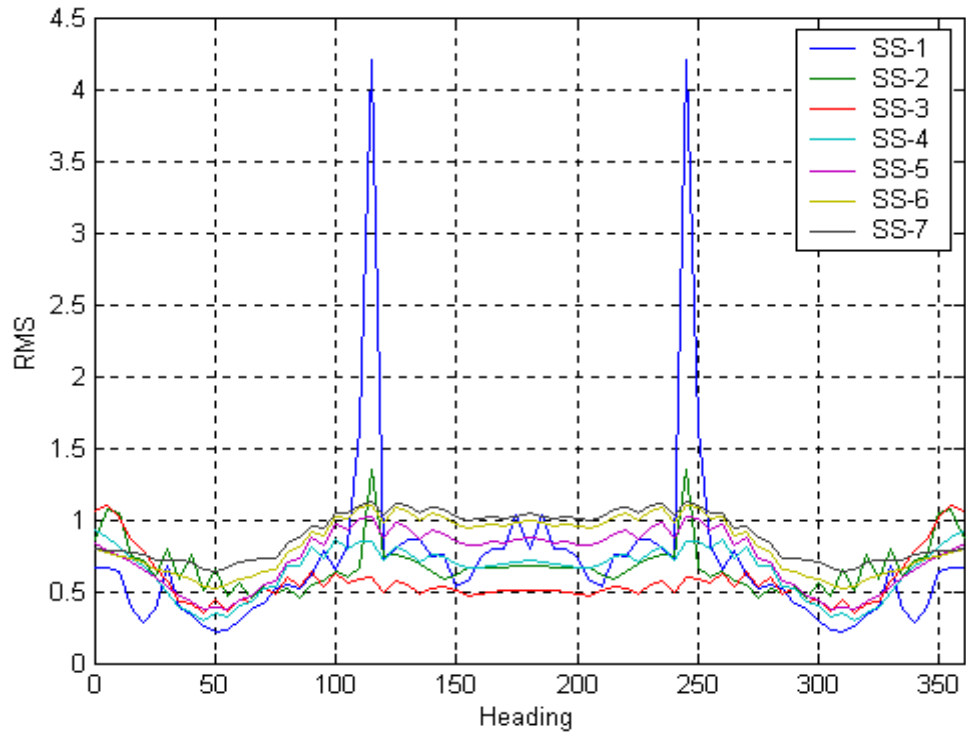


Figure B-25. Vertical Motion vs. Heading when  $V=5\text{kts}$  and  $l/L=0.1$

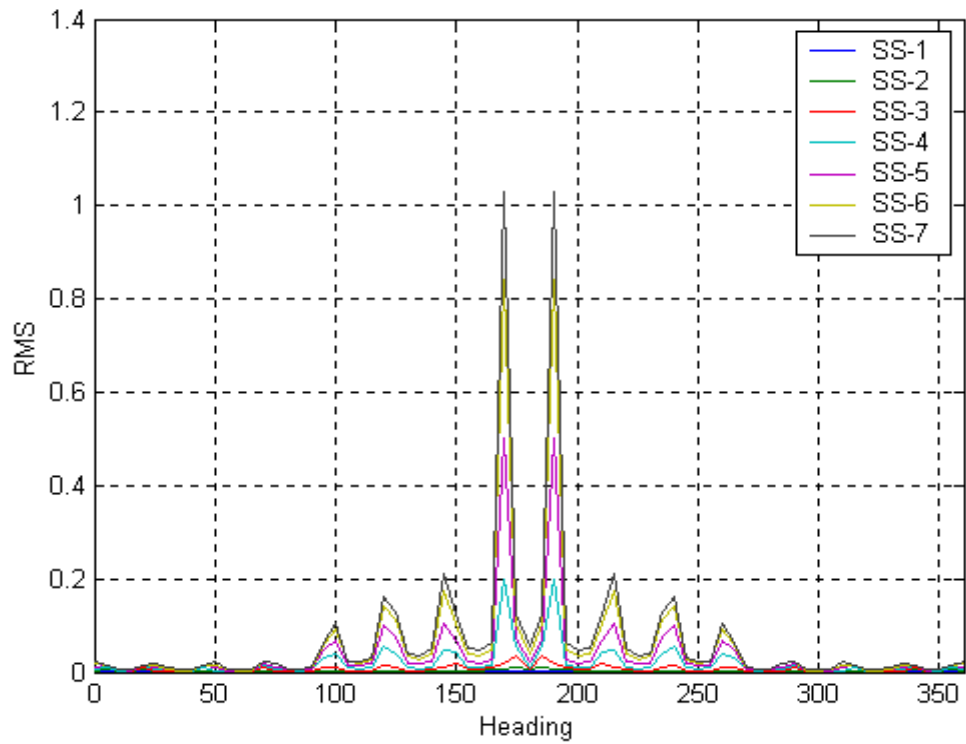


Figure B-26. RMS of Connection Force vs. Heading when  $V=15\text{kts}$  and  $l/L=0.1$

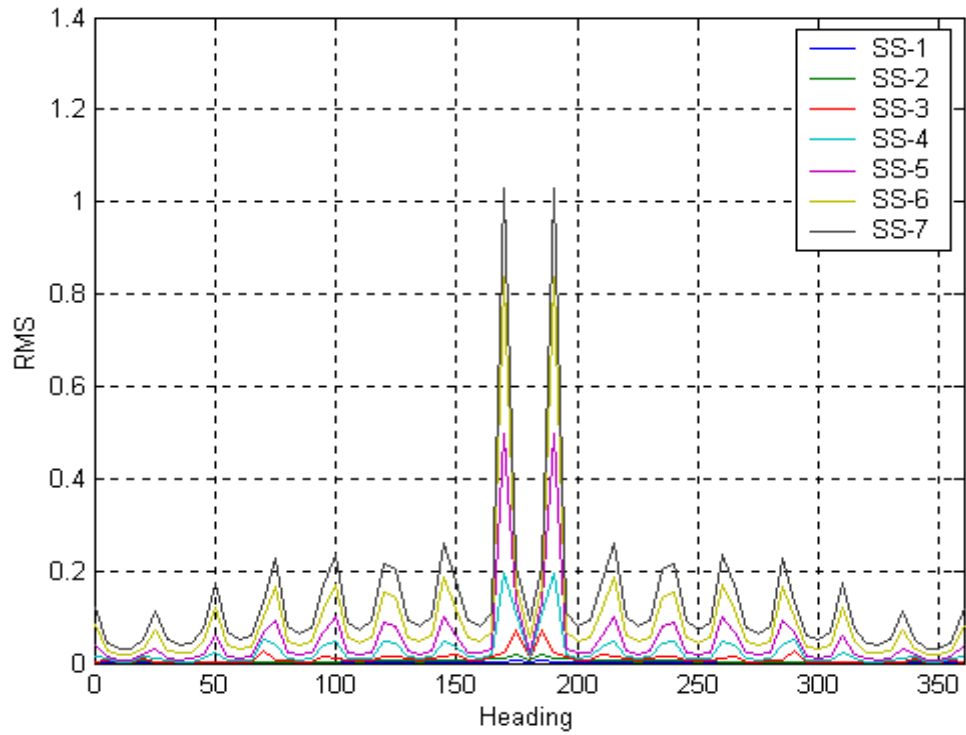


Figure B-27. RMS of Heave Force vs. Heading when  $V=15\text{kts}$  and  $l/L=0.1$

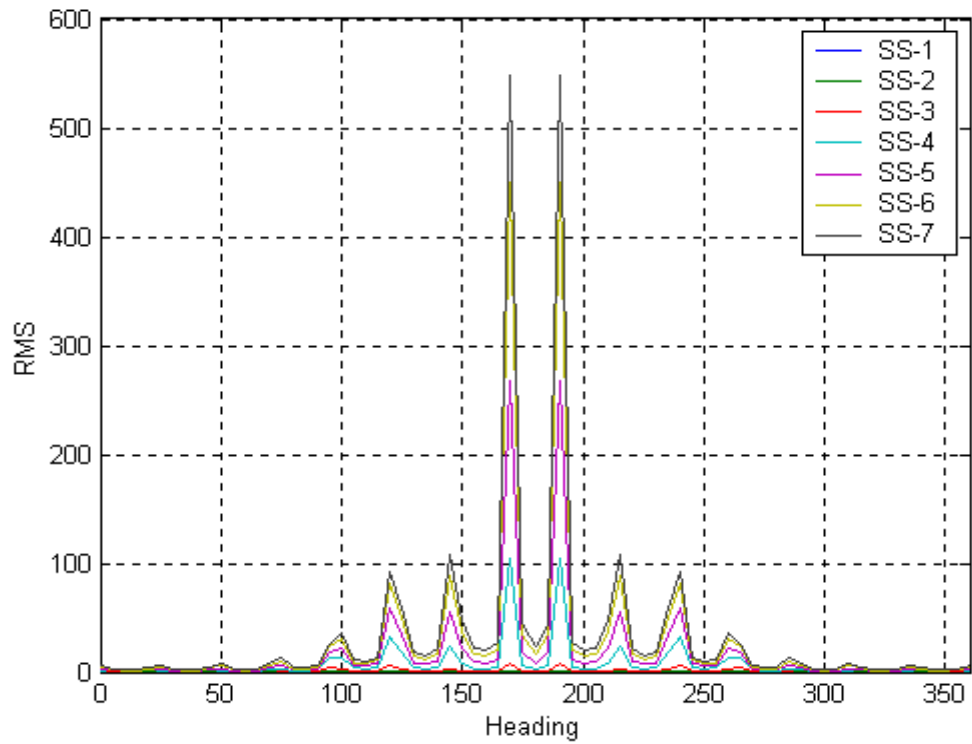


Figure B-28. RMS Value of Vertical Motion vs. Heading when  $V=15\text{kts}$  and  $l/L=0.1$

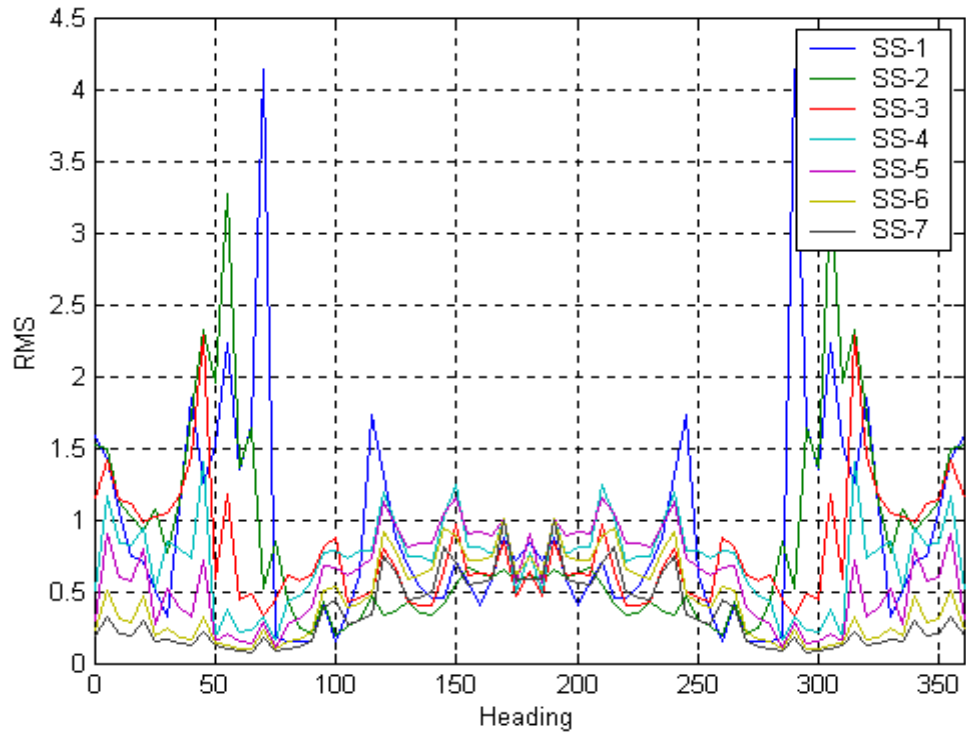


Figure B-29. Normalized Force ( $f/F_3$ ) vs. Heading when  $V=15$  kts and  $l/L=0.1$

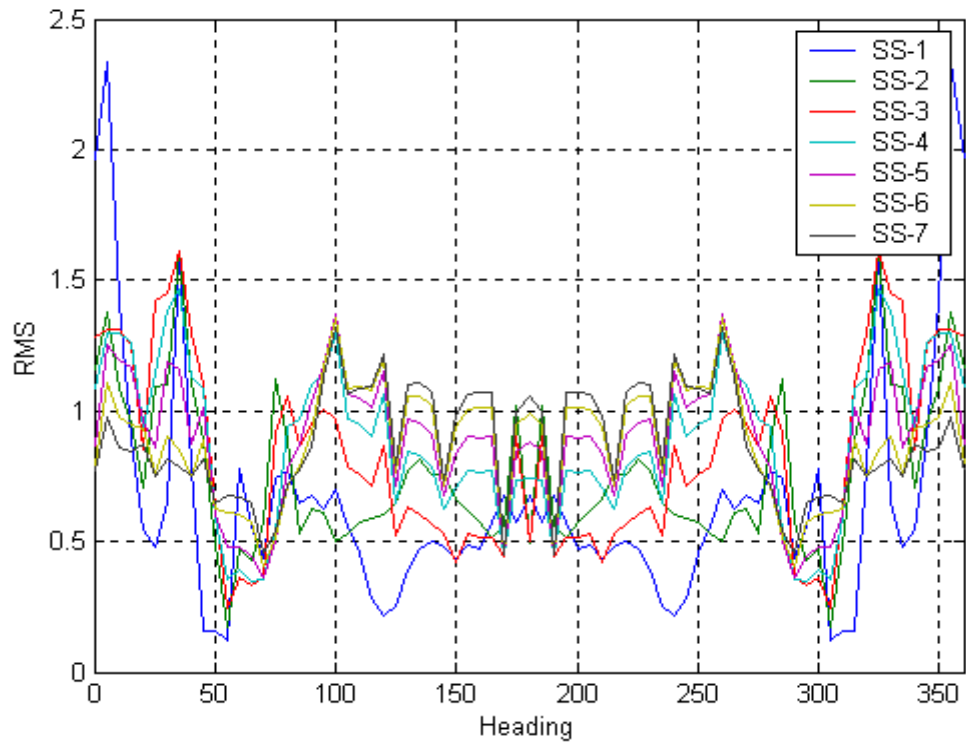


Figure B-30. Normalized Vertical Motion vs. Heading when  $V=15$  kts and  $l/L=0.1$

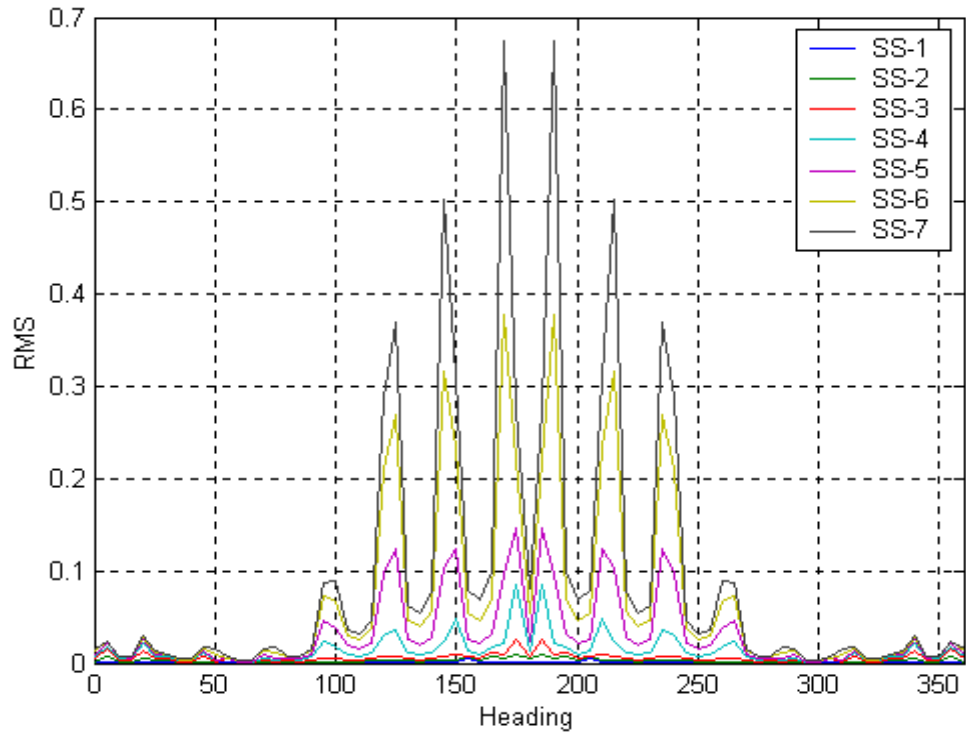


Figure B-31. RMS of Connection Force vs. Heading when  $V=20\text{kts}$  and  $l/L=0.1$

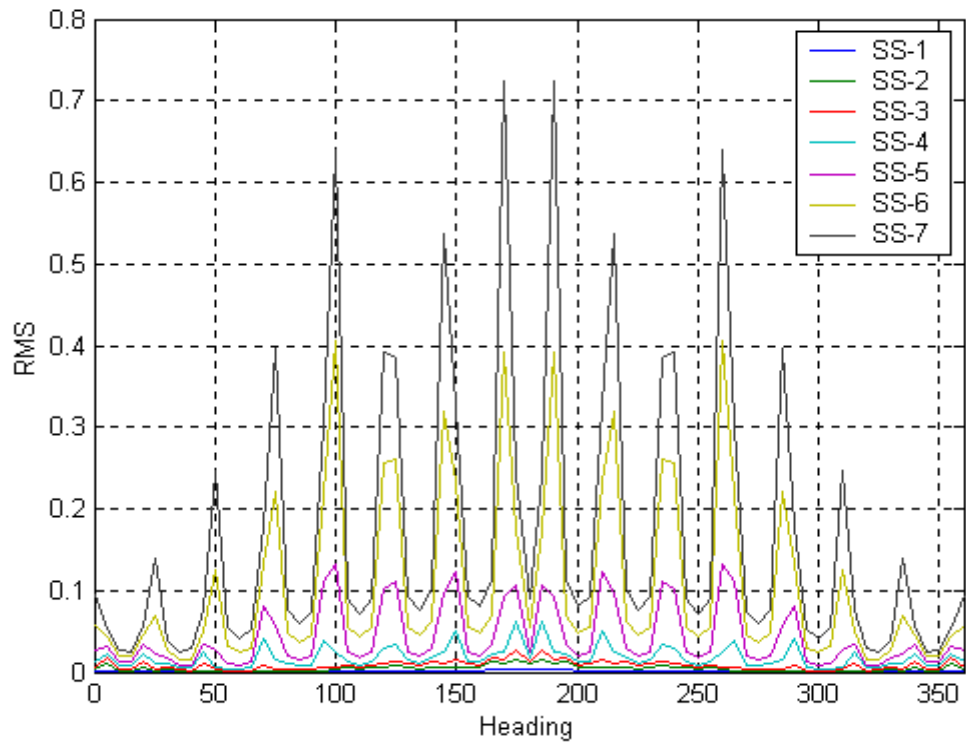


Figure B-32. RMS of Heave Force vs. Heading when  $V=20\text{kts}$  when  $l/L=0.1$

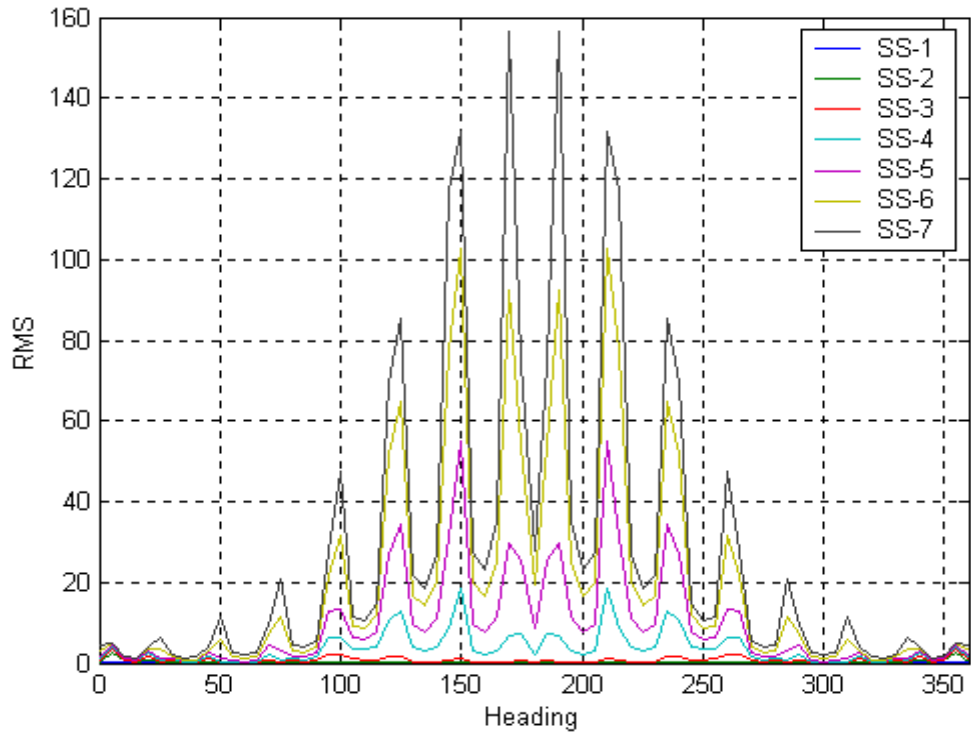


Figure B-33. RMS Value of Vertical motion vs. Heading when  $V=20\text{kts}$  and  $l/L=0.1$

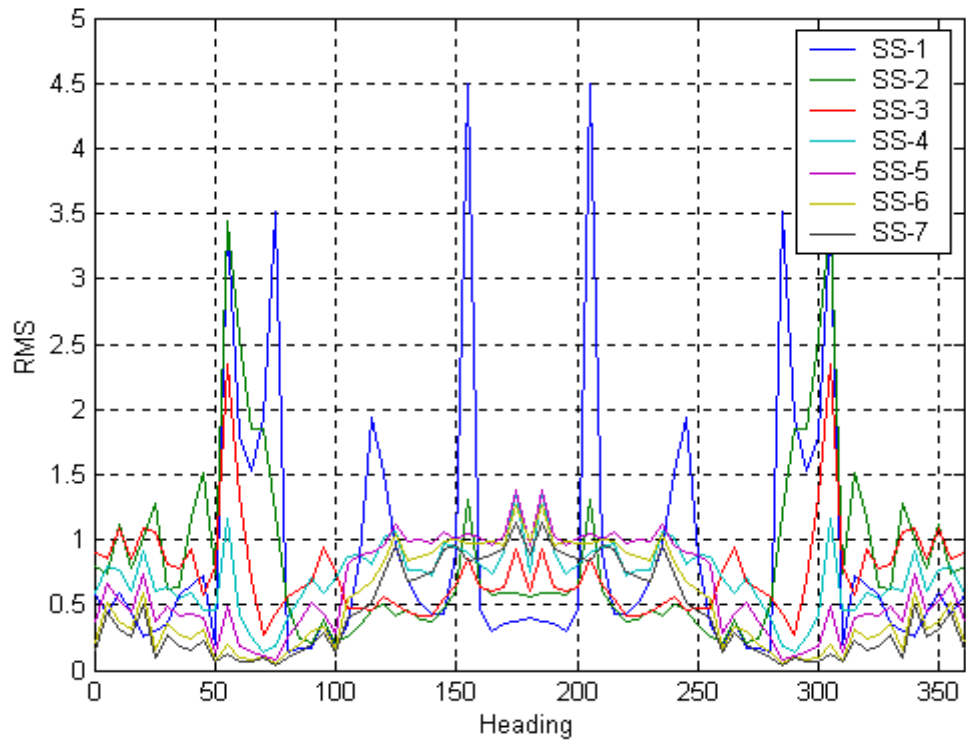


Figure B-34. Normalized Force ( $f/F_3$ ) vs. Heading when  $V=20\text{kts}$  and  $l/L=0.1$

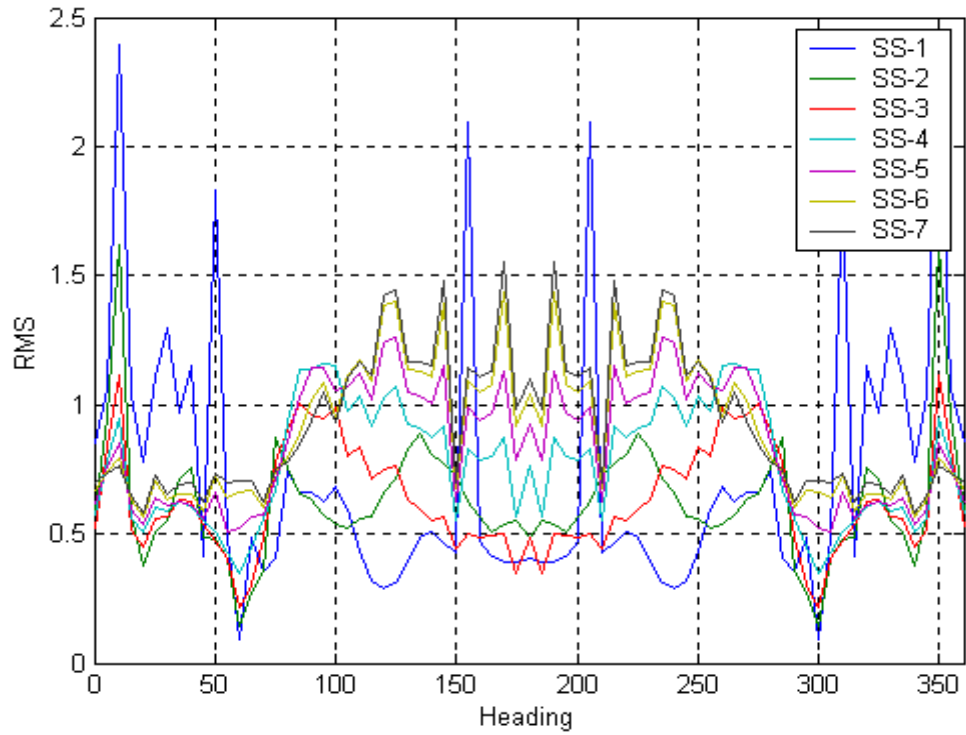


Figure B-35. Vertical Motion vs. Heading when  $V=20\text{kts}$  and  $l/L=0.1$

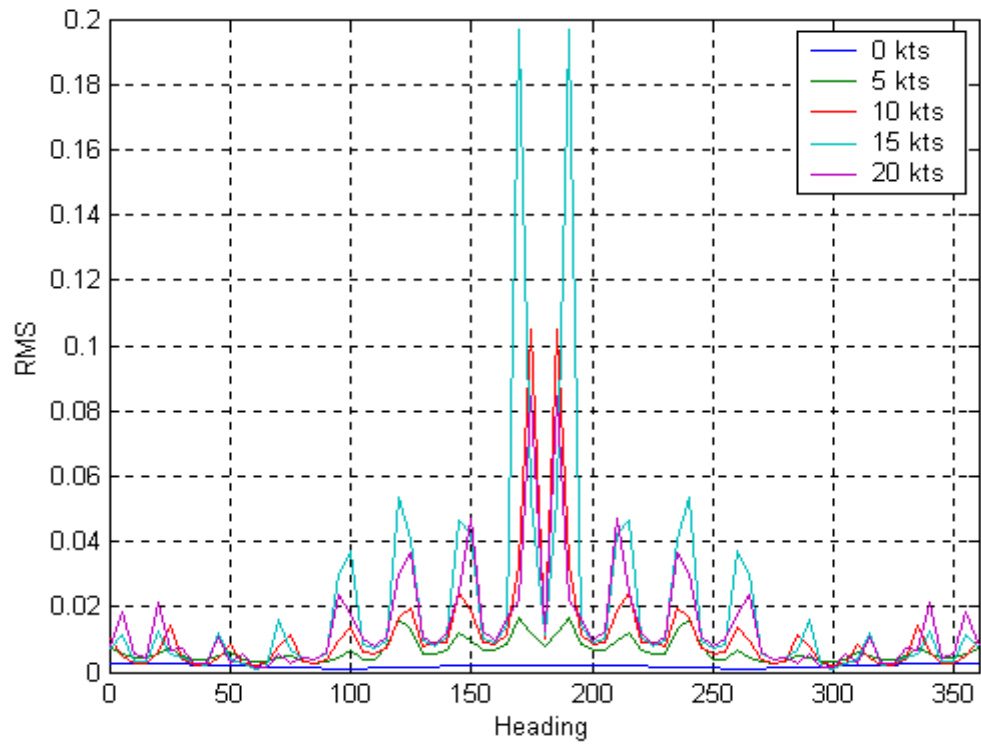


Figure B-36. RMS of Connection Force vs. Heading when  $l/L=0.1$  and Sea State 4

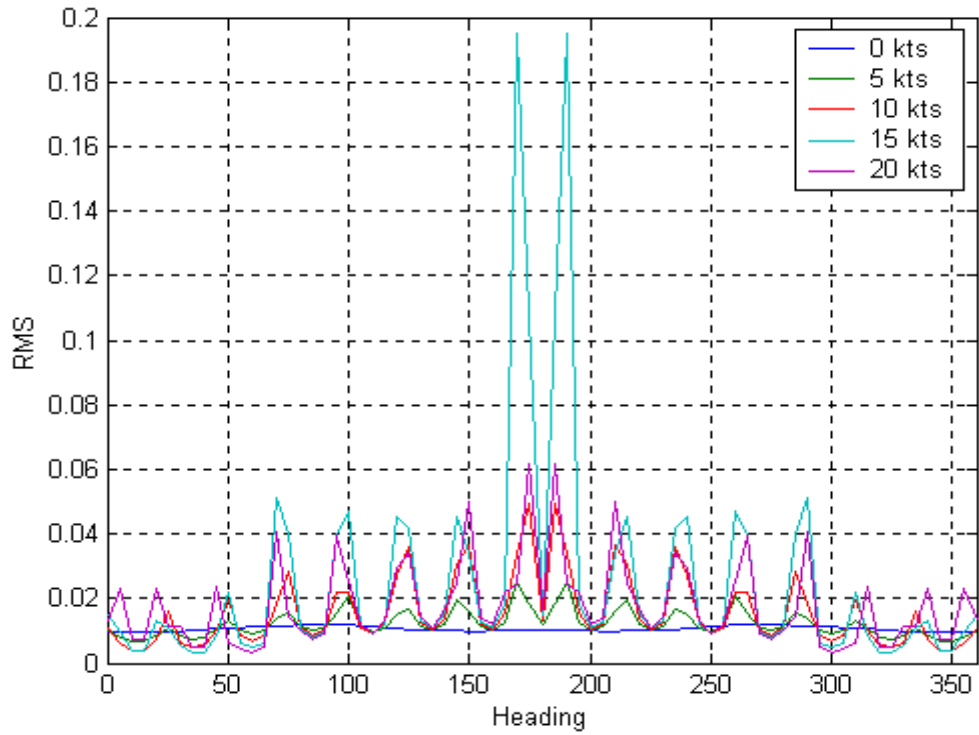


Figure B-37. RMS of Heave Force vs. Heading when  $l/L=0.1$  and Sea State 4

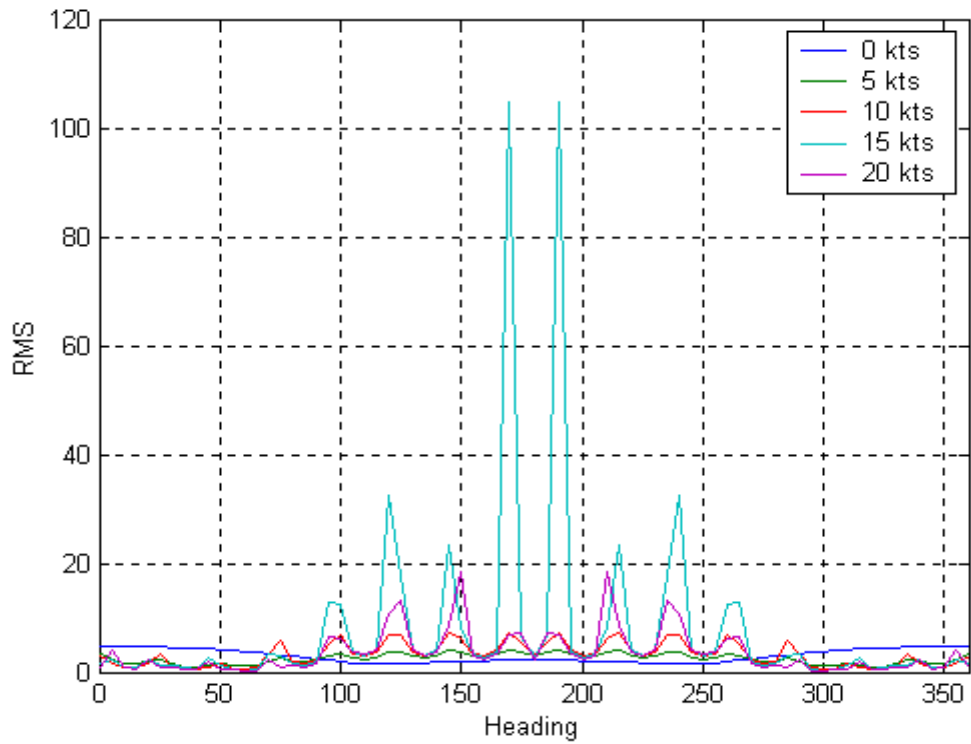


Figure B-38. RMS Value of Vertical Motion vs. Heading when  $l/L=0.1$  and Sea State 4

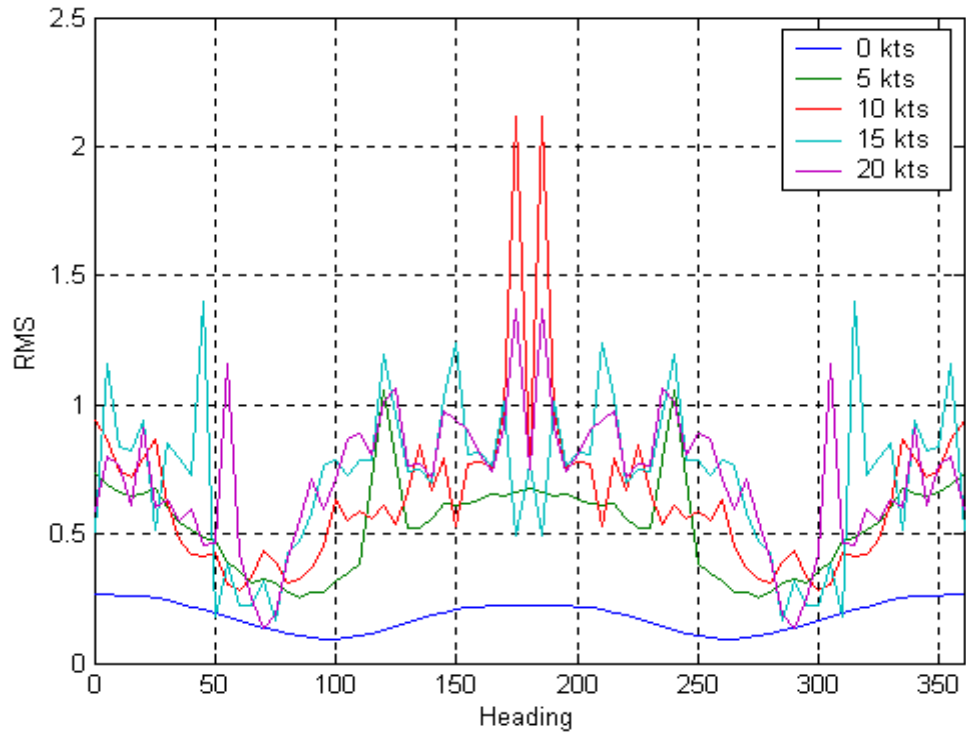


Figure B-39. Normalized Force ( $f/F_3$ ) vs. Heading when  $l/L=0.1$  and Sea State 4

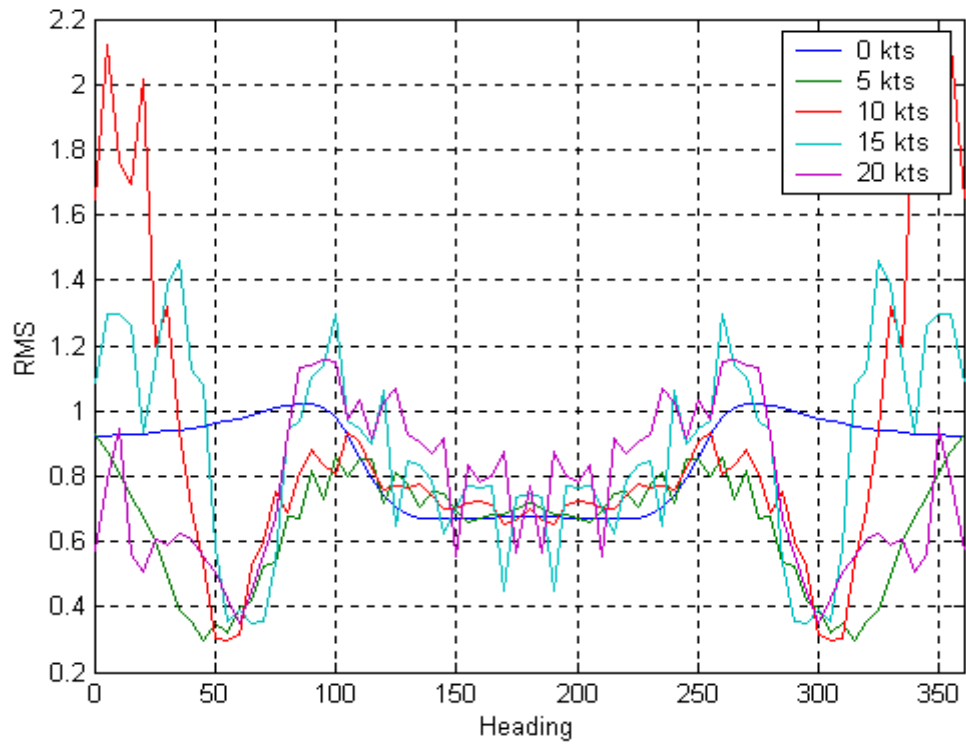


Figure B-40. Vertical Motion vs. Heading when  $l/L=0.1$  and Sea State 4

THIS PAGE INTENTIONALLY LEFT BLANK

## **APPENDIX C. SEAKEEPING RESULTS**

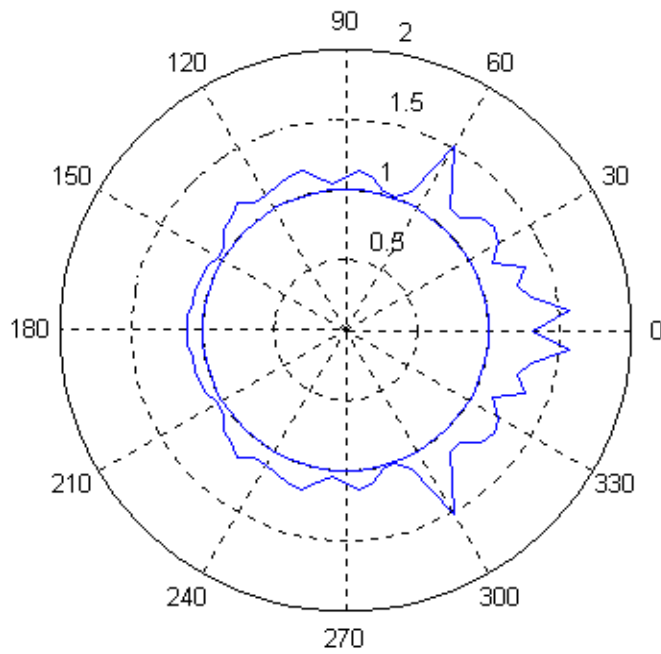


Figure C-1. Sea state variation when  $V=10\text{kts}$ ,  $l/L=0.01$  and Sea State 1

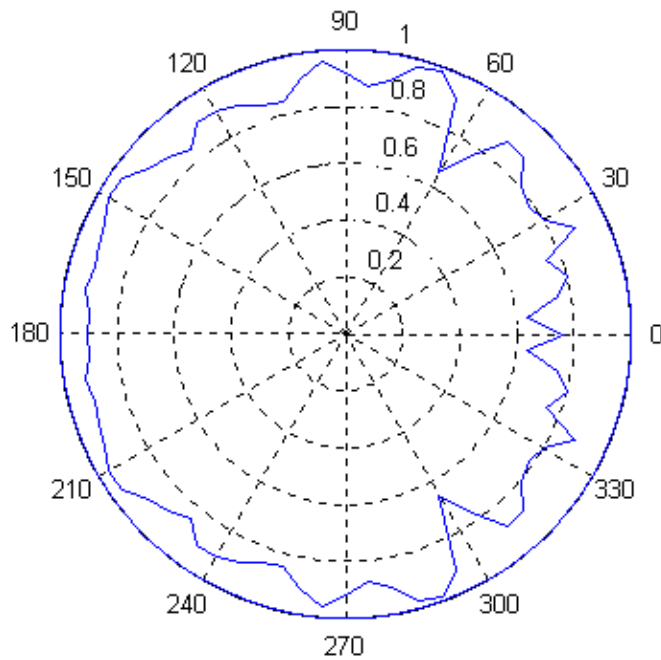


Figure C-2. Sea state degradation when  $V=10\text{kts}$ ,  $l/L=0.01$  and Sea State 1

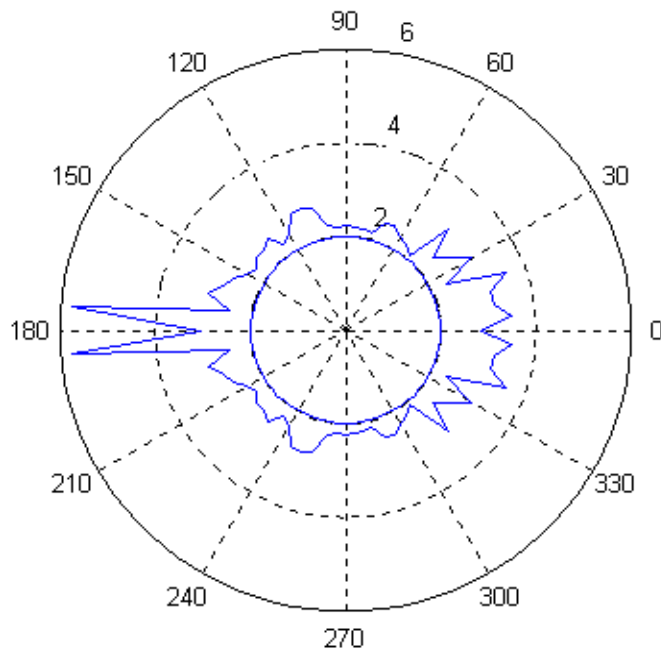


Figure C-3. Sea state variation when  $V=10\text{kts}$ ,  $l/L=0.01$  and Sea State 2

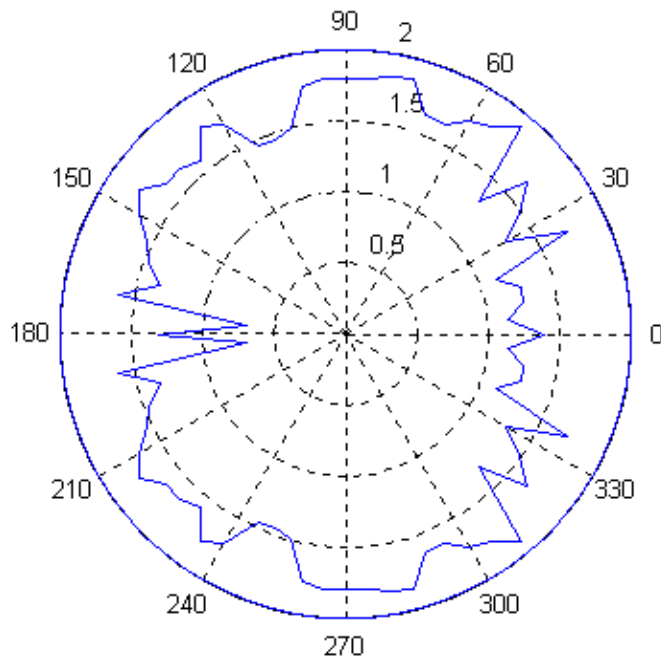


Figure C-4. Sea state degradation when  $V=10\text{kts}$ ,  $l/L=0.01$  and Sea State 2

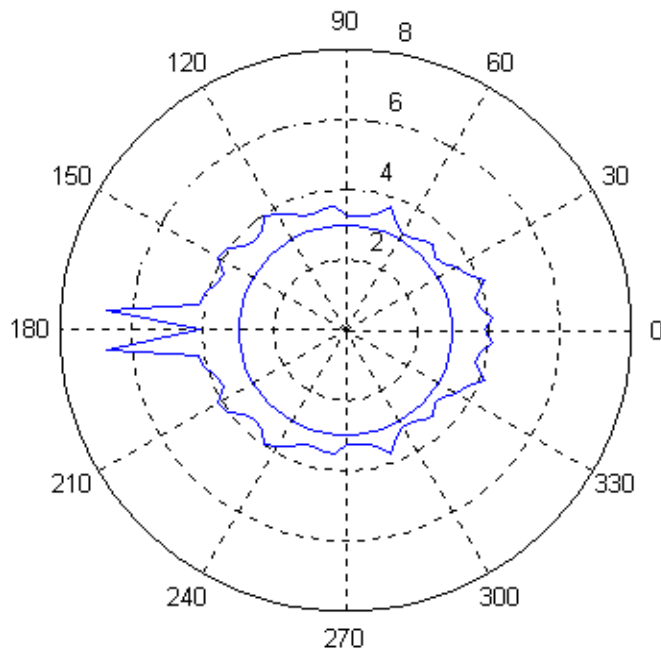


Figure C-5. Sea state variation when  $V=10\text{kts}$ ,  $l/L=0.01$  and Sea State 3

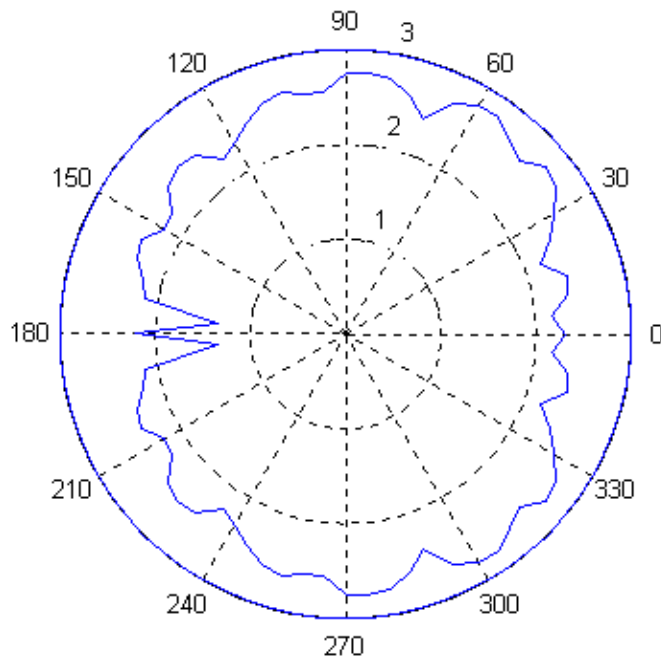


Figure C-6. Sea state degradation when  $V=10\text{kts}$ ,  $l/L=0.01$  and Sea State 3

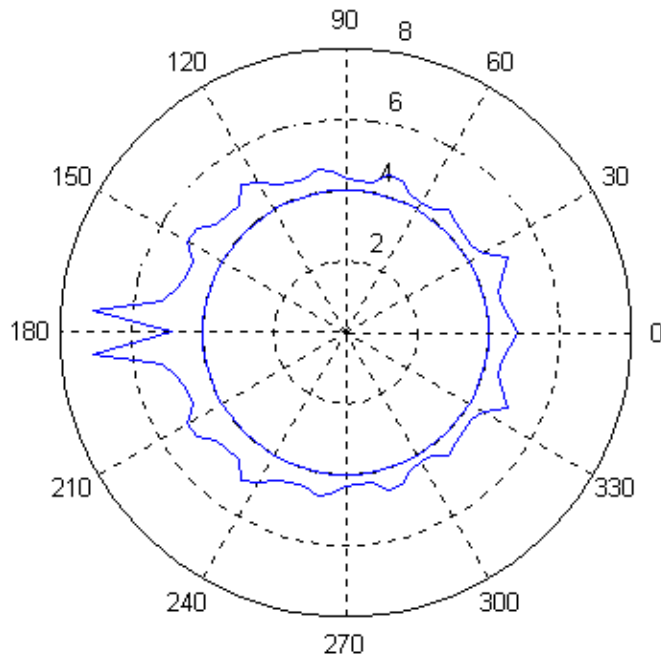


Figure C-7. Sea state variation when  $V=10\text{kts}$ ,  $l/L=0.01$  and Sea State 4

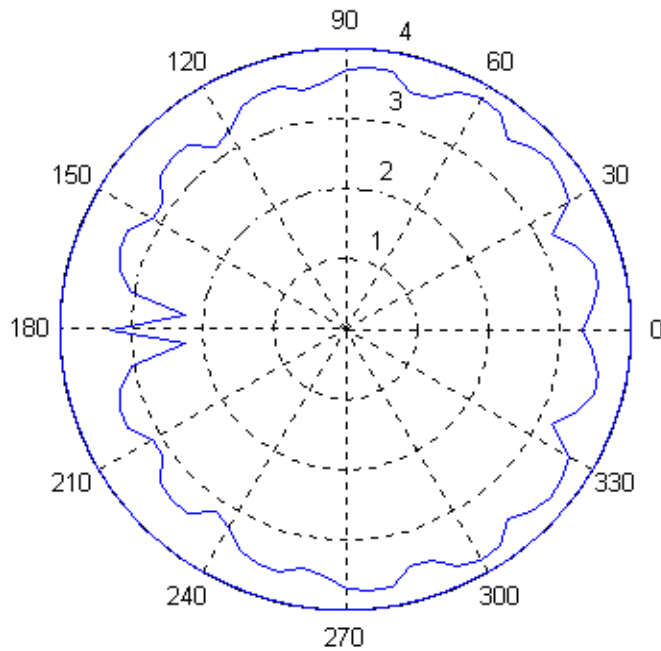


Figure C-8. Sea state degradation when  $V=10\text{kts}$ ,  $l/L=0.01$  and Sea State 4

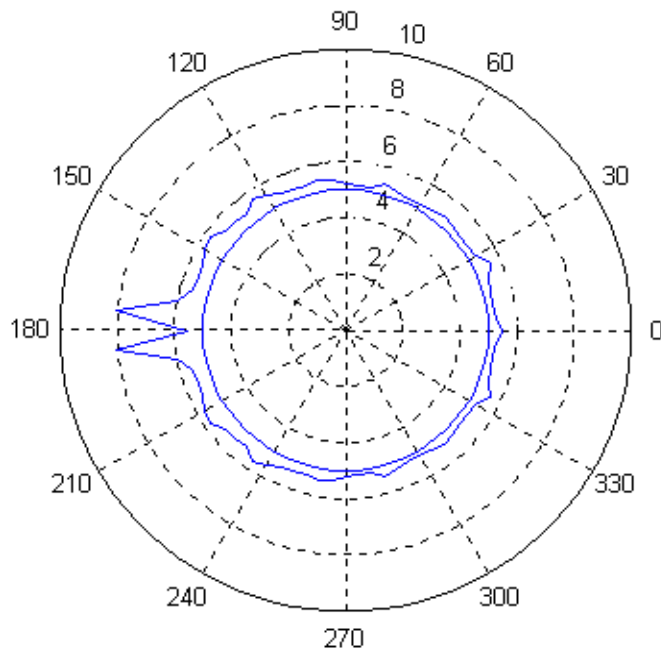


Figure C-9. Sea state variation when  $V=10\text{kts}$ ,  $l/L=0.01$  and Sea State 5

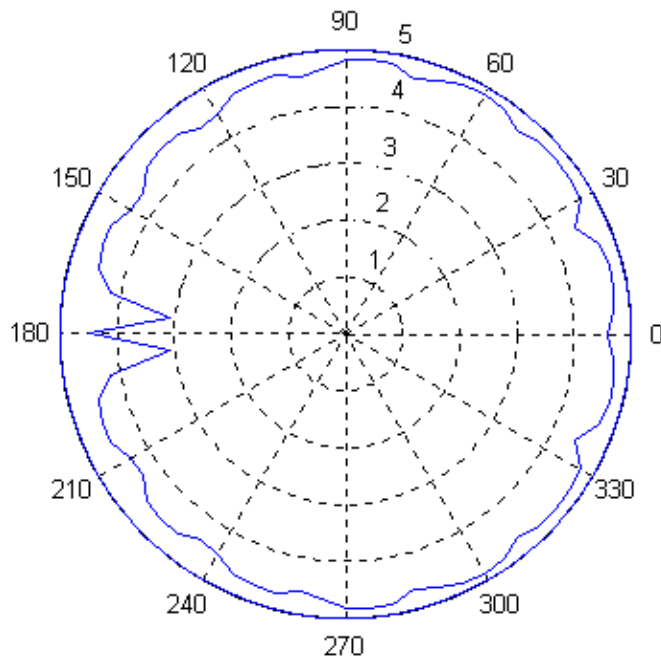


Figure C-10. Sea state degradation when  $V=10\text{kts}$ ,  $l/L=0.01$  and Sea State 5

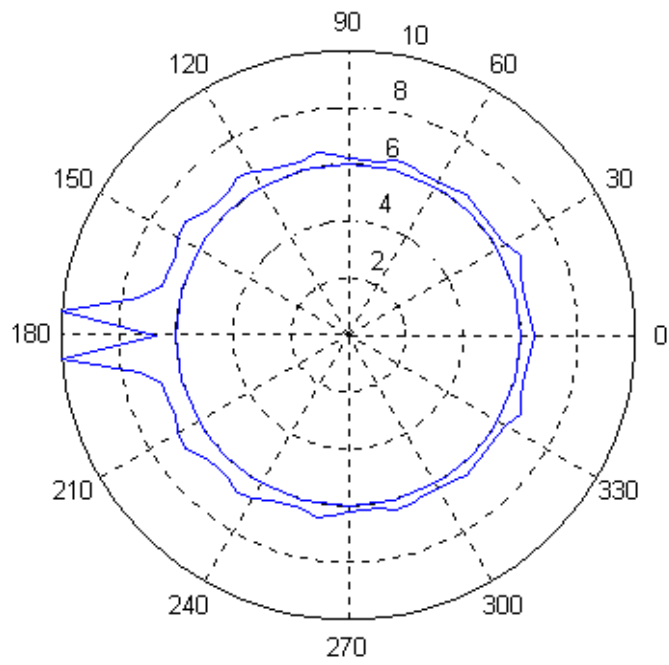


Figure C-11. Sea state variation when  $V=10\text{kts}$ ,  $l/L=0.01$  and Sea State 6

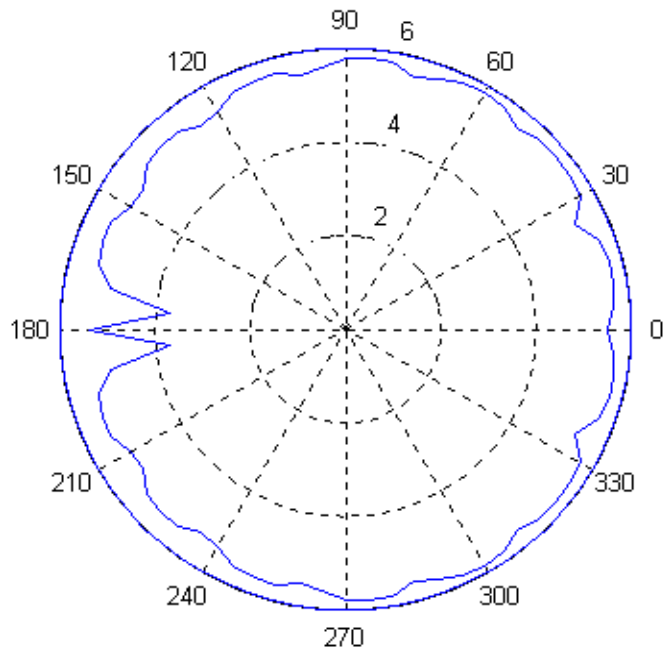


Figure C-12. Sea state degradation when  $V=10\text{kts}$ ,  $l/L=0.01$  and Sea State 6

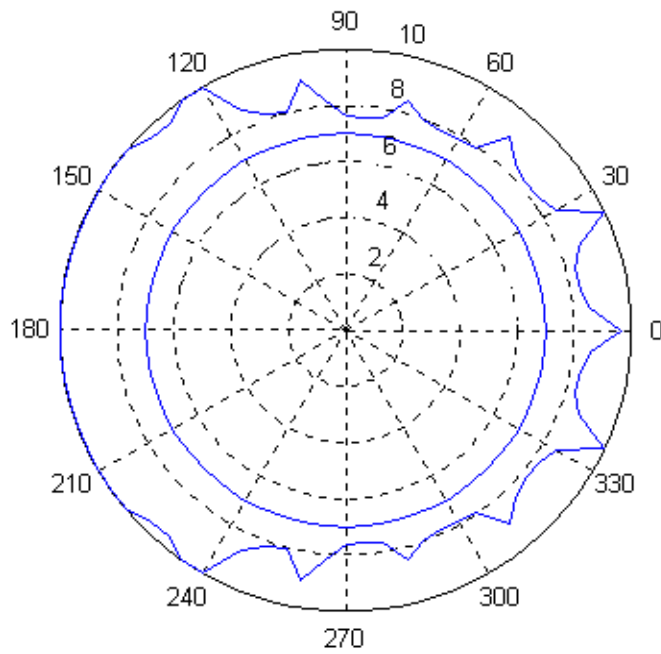


Figure C-13. Sea state variation when  $V=10\text{kts}$ ,  $l/L=0.01$  and Sea State 7

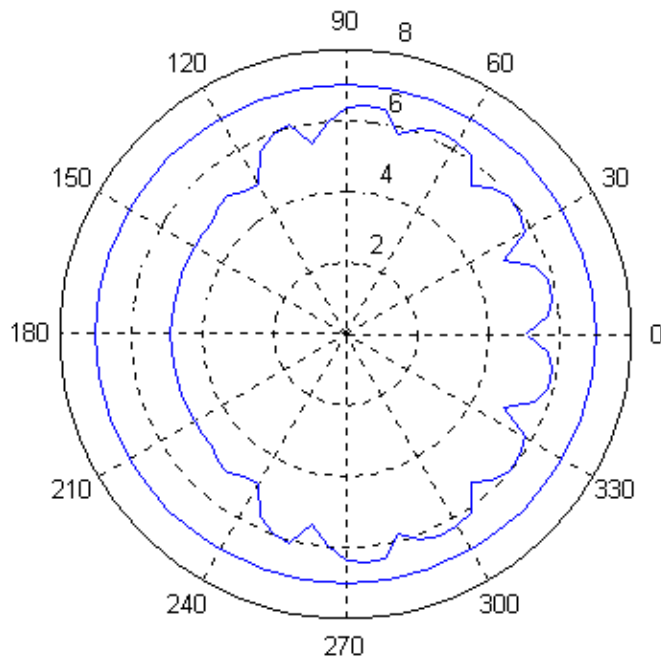


Figure C-14. Sea state degradation when  $V=10\text{kts}$ ,  $l/L=0.01$  and Sea State 7

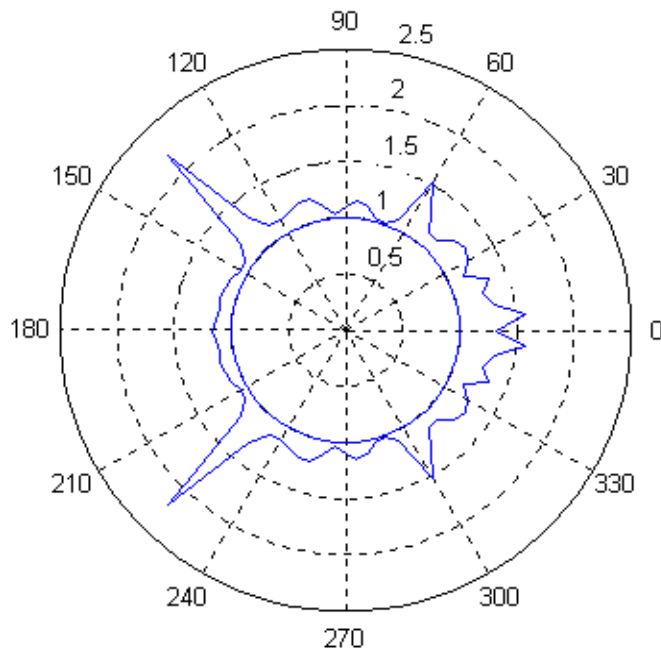


Figure C-15. Sea state variation when  $V=10\text{kts}$ ,  $l/L=0.1$  and Sea State 1

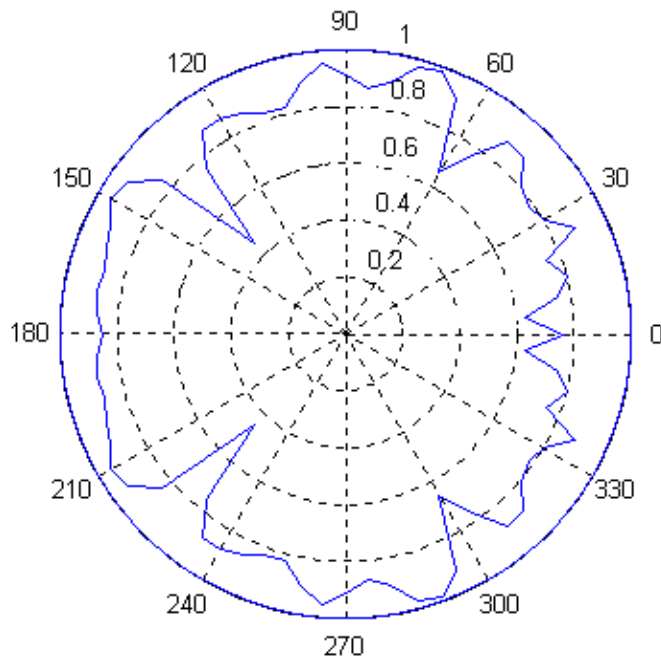


Figure C-16. Sea state degradation when  $V=10\text{kts}$ ,  $l/L=0.1$  and Sea State 1

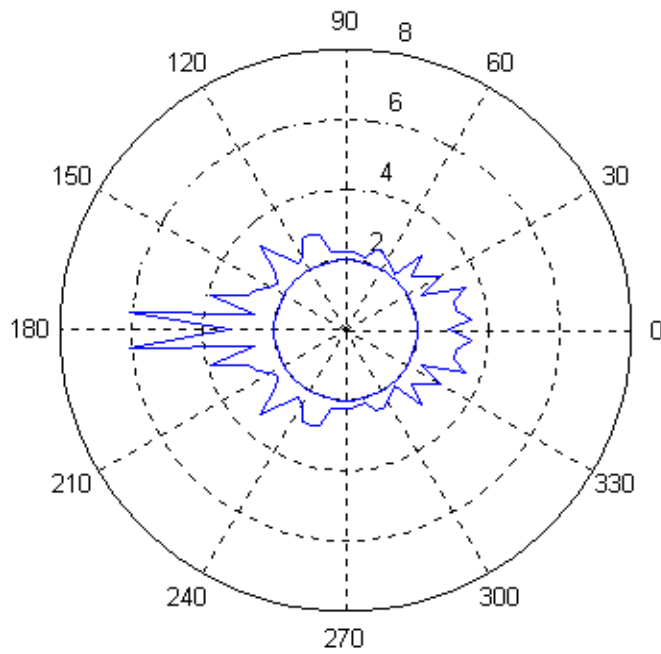


Figure C-17. Sea state variation when  $V=10\text{kts}$ ,  $l/L=0.1$  and Sea State 2

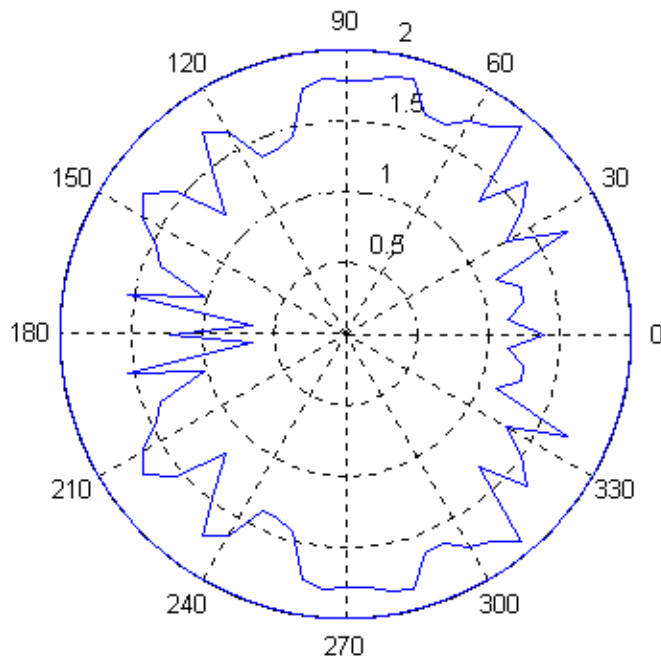


Figure C-18. Sea state degradation when  $V=10\text{kts}$ ,  $l/L=0.1$  and Sea State 2

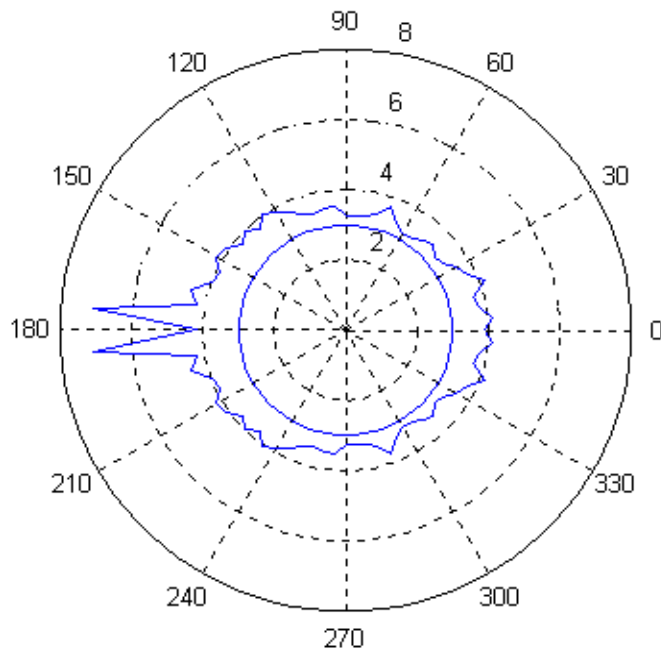


Figure C-19. Sea state variation when  $V=10\text{kts}$ ,  $l/L=0.1$  and Sea State 3

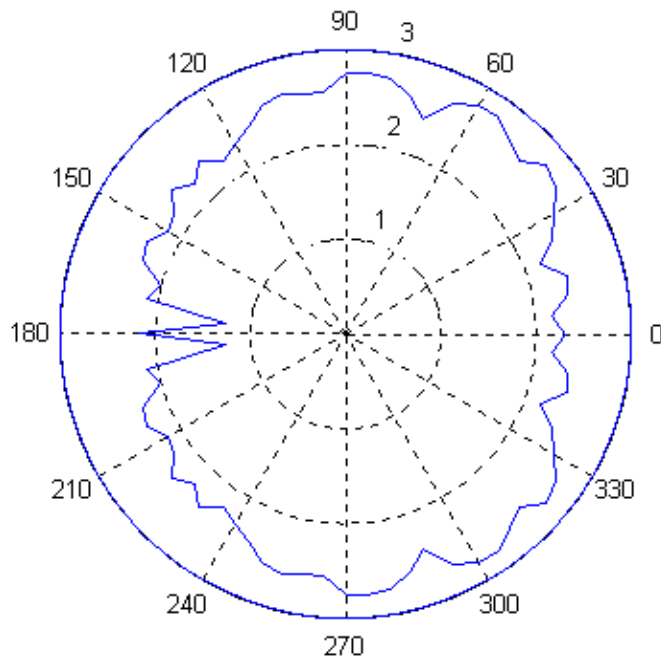


Figure C-20. Sea state degradation when  $V=10\text{kts}$ ,  $l/L=0.1$  and Sea State 3

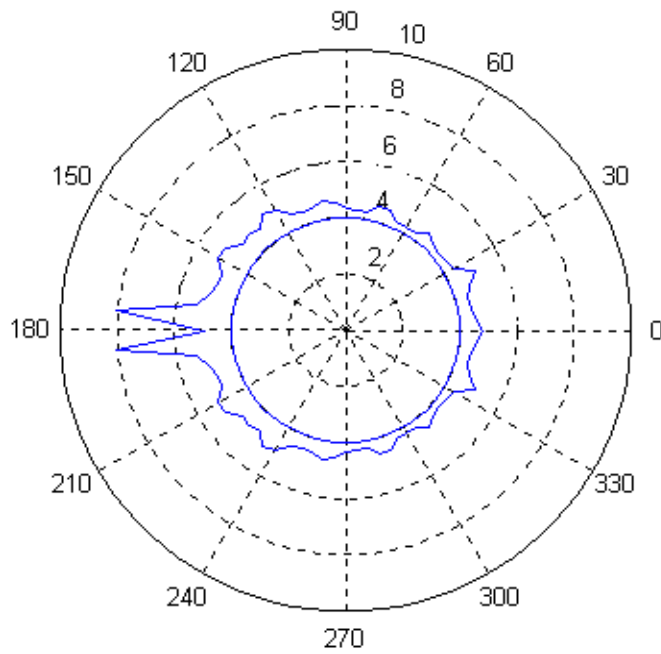


Figure C-21. Sea state variation when  $V=10\text{kts}$ ,  $l/L=0.1$  and Sea State 4

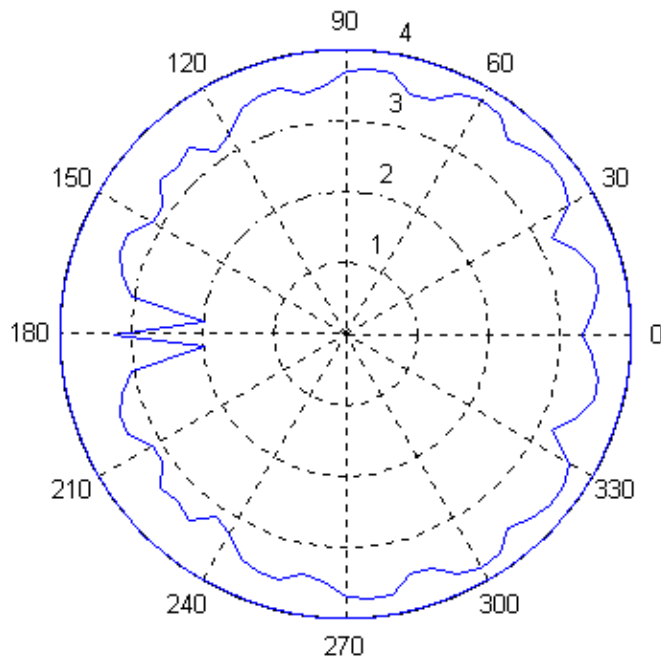


Figure C-22. Sea state degradation when  $V=10\text{kts}$ ,  $l/L=0.1$  and Sea State 4

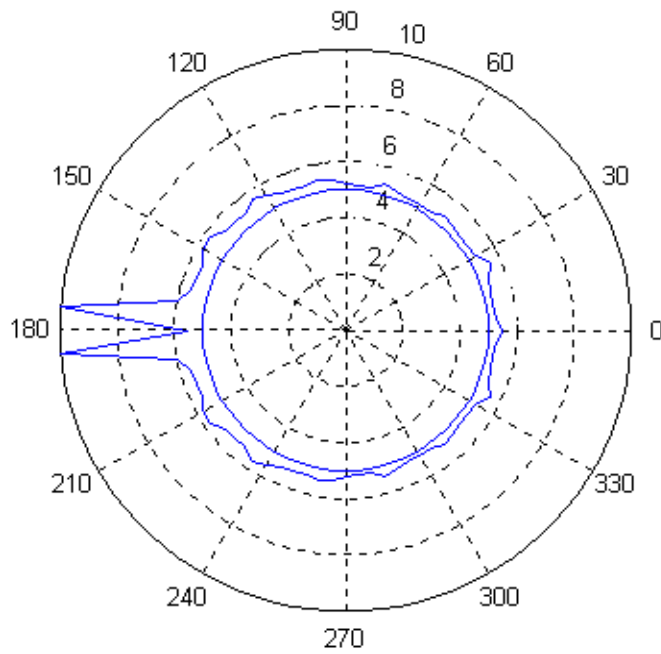


Figure C-23. Sea state variation when  $V=10\text{kts}$ ,  $l/L=0.1$  and Sea State 5

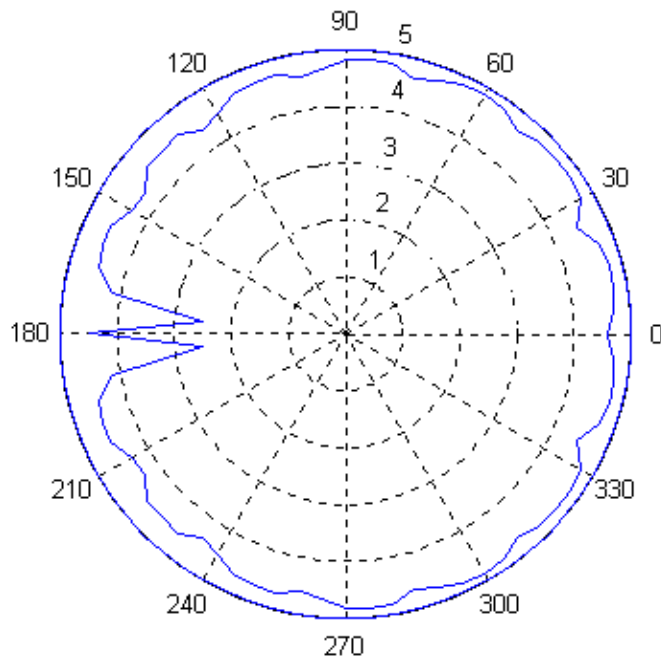


Figure C-24. Sea state degradation when  $V=10\text{kts}$ ,  $l/L=0.1$  and Sea State 5

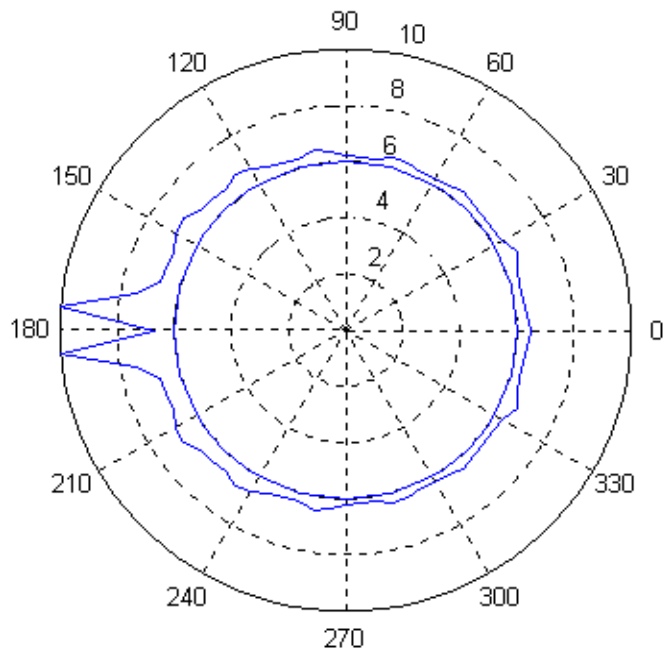


Figure C-25. Sea state variation when  $V=10\text{kts}$ ,  $l/L=0.1$  and Sea State 6

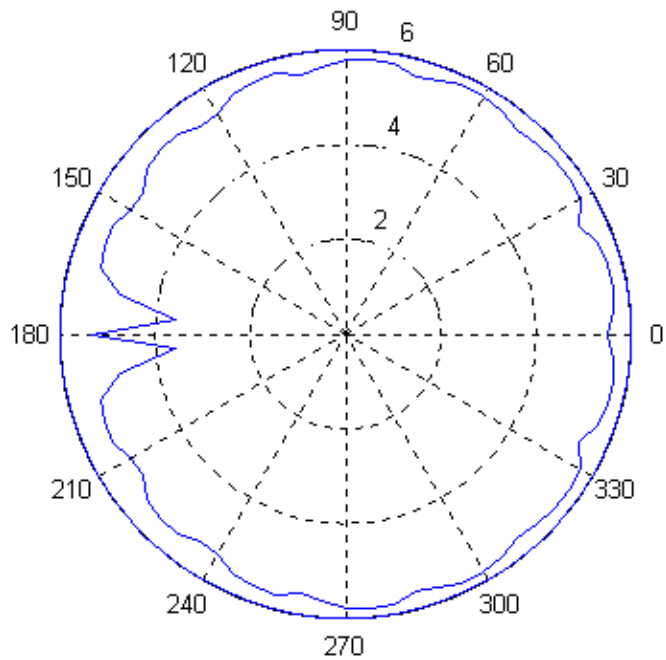


Figure C-26. Sea state degradation when  $V=10\text{kts}$ ,  $l/L=0.1$  and Sea State 6

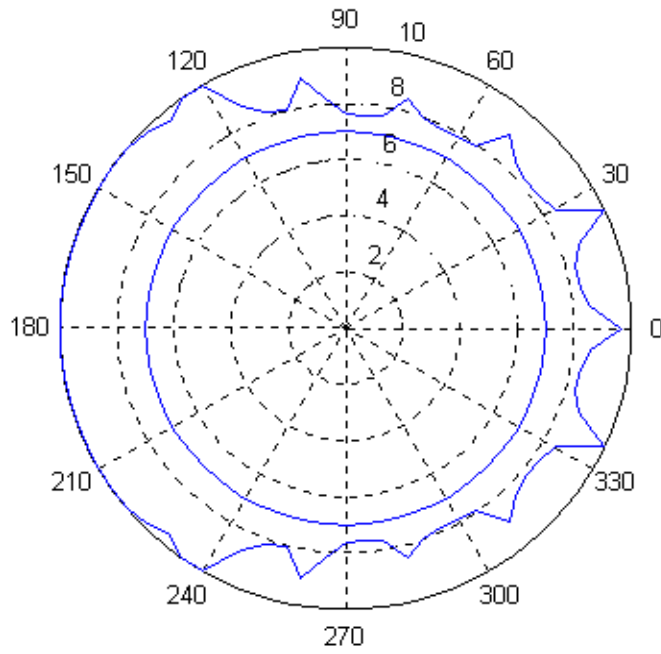


Figure C-27. Sea state variation when  $V=10\text{kts}$ ,  $l/L=0.1$  and Sea State 7

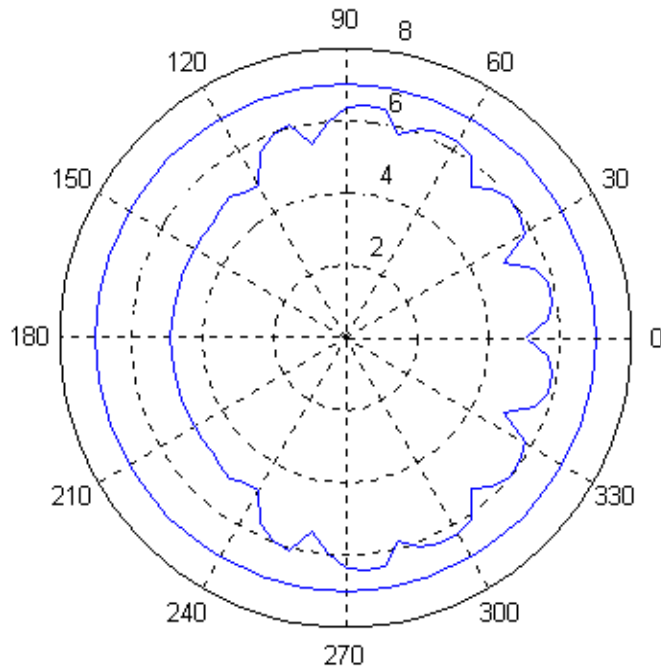


Figure C-28. Sea state degradation when  $V=10\text{kts}$ ,  $l/L=0.1$  and Sea State 7

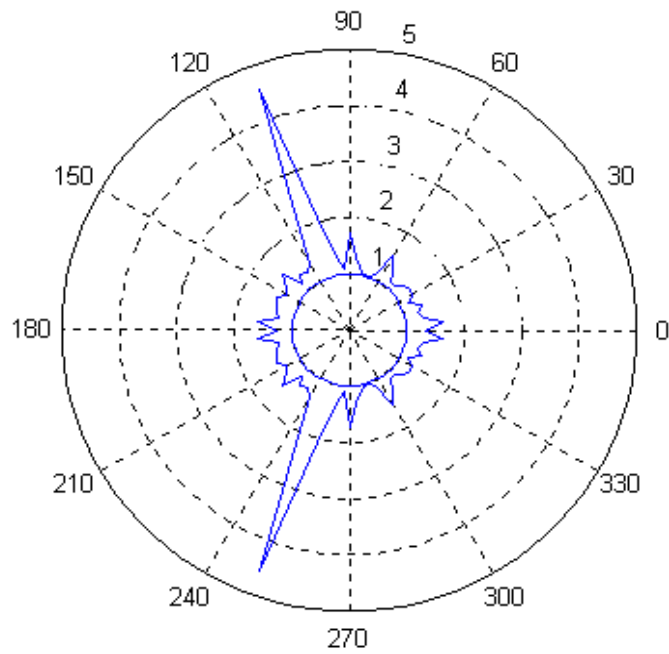


Figure C-29. Sea state variation when  $V=10\text{kts}$ ,  $l/L=0.5$  and Sea State 1

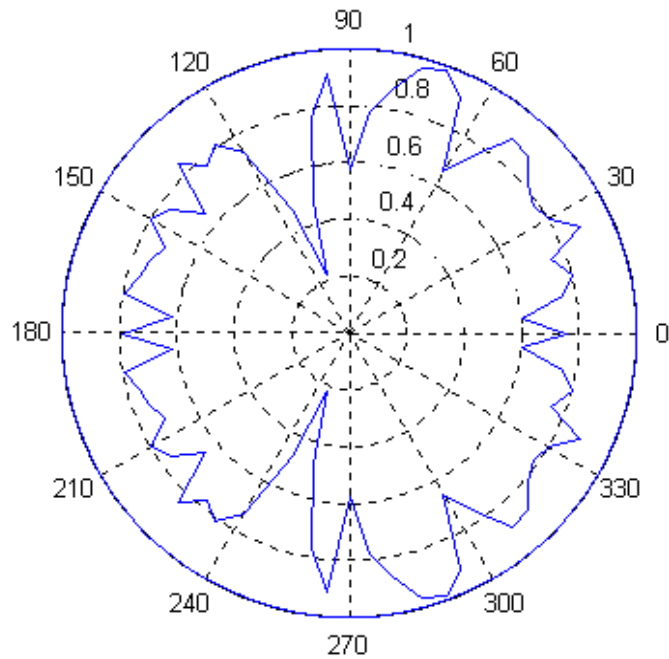


Figure C-30. Sea state degradation when  $V=10\text{kts}$ ,  $l/L=0.5$  and Sea State 1

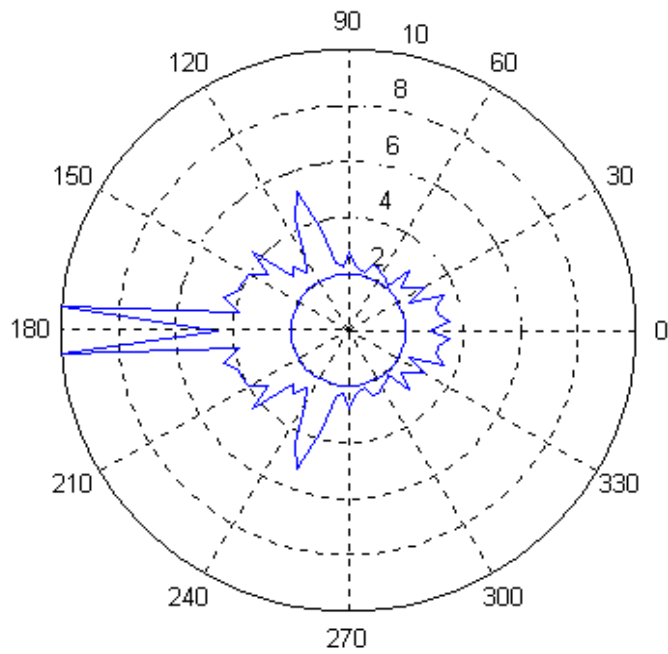


Figure C-31. Sea state variation when  $V=10\text{kts}$ ,  $l/L=0.5$  and Sea State 2

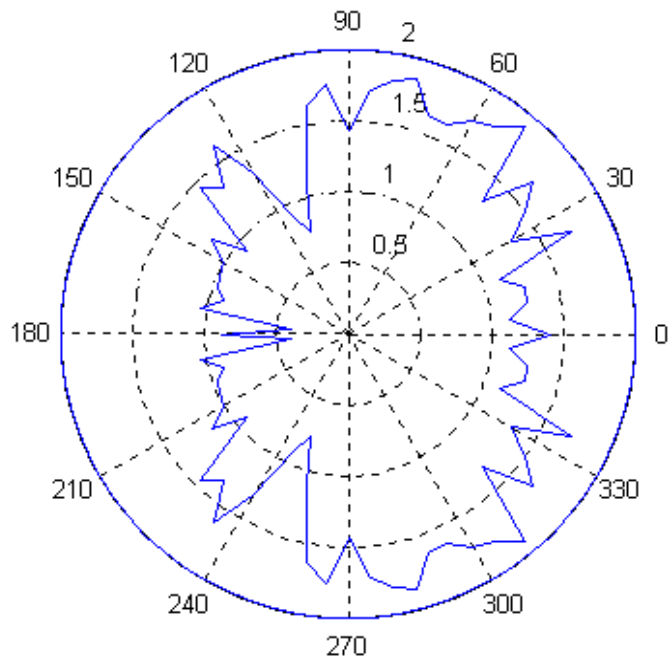


Figure C-32. Sea state degradation when  $V=10\text{kts}$ ,  $l/L=0.5$  and Sea State 2

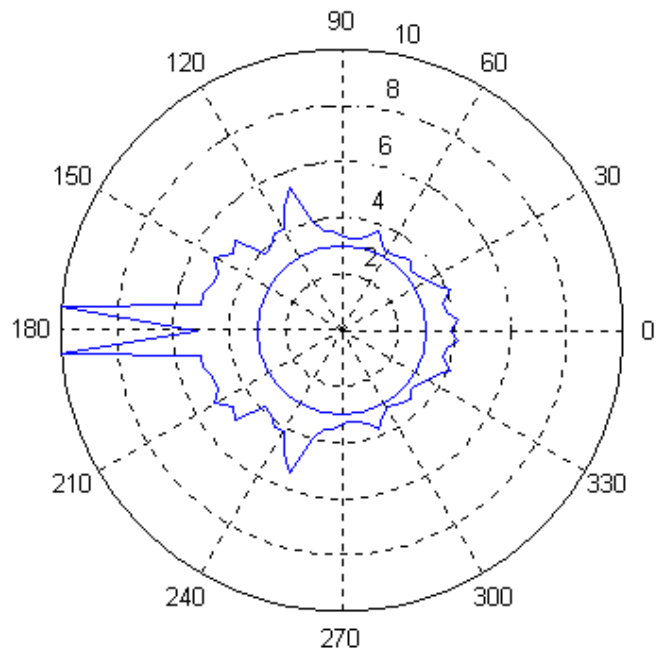


Figure C-33. Sea state variation when  $V=10\text{kts}$ ,  $I/L=0.5$  and Sea State 3

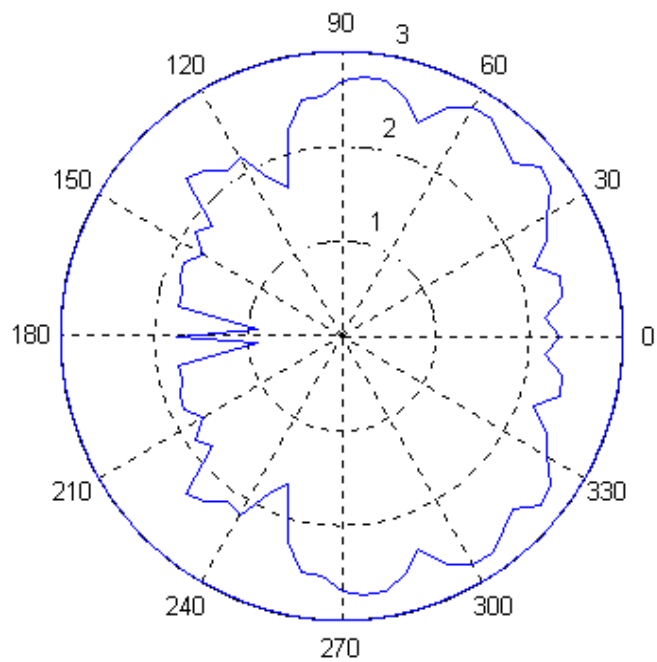


Figure C-34. Sea state degradation when  $V=10\text{kts}$ ,  $I/L=0.5$  and Sea State 3

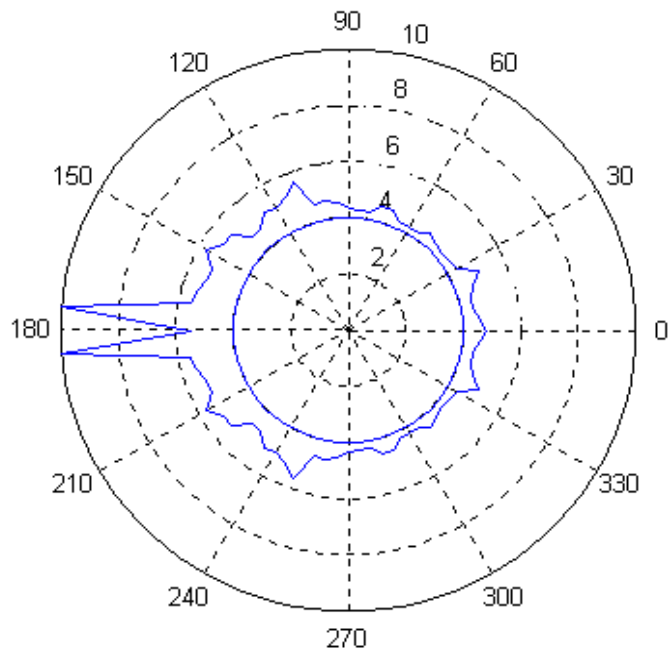


Figure C-35. Sea state variation when  $V=10\text{kts}$ ,  $l/L=0.5$  and Sea State 4

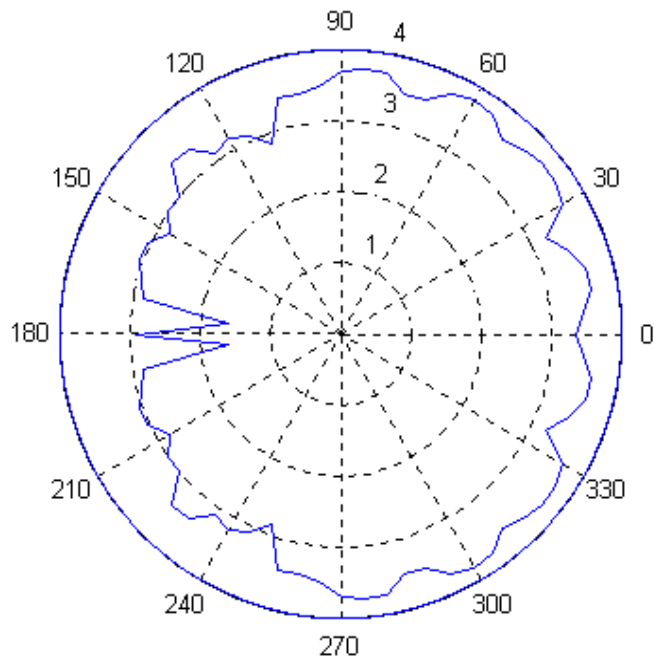


Figure C-36. Sea state degradation when  $V=10\text{kts}$ ,  $l/L=0.5$  and Sea State 4

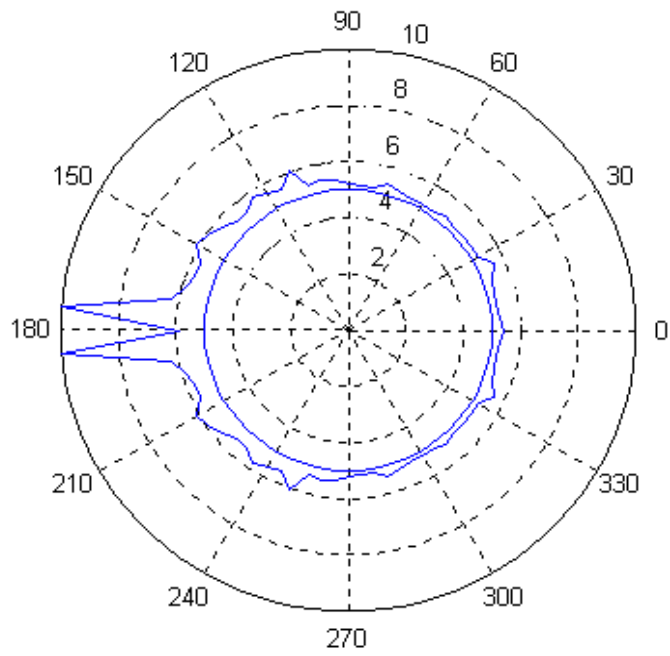


Figure C-37. Sea state variation when  $V=10\text{kts}$ ,  $l/L=0.5$  and Sea State 5

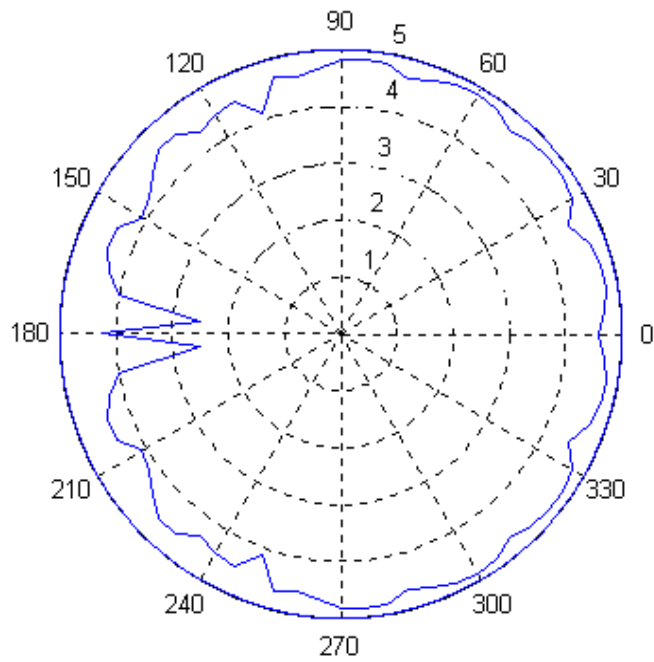


Figure C-38. Sea state degradation when  $V=10\text{kts}$ ,  $l/L=0.5$  and Sea State 5

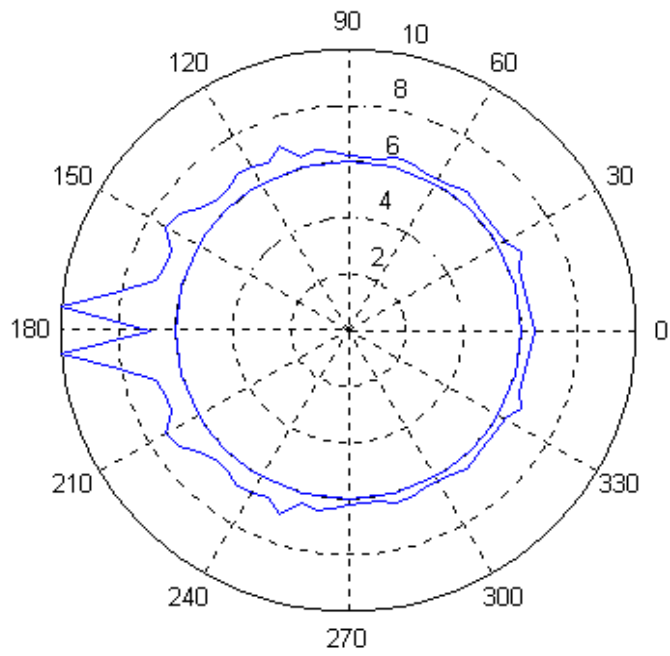


Figure C-39. Sea state variation when  $V=10\text{kts}$ ,  $l/L=0.5$  and Sea State 6

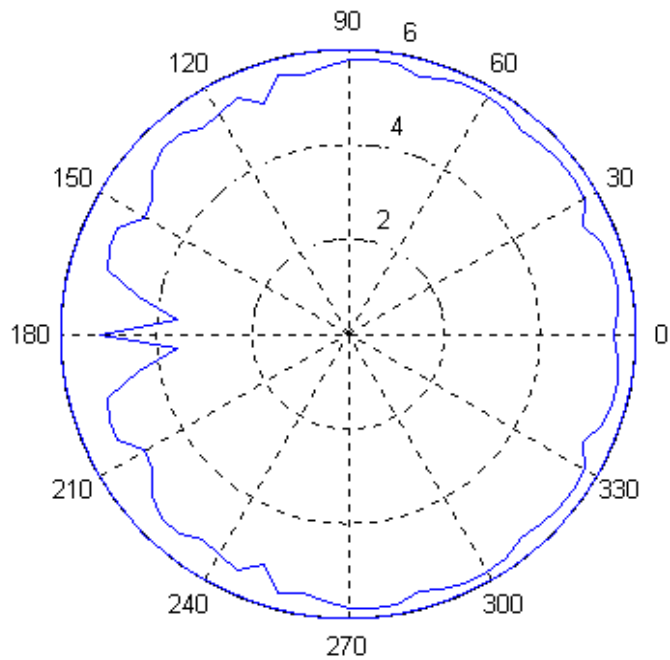


Figure C-40. Sea state degradation when  $V=10\text{kts}$ ,  $l/L=0.5$  and Sea State 6

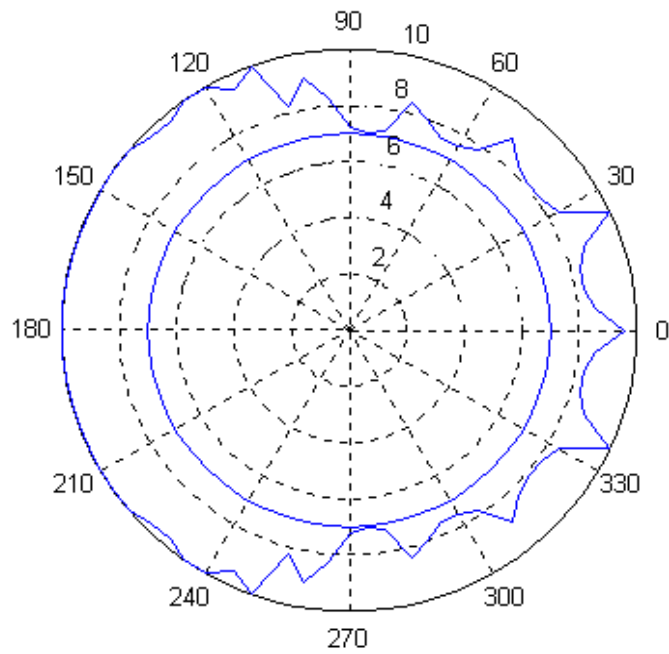


Figure C-41. Sea state variation when  $V=10\text{kts}$ ,  $I/L=0.5$  and Sea State 7

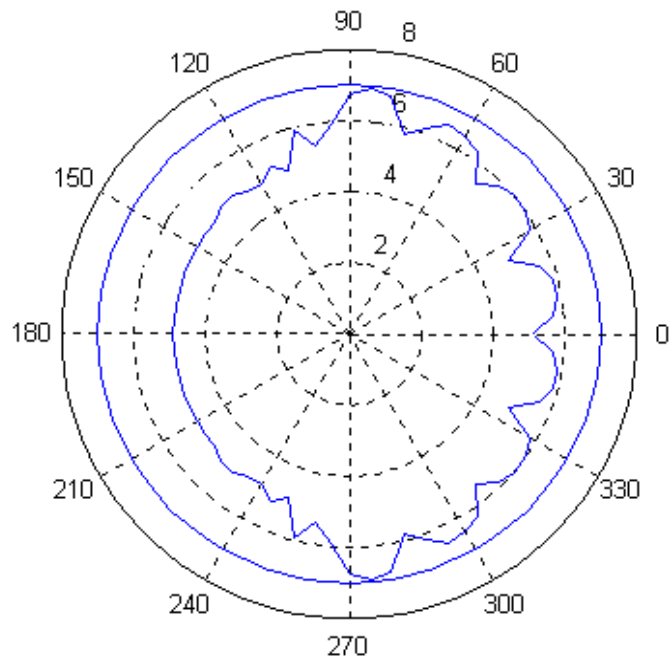


Figure C-42. Sea state degradation when  $V=10\text{kts}$ ,  $I/L=0.5$  and Sea State 7

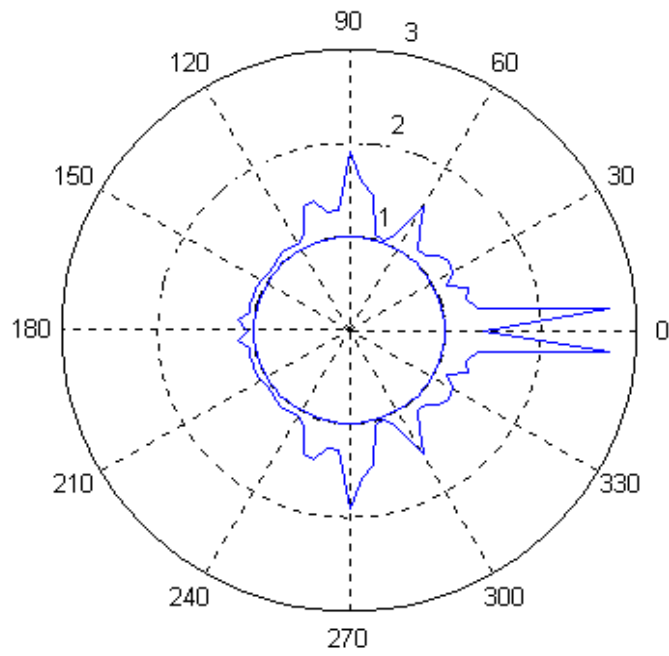


Figure C-43. Sea state variation when  $V=10\text{kts}$ ,  $l/L=1$  and Sea State 1

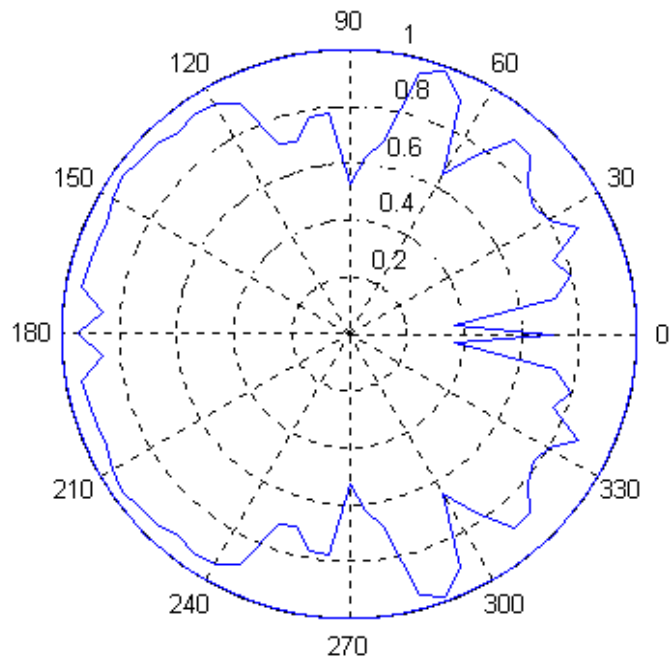


Figure C-44. Sea state degradation when  $V=10\text{kts}$ ,  $l/L=1$  and Sea State 1

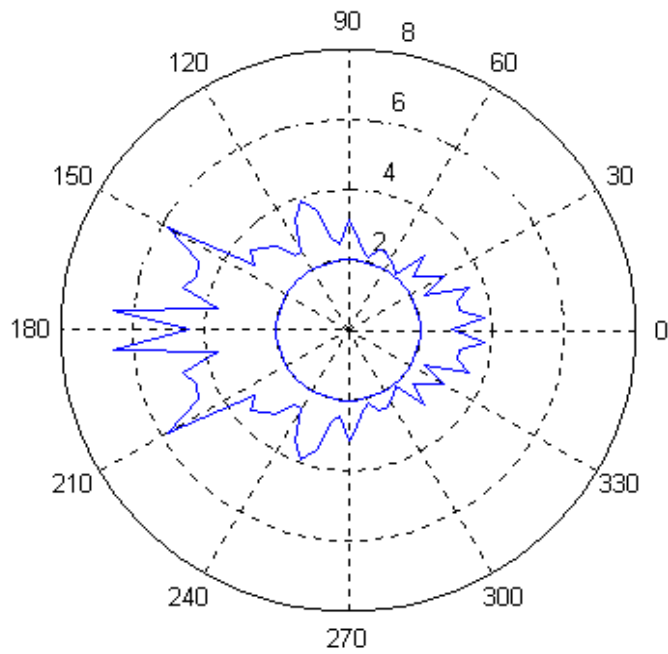


Figure C-45. Sea state variation when  $V=10$  kts,  $l/L=1$  and Sea State 2

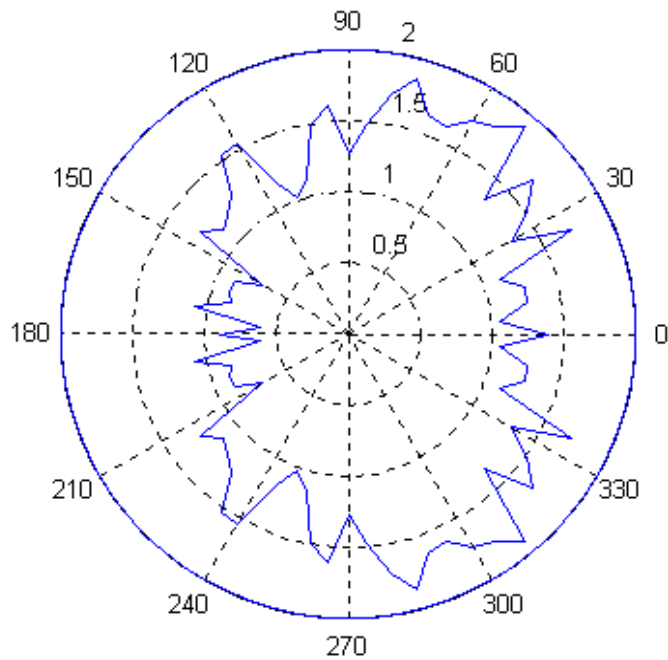


Figure C-46. Sea state degradation when  $V=10$  kts,  $l/L=1$  and Sea State 2

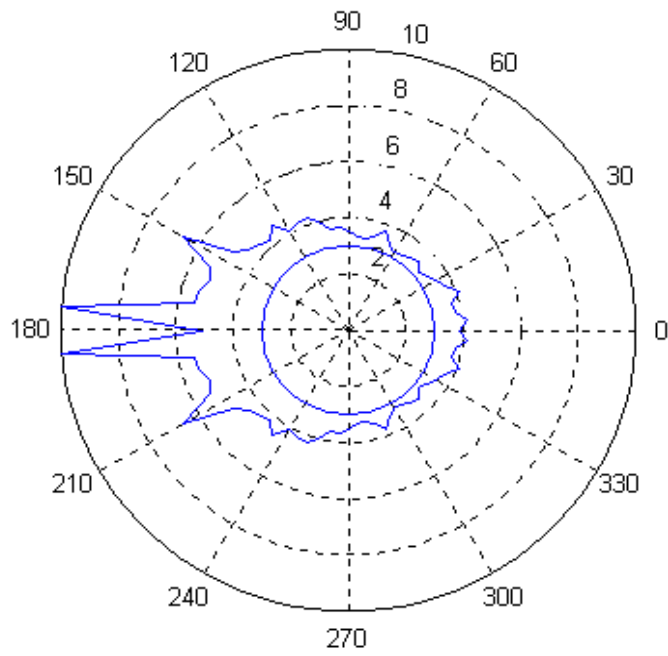


Figure C-47. Sea state variation when  $V=10\text{kts}$ ,  $l/L=1$  and Sea State 3

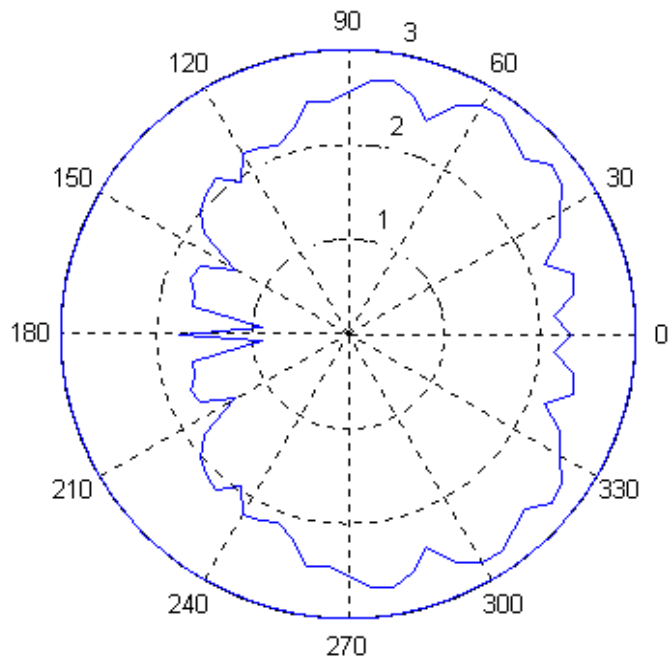


Figure C-48. Sea state degradation when  $V=10\text{kts}$ ,  $l/L=1$  and Sea State 3

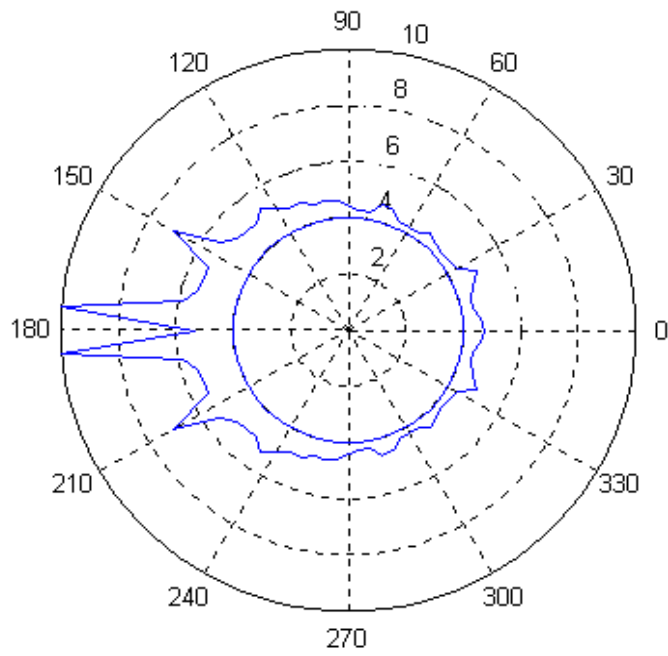


Figure C-49. Sea state variation when  $V=10\text{kts}$ ,  $l/L=1$  and Sea State 4

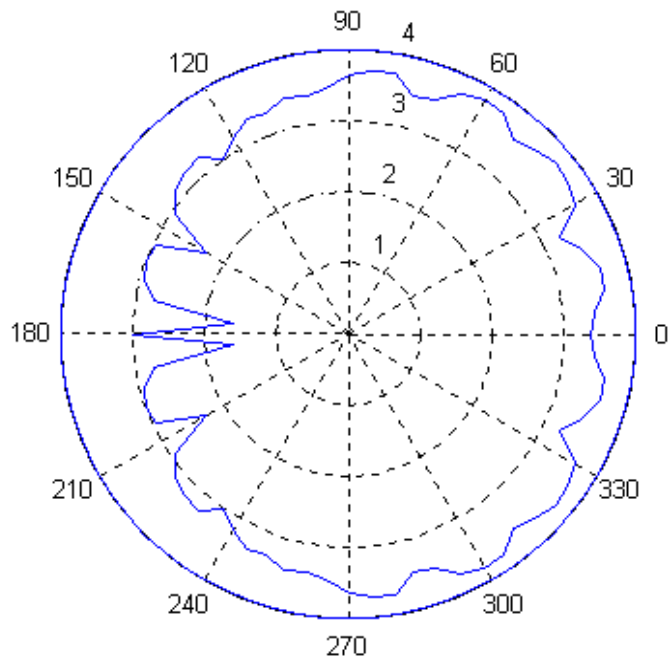


Figure C-50. Sea state degradation when  $V=10\text{kts}$ ,  $l/L=1$  and Sea State 4

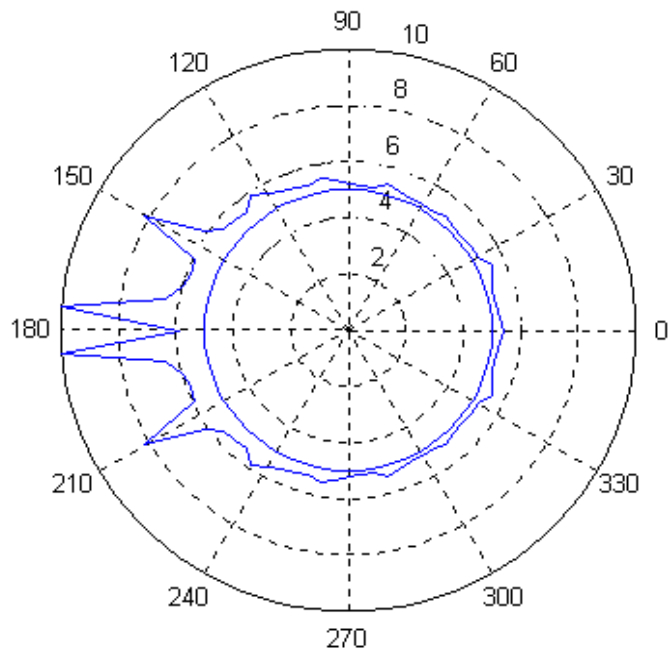


Figure C-51. Sea state variation when  $V=10\text{kts}$ ,  $l/L=1$  and Sea State 5

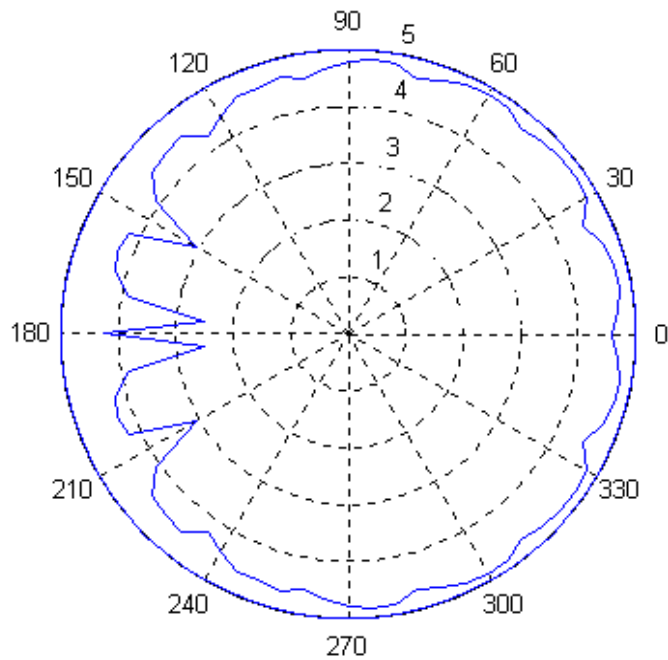


Figure C-52. Sea state degradation when  $V=10\text{kts}$ ,  $l/L=1$  and Sea State 5

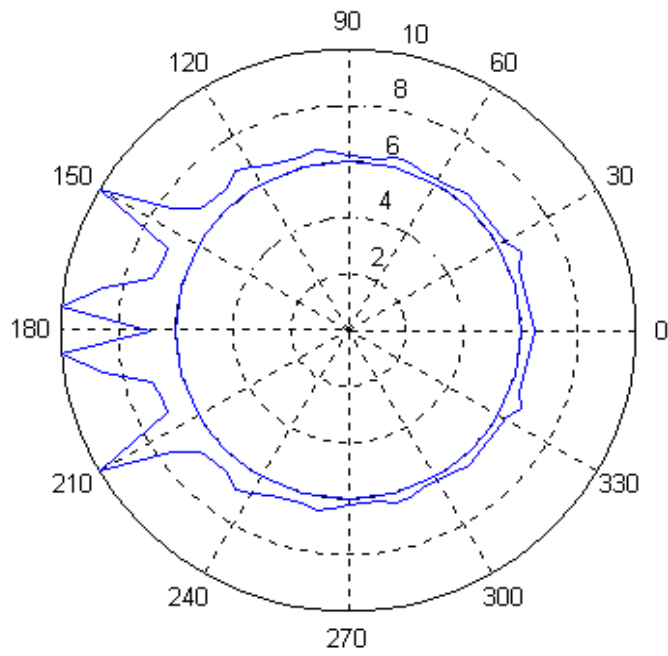


Figure C-53. Sea state variation when  $V=10\text{kts}$ ,  $l/L=1$  and Sea State 6

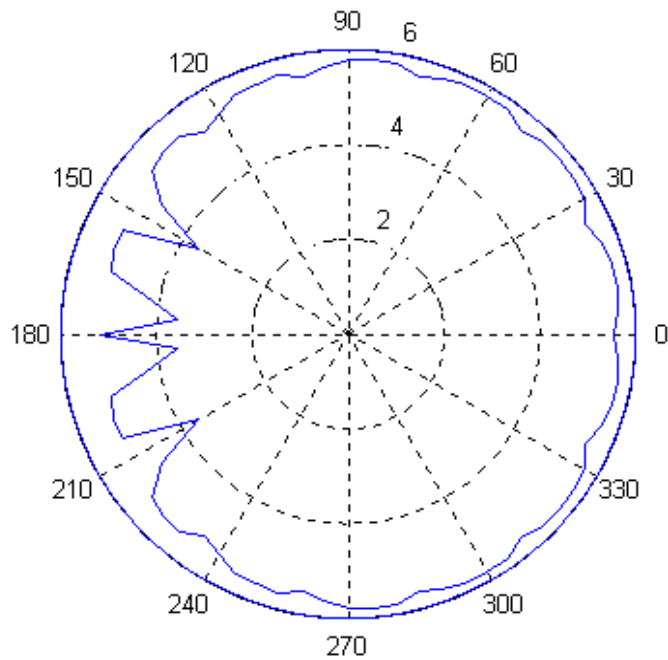


Figure C-54. Sea state degradation when  $V=10\text{kts}$ ,  $l/L=1$  and Sea State 6

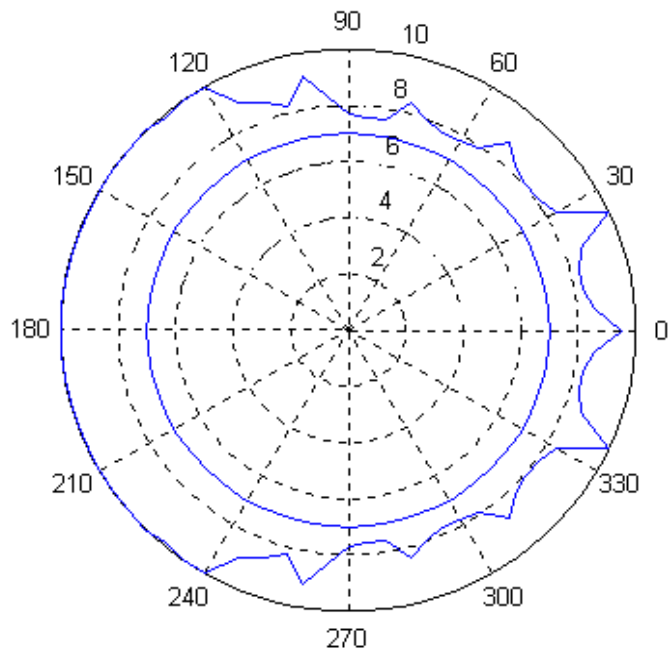


Figure C-55. Sea state variation when  $V=10\text{kts}$ ,  $l/L=1$  and Sea State 7

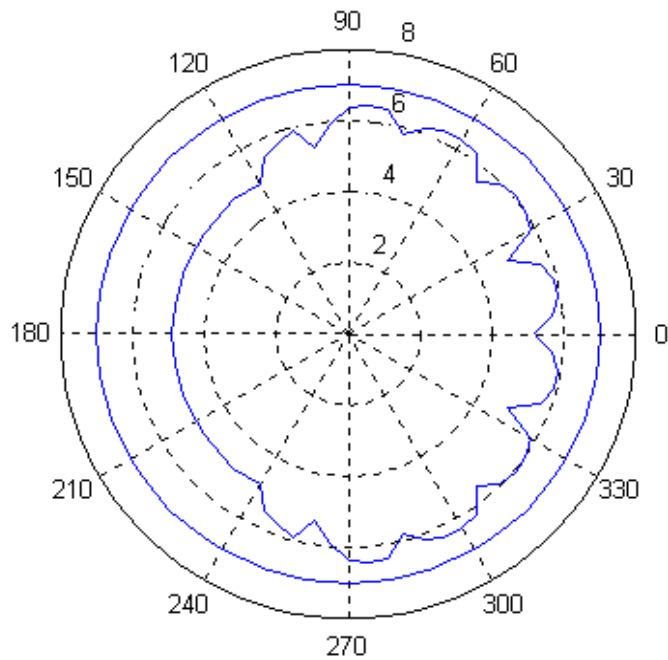


Figure C-56. Sea state degradation when  $V=10\text{kts}$ ,  $l/L=1$  and Sea State 7

THIS PAGE INTENTIONALLY LEFT BLANK

## APPENDIX D. HYDRODYNAMICS DATA

“MATDATA” output files are generated by SHIPMO (Nash). These files provide regular wave response mass added and excitation force matrix constants for given ship, speed, and wave angle. File names are described in the following format:

m -matdata.  
s or k -Vessel simulated, s-SLICE; k-KAIMALINO.  
v or vh -Motion simulated, v-vertical; vh-all six degrees of freedom.  
Speed -Zero to twenty knots in one-knot increments.  
Angle -Zero to 180 degrees in five-degree increments.

Example:

mkvh5\_180.txt = Kaimalino, motion in 6-dof, at 5 knots, 180° wave angle.

SLICE matdata files	KAIMALINO matdata files
mkvh0_0.txt	msvh0_0.txt
mkvh1_0.txt	msvh1_0.txt
mkvh2_0.txt	msvh2_0.txt
mkvh3_0.txt	msvh3_0.txt
mkvh4_0.txt	msvh4_0.txt
mkvh5_0.txt	msvh5_0.txt
.	.
.	.
.	.
<b><u>mkvh20_0.txt</u></b>	<b><u>msvh20_0.txt</u></b>
mkvh0_5.txt	msvh0_5.txt
mkvh1_5.txt	msvh1_5.txt
mkvh2_5.txt	msvh2_5.txt
.	.
.	.
.	.
<b><u>mkvh20_180.txt</u></b>	<b><u>msvh20_180.txt</u></b>

(2 ships) X (21 speeds) X (37 angles) = 1554 files

THIS PAGE INTENTIONALLY LEFT BLANK

## APPENDIX E. MATLAB CODES FOR REGULAR WAVES

```
% Vertical Plane
%
clear
%
% Get run info
%
V =input('Speed (knots) = ');
beta=input('Heading (deg) = ');
l =input('Length (l/L) = ');
%
% Get tension from curvefitting data.
% Applicable for speeds between 1 and 20 ft/sec.
%
T=-1.762*V^4+63.675*V^3-580.8*V^2+2485.9*V-34.047;
%
V_string =num2str(V);
beta_string=num2str(beta);
%
% The matdata output files default to the vertical only format when the
% heading angle is 0 or 180 degrees.
% Set up file reading format.
%
trigg = 30;
f3loc = 27; f5loc=29;
if beta==0
    trigg = 27;
    f3loc = 26; f5loc=27;
elseif beta==180
    trigg = 27;
    f3loc = 26; f5loc=27;
```

```

end
%
% Load FRONT SHIP data file msvhV_beta.txt
%
load_filename=strcat('msvh',V_string,'_',beta_string,'.txt');
filename_s=load(load_filename);
%
% Load REAR SHIP data file
%
load_filename=strcat('mkvh',V_string,'_',beta_string,'.txt');
filename_k=load(load_filename);
%
% GENERAL DATA
%
V=V*1.6878;      % Convert to ft/sec
lambda_min=20;   % Min wave length (ft)
lambda_max=1000; % Max wave length (ft)
delta_lambda=20; % Wave length increment (ft)
rho=1.9905;      % Water density
zeta=1;          % Regular wave height
L=105;           % Reference length for nondimensionalization
g=32.2;          % Gravitational constant
x_s=-46;         % FRONT SHIP attachment point
x_k=+40;         % REAR SHIP attachment point
beta    = beta*pi/180;
lambda  =lambda_min:delta_lambda:lambda_max; % Vector of wavelengths
wavenumber = 2.0*pi./lambda;                % Wave number
omega    = sqrt(wavenumber*g);               % Wave frequency
omegae   = omega-wavenumber*V*cos(beta);     % Frequency of encounter
period   = 2.0*pi./omega;
periode  = 2.0*pi./omegae;
omega    = omega';
omegae   = omegae';

```

```

filesize = size(lambda);
lambda_size= trigg*filesize(2);
%
% FRONT SHIP
%
% Set mass matrix elements
%
M33s=filename_s(3:trigg:lambda_size,3);
M35s=filename_s(3:trigg:lambda_size,5);
M53s=filename_s(5:trigg:lambda_size,3);
M55s=filename_s(5:trigg:lambda_size,5);
%
% Added mass terms
%
A33s=filename_s(9:trigg:lambda_size,3);
A35s=filename_s(9:trigg:lambda_size,5);
A53s=filename_s(11:trigg:lambda_size,3);
A55s=filename_s(11:trigg:lambda_size,5);
%
% Damping terms
%
B33s=filename_s(15:trigg:lambda_size,3);
B35s=filename_s(15:trigg:lambda_size,5);
B53s=filename_s(17:trigg:lambda_size,3);
B55s=filename_s(17:trigg:lambda_size,5);
%
% Hydrostatic terms
%
C33s=filename_s(21:trigg:lambda_size,3);
C35s=filename_s(21:trigg:lambda_size,5);
C53s=filename_s(23:trigg:lambda_size,3);
C55s=filename_s(23:trigg:lambda_size,5);
%
```

```

% Total exciting forces
%
F3s_t_amp=filename_s(f3loc:trigg:lambda_size,5);
F5s_t_amp=filename_s(f5loc:trigg:lambda_size,5);
F3s_t_pha=filename_s(f3loc:trigg:lambda_size,6);
F5s_t_pha=filename_s(f5loc:trigg:lambda_size,6);
F3s_t=F3s_t_amp.*exp(i*F3s_t_pha.*pi/180.0);
F5s_t=F5s_t_amp.*exp(i*F5s_t_pha.*pi/180.0);
%
% Froude/Krylov exciting forces
%
F3s_f_amp=filename_s(f3loc:trigg:lambda_size,1);
F5s_f_amp=filename_s(f5loc:trigg:lambda_size,1);
F3s_f_pha=filename_s(f3loc:trigg:lambda_size,2);
F5s_f_pha=filename_s(f5loc:trigg:lambda_size,2);
F3s_f=F3s_f_amp.*exp(i*F3s_f_pha.*pi/180.0);
F5s_f=F5s_f_amp.*exp(i*F5s_f_pha.*pi/180.0);
%
% Diffraction exciting forces
%
F3s_d_amp=filename_s(f3loc:trigg:lambda_size,3);
F5s_d_amp=filename_s(f5loc:trigg:lambda_size,3);
F3s_d_pha=filename_s(f3loc:trigg:lambda_size,4);
F5s_d_pha=filename_s(f5loc:trigg:lambda_size,4);
F3s_d=F3s_d_amp.*exp(i*F3s_d_pha.*pi/180.0);
F5s_d=F5s_d_amp.*exp(i*F5s_d_pha.*pi/180.0);
%
% REAR SHIP
%
% Set mass matrix elements
%
M33k=filename_k(3:trigg:lambda_size,3);
M35k=filename_k(3:trigg:lambda_size,5);

```

```

M53k=filename_k(5:trigg:lambda_size,3);
M55k=filename_k(5:trigg:lambda_size,5);
%
% Added mass terms
%
A33k=filename_k(9:trigg:lambda_size,3);
A35k=filename_k(9:trigg:lambda_size,5);
A53k=filename_k(11:trigg:lambda_size,3);
A55k=filename_k(11:trigg:lambda_size,5);
%
% Damping terms
%
B33k=filename_k(15:trigg:lambda_size,3);
B35k=filename_k(15:trigg:lambda_size,5);
B53k=filename_k(17:trigg:lambda_size,3);
B55k=filename_k(17:trigg:lambda_size,5);
%
% Hydrostatic terms
%
C33k=filename_k(21:trigg:lambda_size,3);
C35k=filename_k(21:trigg:lambda_size,5);
C53k=filename_k(23:trigg:lambda_size,3);
C55k=filename_k(23:trigg:lambda_size,5);
%
% Total exciting forces
%
F3k_t_amp=filename_k(f3loc:trigg:lambda_size,5);
F5k_t_amp=filename_k(f5loc:trigg:lambda_size,5);
F3k_t_pha=filename_k(f3loc:trigg:lambda_size,6);
F5k_t_pha=filename_k(f5loc:trigg:lambda_size,6);
F3k_t=F3k_t_amp.*exp(i*F3k_t_pha.*pi/180.0);
F5k_t=F5k_t_amp.*exp(i*F5k_t_pha.*pi/180.0);
%

```

```

% Froude/Krylov exciting forces
%
F3k_f_amp=filename_k(f3loc:trigg:lambda_size,1);
F5k_f_amp=filename_k(f5loc:trigg:lambda_size,1);
F3k_f_pha=filename_k(f3loc:trigg:lambda_size,2);
F5k_f_pha=filename_k(f5loc:trigg:lambda_size,2);
F3k_f=F3k_f_amp.*exp(i*F3k_f_pha.*pi/180.0);
F5k_f=F5k_f_amp.*exp(i*F5k_f_pha.*pi/180.0);
%
% Diffraction exciting forces
%
F3k_d_amp=filename_k(f3loc:trigg:lambda_size,3);
F5k_d_amp=filename_k(f5loc:trigg:lambda_size,3);
F3k_d_pha=filename_k(f3loc:trigg:lambda_size,4);
F5k_d_pha=filename_k(f5loc:trigg:lambda_size,4);
F3k_d=F3k_d_amp.*exp(i*F3k_d_pha.*pi/180.0);
F5k_d=F5k_d_amp.*exp(i*F5k_d_pha.*pi/180.0);
%
% MATCHING CONDITION
%
A33bar_s=- (omegae.^2).*(M33s+A33s)+i*omegae.*B33s+C33s;
A35bar_s=- (omegae.^2).*(M35s+A35s)+i*omegae.*B35s+C35s;
A53bar_s=- (omegae.^2).*(M53s+A53s)+i*omegae.*B53s+C53s;
A55bar_s=- (omegae.^2).*(M55s+A55s)+i*omegae.*B55s+C55s;
A33bar_k=- (omegae.^2).*(M33k+A33k)+i*omegae.*B33k+C33k;
A35bar_k=- (omegae.^2).*(M35k+A35k)+i*omegae.*B35k+C35k;
A53bar_k=- (omegae.^2).*(M53k+A53k)+i*omegae.*B53k+C53k;
A55bar_k=- (omegae.^2).*(M55k+A55k)+i*omegae.*B55k+C55k;
%
mu3_s=(A55bar_s.*F3s_t-A35bar_s.*F5s_t)/(A33bar_s.*A55bar_s-
A35bar_s.*A53bar_s);
nu3_s=(A55bar_s+A35bar_s*x_s)/(A33bar_s.*A55bar_s-A35bar_s.*A53bar_s);

```

```

mu5_s=(A53bar_s.*F3s_t-A33bar_s.*F5s_t)/(A53bar_s.*A35bar_s-
A33bar_s.*A55bar_s);
nu5_s=(A53bar_s+A33bar_s*x_s)/(A53bar_s.*A35bar_s-A33bar_s.*A55bar_s);
mu3_k=(A55bar_k.*F3k_t-A35bar_k.*F5k_t)/(A33bar_k.*A55bar_k-
A35bar_k.*A53bar_k);
nu3_k=(A55bar_k+A35bar_k*x_k)/(A33bar_k.*A55bar_k-
A35bar_k.*A53bar_k);
mu5_k=(A53bar_k.*F3k_t-A33bar_k.*F5k_t)/(A53bar_k.*A35bar_k-
A33bar_k.*A55bar_k);
nu5_k=(A53bar_k+A33bar_k*x_k)/(A53bar_k.*A35bar_k-
A33bar_k.*A55bar_k);
%
a=mu3_s-mu5_s*x_s-mu3_k+mu5_k*x_k;
b=nu3_s-nu5_s*x_s+nu3_k-nu5_k*x_k;
f=a./(l/T+b);
%
f_s=-f; % Connection force on FRONT SHIP
f_k=f; % Connection force on REAR SHIP
eta3_s=mu3_s+nu3_s.*f_s; % FRONT SHIP heave
eta5_s=mu5_s+nu5_s.*f_s; % FRONT SHIP pitch
eta3_k=mu3_k+nu3_k.*f_k; % REAR SHIP heave
eta5_k=mu5_k+nu5_k.*f_k; % REAR SHIP pitch
xi_s=eta3_s-eta5_s*x_s; % FRONT SHIP motion at connection
xi_k=eta3_k-eta5_k*x_k; % REAR SHIP motion at connection
xi0_s=mu3_s-mu5_s*x_s; % FRONT SHIP motion at connection for zero f
xi0_k=mu3_k-mu5_k*x_k; % REAR SHIP motion at connection for zero f
%
% SAMPLE FIGURES
%
figure (1)
plot(period,abs(xi0_s),'r',period,abs(xi_s),'b'),grid,legend('w/o connection','with
connection')
title('Leading Ship Motion'),xlabel('T [sec]'),ylabel('\xi_V [ft/ft]')

```

```
figure (2)
plot(period,abs(xi0_k),'r',period,abs(xi_k),'b'),grid,legend('w/o connection','with
connection')
title('Trailing Ship Motion'),xlabel('T [sec]'),ylabel('\xi_V [ft/ft]')
```

```
figure (3)
plot(period,abs(f),'r',period,F3s_t_amp,'b',period,F3k_t_amp,'g'),grid,legend('conn
ection force','wave, leading ship','wave, trailing ship')
title('Exciting Forces'),xlabel('T [sec]'),ylabel('F [lbs/ft]')
```

## APPENDIX F. MATLAB CODES FOR RANDOM WAVES

```
% This section is added to the codes for regular waves
hs=[.85 2.25 4.25 6.75 10 17 32.5];
%
% Begin random wave calculations
% Fully developed seas - PM spectrum
%
iHS=0;
for I=1:7;          % Loop on significant wave height
    HS=hs(I);
    iHS=iHS+1;
    %
    % Random wave calculations
    % Pierson-Moscowitz spectrum
    %
    POWER =-.032*(g/HS)^2;
    S    =(0.0081*g^2).*exp(POWER./(omega.^4))./(omega.^5);
    Se   =S./(1-(2.0/g)*omega*V*cos(beta));    % Convert S(w) to S(we)
    %
    % Define response spectra
    %
    Sf   =((abs(f)).^2).*Se;
    Sxi_s =((abs(xi_s)).^2).*Se;
    Sxi_k =((abs(xi_k)).^2).*Se;
    Sxi0_s =((abs(xi0_s)).^2).*Se;
    Sxi0_k =((abs(xi0_k)).^2).*Se;
    SF3s_t =((abs(F3s_t)).^2).*Se;
    SF3k_t =((abs(F3k_t)).^2).*Se;
    %
    % Initializations
    %
    Sf_i=0;
```

```

Sxi_s_i=0;
Sxi_k_i=0;
Sxi0_s_i=0;
Sxi0_k_i=0;
SF3s_t_i=0;
SF3k_t_i=0;
%
% Integral S(w)*|RAO|^2
%
    for I=2:1:filesize(2),
        Sf_i=Sf_i+0.5*abs((Sf(I)+Sf(I-1)))*abs((omegae(I-1)-
omegae(I)));
        Sxi_s_i=Sxi_s_i+0.5*abs((Sxi_s(I)+Sxi_s(I-
1)))*abs((omegae(I-1)-omegae(I)));
        Sxi_k_i=Sxi_k_i+0.5*abs((Sxi_k(I)+Sxi_k(I-
1)))*abs((omegae(I-1)-omegae(I)));
        Sxi0_s_i= Sxi0_s_i + 0.5*abs((Sxi0_s(I) + Sxi0_s(I-1))) *
abs((omegae(I-1)-omegae(I)));
        Sxi0_k_i= Sxi0_k_i + 0.5*abs((Sxi0_k(I) + Sxi0_k(I-1))) *
abs((omegae(I-1)-omegae(I)));
        SF3s_t_i= SF3s_t_i + 0.5*abs((SF3s_t(I) + SF3s_t(I-1))) *
abs((omegae(I-1)-omegae(I)));
        SF3k_t_i= SF3k_t_i + 0.5*abs((SF3k_t(I) + SF3k_t(I-1)))
* abs((omegae(I-1)-omegae(I)));
    end
%
% RMS values
%
RMS_f = sqrt(Sf_i);
RMS_xi_s = sqrt(Sxi_s_i);
RMS_xi_k = sqrt(Sxi_k_i);
RMS_xi0_s = sqrt(Sxi0_s_i);
RMS_xi0_k = sqrt(Sxi0_k_i);
RMS_F3s_t = sqrt(SF3s_t_i);
RMS_F3k_t = sqrt(SF3k_t_i);

```

$v_{HS}(i\beta, iHS) = HS;$   
 $RMS\_fF(i\beta, iHS) = RMS\_f / RMS\_F3s\_t;$   
 $RMS\_xX(i\beta, iHS) = RMS\_xi\_s / RMS\_xi0\_s;$   
 $RMS\_ff(i\beta, iHS) = RMS\_f;$   
 $RMS\_xx(i\beta, iHS) = RMS\_xi\_s;$   
 $RMS\_FF3s\_t(i\beta, iHS) = RMS\_F3s\_t;$

THIS PAGE INTENTIONALLY LEFT BLANK

## APPENDIX G. MATLAB CODES FOR SEAKEEPING EVALUATION

```
% This section is added at the end the codes for random waves
RMS_con=RMS_ff+RMS_FF3s_t;
RMS_uncon=RMS_FF3s_t;

% This section is a sample for getting sea state figures of Appendix. C after you
build a matrix of RMS values above for different conditions
t=linspace(0,2*pi,73)';
figure(1)
polar(t,SS1005(:,23)),hold on
polar(t,7*ones(73,1))
figure(2)
polar(t,SS1005(:,22)),hold on
polar(t,6*ones(73,1))
figure(3)
polar(t,SS1005(:,21)),hold on
polar(t,5*ones(73,1))
figure(4)
polar(t,SS1005(:,20)),hold on
polar(t,4*ones(73,1))
figure(5)
polar(t,SS1005(:,19)),hold on
polar(t,3*ones(73,1))
figure(6)
polar(t,SS1005(:,18)),hold on
polar(t,2*ones(73,1))
figure(7)
polar(t,SS1005(:,17)),hold on
polar(t,1*ones(73,1))
```

THIS PAGE INTENTIONALLY LEFT BLANK

## LIST OF REFERENCES

Beck, R. F., "Principles of Naval Architecture," Volume III, Chapter VIII, Section 3, 1989.

Beck, R. F., and Reed, A. M., "Modern Computational Methods for Ships in a Seaway," August 2001.

Beck, R. F., and Troesch, A. W., "Documentation and User's Manual for the Computer Program SHIPMO.BM," Report No. 89-2, 1989.

Cummins, W. E., "Principles of Naval Architecture," Volume III, Chapter VIII, Section 2, 1989.

Korsmeyer, T., and Kring, D., "Coupling Structural and Hydrodynamic Analyses," December 1998.

McCreight, K. K., "A Note on the Selection of Wave Spectra for Design Evaluation," Naval Surface Warfare Center, January 1998.

Nash, C., "Vertical Plane Response of Surface Ships in Close Proximity Towing," Naval Postgraduate School, Monterey, CA, June 2001.

Newman, J. N., "Marine Hydrodynamics," Section 6.2, Massachusetts Institute of Technology Press, Cambridge, Massachusetts, 1977

Ochi, J. K., and Hubble, E. N., "On Six-Parameter Wave Spectra," Proceeding of the Fifteenth Conference on Coastal Engineering, July 1976.

Pierson, W. J. and Moscovitz, L., "A Proposed Spectral Form for Fully Developed Wind Seas Based on the Similarity Theory of S.A. Kitaigorodskii," Journal of Geophysical Research, Volume 69, 1964

Pierson, W. J., "The Spectral Ocean Wave Model (SOWM), A Northern Hemisphere Computer Model for Specifying and Forecasting Ocean Wave Spectra," DTNSRDC Report 82/011, July 1982.

TSSE, Total Ship Systems Engineering, "Sea Lance Littoral Warfare Small Combatant System," Naval Postgraduate School, Monterey, CA, January 2001

THIS PAGE INTENTIONALLY LEFT BLANK

## INITIAL DISTRIBUTION LIST

1. Defense Technical Information Center  
Ft. Belvoir, VA
2. Dudley Knox Library  
Naval Postgraduate School  
Monterey, CA
3. Chairman  
Department of Mechanical Engineering  
Naval Postgraduate School  
Monterey, CA
4. Professor Fotis A. Papoulias  
Department of Mechanical Engineering  
Naval Postgraduate School  
Monterey, CA
5. Naval Engineering Curricular Office  
Naval Postgraduate School  
Monterey, CA
6. LTJG Orhan Barbaros Okan  
Dereboyu Sk. 25-5  
Yenimahalle, ANKARA 06170  
TURKEY
7. Deniz Kuvvetleri Komutanligi  
Bakanliklar, ANKARA 06100  
TURKEY